Final Thesis
Industrial Engineer

Development of a surrogate model for simplified neutronic calculations involved in the design stage of a thermonuclear fusion reactor

Volume I

REPORT

Author: Javier Martínez Arroyo
Thesis Director: Antonella Li Puma
Thesis Co-Director: Jean-Charles Jaboulay
University Director: Javier Dies Llovera
Session: September 2012

Commissariat à l'Energie Atomique
DEN/DANS/DM2S/SERMA/LPEC
Centre de Saclay

Escola Tècnica Superior
d'Enginyeria Industrial de Barcelona

Methodology developed during the project, results and conclusions will be presented at the conference ***27th Symposium on Fusion Technology (SOFT 2012)*** (1) on September the 24th, 2012 in Liège (Belgium).

A scientific paper based on the work developed on this report will be published in the scientific journal ***Fusion Engineering and Design*** (2).

Documents included:

Registration sheet
Authorization to disseminate copyrighted academic works
Abstract
Final thesis report
Acknowledgements
Budget
Bibliography
Electronic version of all the documentation

Abstract

Several system codes have been developed since the eighties, with different objectives and appropriate architecture and level of development, aiming to explore possible operating condition ranges of a fusion power reactor.

In some "system codes" technology/engineering assumptions/models (e.g. thermodynamic efficiency of coolant cycle, neutron multiplication coefficient, Tritium Breeding Ratio, radial built) are treated as input data inserted by the user and integrated in a main module essentially describing "plasma physics" aspects. In a first stage, these values come from previous studies on equivalent reactor concepts. Subsequent and more complete analyses with detailed models allow to confirm/deny these values and modify, if needed, for a second run and most likely several run, up to convergence. Some other codes consist of different specific modules (calculation tools) each one treating a separate aspects (e.g. physics, engineering, costing...) and integrated together in a common multiphysics calculation platform. Appropriate modules consistently calculate needed values using simplified models or surrogate models that enable an acceleration of the convergence of these systems codes. A system code based on this approach, SYCOMORE, is under development at CEA. The characteristics of the plasma and of the various reactor subsystems are addressed by various codes/models which are linked together via an integrated tokamak modelling platform. This platform allows creating a system design workflow by chaining the execution of the various modules.

In this framework, this document describes a methodology developed to build the neutronic module of SYCOMORE: a surrogate model, based on neural network giving main neutronic parameters characterizing a fusion reactor (tokamak): tritium breeding ration (TBR), multiplication factor, and nuclear heating as a function of the reactor main geometrical parameters (major radius, elongation…), of the radial built, Li enrichment, blanket and shield thickness, etc. (3)

In order to obtain a reliable surrogate model, a consistent database is needed. Simplified 1D and 2D neutronic calculation carried out with APOLLO2 (deterministic) and and TRIPOLI-4 (Montecarlo) codes codes are therefore used to fill the database. The URANIE platform is used to build the surrogate model from neutronic results. The simplified 1D and 2D models are validated against more detailed 3D Monte-Carlo model conducted with TRIPOLI-4. This methodology is devoted to helium cooled lithium lead (HCLL) blanket, but it could be applied to any breeder blanket concept provided that appropriate validation could be carried out.

Table of Contents

(Volume I)

Registration Sheet

Abstract

Glossary of signs, symbols, abbreviations, acronyms and terms 7

Preface 9

i. Context 9

ii. Organizations overview 9

iii. Thesis topic in the context 11

iv. Host organization 13

v. Brief introduction to fusion reactors 13

vi. Presentation of the HCLL DEMO thermonuclear reactor 14

1. Introduction 17

2. Methodology 19

2.1. Approach 19

2.1.1. Selection of a physical model for the proposed problem 19

Ideal response function 19

2.1.2. Creation of a plan of experience 20

Physical Model 20

2.1.3. Sensitivity analysis and creation of a response function 22

2.2. Presentation of the codes and tools 26

2.2.1. Apollo2 27

2.2.2. Tripoli4 27

2.2.3. Uranie 28

3. Creation of a parameterized physical model describing the neutronic behaviors of a thermonuclear fusion reactor 31

3.1. Parameterization of the Apollo2 model 32

3.2. Geometry definition of the Apollo2 model 32
3.2.1. 1-Dimension Cylindrical Geometry 32
3.2.2. R-Z Square-Based Geometry 33
3.3. Materials' compositions and definitions 35
3.4. Source definition 36
3.4.1. Energy spectrum 37
3.4.2. Spatial Spectrum 41
3.5. Energy corrections and gamma transport 41
3.6. Scores and result post-treatment 41
3.6.1. 1D Model 42
3.6.2. RZ Model 43
4. Validation of the Apollo2 model 45
4.1. Comparison between different Apollo2 energy grids 45
4.1.1. 1D Apollo2 model 45
4.2. Development of a Monte-Carlo model using Tripoli4 48
4.2.1. 3D Geometry Tripoli4 48
4.2.2. 1D Geometry Tripoli4 51
4.2.3. Neutron and Neutron-Photon simulations 52
4.3. Validation of the Apollo2 model with Tripoli4 55
4.3.1. RZ geometry model 55
4.3.2. 1D geometry model 56
4.3.2.1 1D Tripoli4 model validation 56
4.3.2.2 1D Apollo2 model peak fast neutron flux 58
4.3.2.3 1D Apollo2 model deposited energy 62
4.4. Selection of the final physical models: correcting factors 64
5. Coupling the physical model with URANIE 65
5.1. Plan of experience RZ geometry Apollo2 model 65

5.1.1. Creation 65
5.1.2. Evaluation 65
5.2. Plan of experience 1D geometry Apollo2 model 67
5.2.1. Creation 67
5.2.2. Evaluation 67
5.3. Plan of experience 1D geometry Tripoli4 model 71
5.3.1. Creation 71
5.3.2. Evaluation 71
5.4. Conclusions on plans of experience 72
6. Creation of neural networks using URANIE 73
6.1. Neural networks 73
6.1.1. Creation of neural networks 73
6.1.2. Evaluation of neural networks 74
6.1.3. Automatization of the creation and evaluation of neural networks 77
6.2. Neural networks and correcting factors 77
7. Creation of the surrogate model 81
7.1. Coupling python and C++ 81
7.2. The Neutronic Module 82
8. Environmental impact 87
Conclusions 89
Budget 91
Acknowledgments 93
Bibliography 95
Electronic version 99

(Volume II)

A. Appendix : Parameters, geometries and definitions 107
A.1. Input geometry parameters 107

A.2. Input materials' composition parameters 109
A.3. Other input parameters 111
A.4. Output variables 111
A.5. TBR and M_E definitions 113
A.6. 1-Dimension Cylindrical Geometry 115
A.7. RZ Square-Based Geometry 117
B. Apendix : Results 119
B.1. Apollo2 Peak Radial Flux Results 119
B.2. Apollo2 Energy Deposition Results 120
B.3. RZ Apollo2 performances 121
B.4. 1D Tripoli4 performances 122
B.5. 1D Apollo2 peak neutron flux performances 125
B.6. 1D Apollo2 deposited energy performances 128
B.7. Example of neural network 129
B.8. Neural network performances example 132
B.9. Chosen neural network performances 138
C. Apendix : Programs and Codes 149
C.1. Neutronic Module 149

Glossary of signs, symbols, abbreviations, acronyms and terms

BP: Back Plate

BZ: Breeding Zone

CEA: Comissariat à l'Energie Atomique et aux Energies Alternatives

cm: centimeters

DANS: Direction déléguée aux Activités Nucléaires de Saclay

DE: Deposited energy

DEMO: DEMonstration thermonuclear fusion reactor

DEN: Direction de l'Energie Nucléaire

DM2S: Département de modélisation des systèmes et structures

EFDA: European Fusion Development Agreement

EURATOM: European Atomic Energy Community

F4E: Fusion for Energy (European Domestic Agency for Fusion Energy)

FW: First Wall

GEDEMO: Groupe d'Etudes du réacteur à fusion de DEMOnstration

HCLL: Helium Cooled Lithium Lead

HCPB: Helium Cooled Pebble Bed

Ib: Inboard

IRFM: Institut de recherche sur la fusion par confinement magnétique

ITER: International Thermonuclear Experimental Reactor

JET: Joint European Torus

LHS: Latin Hypercube Sampling

LPEC: Laboratoire de Protection, d'Études et de Conception

m: meters

MAN: Manifold

MC: Monte Carlo simulation method

ME: Multiplication factor

MeV: Mega electronvolts

MW: Mega Watts

NN: Neural Network

Ob: Ouboard

s: seconds

SERMA: Service d'Etudes des Réacteurs et de Mathématiques Apliquées

SH: Shield

TBR: Trithium Breeding Ratio

TFC: Toroidal Field Coils

TFSWP: Toroidal Field Structure in front of the Winding Package

TOL: Tolerance

VV: Vacuum Vessel

W: Watts

Preface

i. Context

The world's increasing energy demand has pushed the international community to look for new energy sources. Among the existing options the thermonuclear fusion energy represents an area of active research, mostly due to its environmental-friendly and safe nature. Many institutions worldwide are working on developing the technologies necessary for the establishment of an industrial fusion reactor.

There are currently several international projects of thermonuclear fusion reactors among them: ITER (International Thermonuclear Experimental Reactor) and DEMO (DEMOnstration Power Plant).

> *ITER is a large-scale scientific experiment intended to prove the viability of fusion as an energy source, and to collect the data necessary for the design and subsequent operation of the first electricity-producing fusion power plant. Launched as an idea for international collaboration in 1985, the ITER Agreement includes China, the European Union, India, Japan, Korea, Russia and the United States. […] ITER will be built adjacent to the CEA Cadarache research center […]. This site in Southern France was chosen for the ITER project in June 2005 by the seven ITER Members.* (4)
>
> *Beyond ITER, it is envisaged that demonstration fusion reactor could be constructed that can produce electrical power and be commercialized. […] While the final design of DEMO will depend to a large extent on the results obtained from the exploitation of ITER and other fusion experiments, it is envisaged that a program of research and development activities in preparation for DEMO will be coordinated by F4E to perform studies, validate technologies, develop prototypes, etc.* (5)

ii. Organizations overview

The seven Members of the international ITER project have all created Domestic Agencies to act as the liaison between national governments and the ITER Organization. In the case of the European Union, the European Domestic Agency serves as the link between the European Commission and the ITER Organization. The Domestic Agencies' role is to handle the procurement of each Member's in-kind contributions to ITER. The Domestic Agencies employ

their own staff and have their own budget, and place contracts with suppliers. They are responsible for organizing and carrying out the procurement for each ITER Member. (6)

The European Domestic Agency is Fusion for Energy (F4E). *F4E is the European Union's Joint Undertaking for ITER and the Development of Fusion Energy. The organization was created under the EURATOM Treaty by a decision of the Council of the European Union in order to meet three objectives:*

- *F4E is responsible for providing Europe's contribution to ITER […]*
- *F4E also supports fusion research and development initiatives through the Broader Approach Agreement signed with Japan – a fusion energy partnership which will last for 10 years*
- *Ultimately, F4E will contribute towards the construction of demonstration fusion reactors*

F4E is established for a period of 35 year from 19 April 2007 and is located in Barcelona. (5)

> *The EURATOM Treaty establishing the European Atomic Energy Community (EURATOM) was initially created to coordinate the Member States' research programs for the peaceful use of nuclear energy. The EURATOM Treaty today helps to pool knowledge, infrastructure, and funding of nuclear energy. It ensures the security of atomic energy supply within the framework of a centralized monitoring system.* (3)

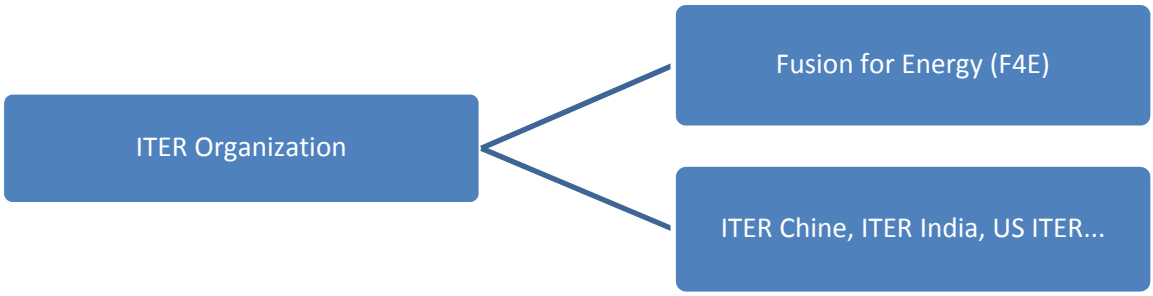

Figure 0-1 : Organizations overview

Among the international institutions working on fusion reactors, the CEA is one of the major players. CEA's responsibilities include, within the European Commission, the design of the HCLL breeding blanket (Helium Cooled Lithium Lead) (see vi) and its mock test for ITER, the TBM (Test Blanket Module). In addition to working on projects for Tore Supra(7), ITER and JET, one of the objectives of the CEA is the creation of a system code that takes into account all the physics involved in a thermonuclear fusion reactor in order to simplify the design process.

In parallel of F4E, there is also the European Fusion Development Agreement (EFDA) which coordinates research about fusion within the European Union. *This is an agreement between European fusion research institutions and the European Commission to strengthen their coordination and collaboration, and participate in collective activities. EFDA activities include coordination of fusion physics and technology research in EU laboratories, the exploitation of the world's largest fusion experiment, the Joint European Torus (JET) in the UK, training and career development in fusion and EU contributions to international collaborations. [4]*

iii. Thesis topic in the context

In the report *Decision of the governing board adopting the project plan (Edition 2010) of the European Joint Undertaking for ITER and the development of fusion energy*, we can read:

> *"DEMO Design*
>
> *The activity has two phases:*
>
> - *Phase One: Analyze common elements for DEMO (2007-2010)*
> - *Phase Two: Develop Potential DEMO Designs (2011-mid 2017)*
>
> *Phase One activities have so far been conducted by a number of workshops/meetings. At the end of Phase One, a major review took place to recommend specific goals for Phase Two, and a small group of experts outlined a proposal for Phase Two joint activities. Proposed Terms of Reference for DEMO Design Activities (DDA) are to be presented at the BASC in December 2010. The joint work would be organized as follows:*
>
> - *Phase Two-A, Jan 2011-Dec 2012: Consolidation of knowledge, to define a sound common basis for DEMO design, definition of priorities for R&D tasks*
>   - ✓ *Definition of design criteria and cost models*
>   - ✓ *Analysis of key design issues and options and launch preliminary work*
>   - ✓ ***Preparation and start implementation of system design code***
> - *Phase Two-B, Jan 2013-Dec 2014: Detailed studies*

- ✓ *Follow-up work on key design issues and options and narrow down design options on which concentrate further analysis work*
- ✓ *Adjustment of Design Criteria, Design Equations, and cost models*
- ✓ *Evaluation of sets of DEMO parameters as a function of uncertainties*
- ✓ *Preparation of intermediate documentation.*

- *Phase Two-C, Jan 2015-Jun2017: Development of pre-conceptual design options for DEMO*
  - ✓ *Develop integrated conceptual design/work final review and*
  - ✓ *Preparation of final documentation.*

It is expected that this design activity will also suggest specific R&D activities, some of which would be carried out on ITER, or on the Satellite Tokamaks (JT-60SA) and other facilities." [F4E10](5)

CEA participates to European reactor studies aiming to define a power plant as a whole system, therefore integrating various aspects intervening in its design (plasma physics, handling, heating and current drive systems, coils, breeding blankets ...). A CEA working group has been namely created: GEDEMO (Groupe d'Etudes du réacteur à fusion de DEMOnstration) in this frame. One of GEDEMO objectives is to build a system code for the pre-design of a fusion reactor, i.e. a computational tool that integrates in a coherent way various tools specialized on the dimensioning of various aspects of a reactor. In such a type of tool the rapidity of execution and flexibility play an important role. For this reason, models aim to estimate trends more than to finely describe concerned phenomena.

Some of the modules of this system code are already available (plasma physics, coils design…) while the neutronic module is missing. So far, in fact, the approach has been to perform neutronic calculations on the Tokamak designs provided by the plasma physics and coil design teams using Monte Carlo simulations that can take weeks. This approach does not lend itself to integration in a system code. It is therefore necessary to find a completely new approach to neutronic calculations in order to create a neutronic module that can be fitted in a system code.

In this frame the scope of this study was to develop a tool able to assess fair-enough calculations on the main neutronic parameters that are concerned in the design stage of a thermonuclear fusion reactor.

iv. Host organization

The CEA is the French Alternative Energies and Atomic Energy Commission (Commissariat à l'énergie atomique et aux énergies alternatives). It is a government-funded technological research organization established in 1945 by General de Gaulle. The CEA is active in four main areas: low-carbon energies, defense and security, information technologies and health technologies and is based in ten research centers in France.

This final thesis took place in a laboratory called *Laboratoire de Protection, d'Études et de Conception* (LPEC) in the CEA Saclay Center. Besides its historical activity on fission reactors simulation focused on the development and improvement of Gen III and Gen IV reactors, radioprotection, neutron fluence on the cuve and the study of RIA's (reactivity initiated accidents); part of the laboratory work is focused on the design of other experimental devices such as a Test Blanket Module for ITER, the design of radioactive waste transport casks as well as the design of experimental irradiation devices for the reactor Osiris… This laboratory is under the authority of a section called the SERMA (Service d'Etudes des Réacteurs et de Mathématiques Apliqées) which is also under the authority of a department called the DM2S (Département de modélisation des systèmes et structures). This department is under the direction of the DANS (Direction déléguée aux Activités Nucléaires de Saclay) which is also under the direction of the DEN (Direction de l'Energie Nucléaire).

v. Brief introduction to fusion reactors

The goal of a fusion reactor is to exploit the energy released by a fusion reaction to produce electricity. Among the possible reactions, the reaction considered here is that between deuterium and tritium (because it is the easiest to implement and control):

$$^{2}_{1}H + ^{3}_{1}H \rightarrow ^{4}_{2}He + n$$

This reaction is achieved in a deuterium-tritium plasma where high temperatures and high neutron fluxes are present. The plasma confinement is the most challenging part involved in a thermonuclear fusion reactor. The plasma physics studies the confinement of the plasma which is achieved using superconducting coils that will generate high fields (up to 5.3 T in ITER) up to ~10T in DEMO).

However, tritium is a rare isotope and industrially very expensive to manufacture, so the fusion reactors have a component called breeding blanket responsible for generating tritium in order to

maintain the fusion reaction. The breeding blanket is made out of a lithiated material that when subjected to a neutron flux from the plasma produces tritium according to the reactions:

$$^{6}_{3}Li + n \rightarrow {}^{3}_{1}H + {}^{4}_{2}He$$

$$^{7}_{3}Li + n \rightarrow {}^{3}_{1}H + {}^{4}_{2}He + n$$

The breeding blanket is also responsible for converting the energy of neutrons in heat operable to generate electricity, and, protecting the superconducting coils against damage due to irradiation by neutrons.

vi. Presentation of the HCLL DEMO thermonuclear reactor

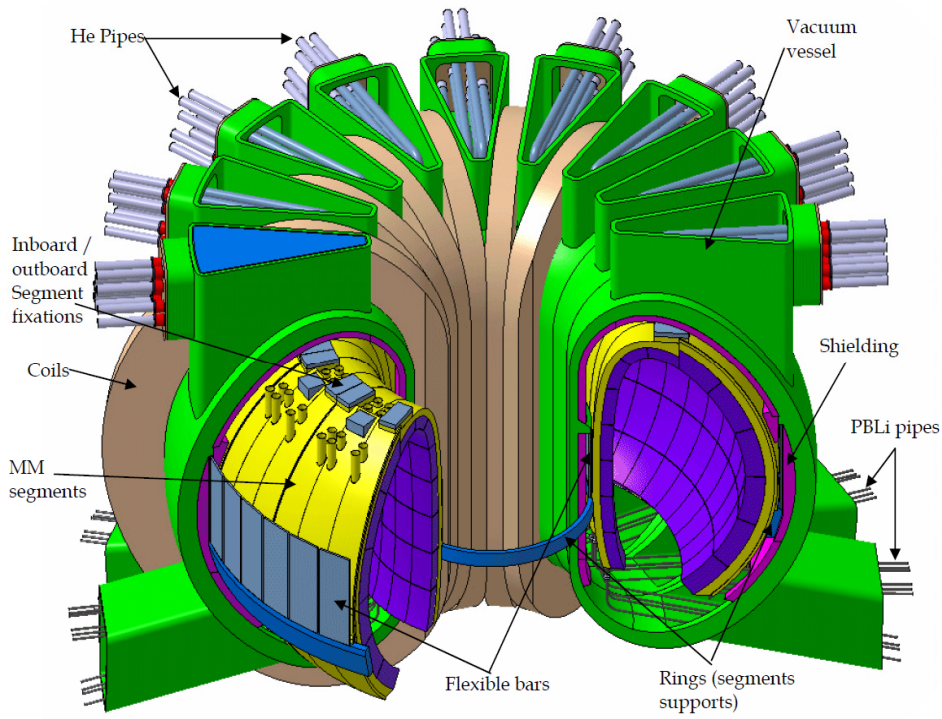

Figure 0-2 : CEA HCLL DEMO-2007 Reactor (8)

DEMO is based on the 'tokamak' concept of magnetic confinement, in which the plasma is contained in a torus-shaped vacuum vessel. The fuel - a mixture of Deuterium and Tritium - is heated to temperatures in excess of 150 million °C, forming hot plasma. Strong magnetic fields are used to keep the plasma away from the walls; these are produced by superconducting coils surrounding the vessel, and by an electrical current driven through the plasma.

One of tritium breeding blankets being studied in Europe as possible candidate for a fusion reactor is the HCLL blanket. This coverage uses lithium-lead (LiPb) as a generator and carrier of

tritium and neutron multiplier, helium as a coolant and a low-activation martensitic steel, Eurofer, as structural material.

Blanket modules (in purple) extract heat from thermal loads, provide shielding from the high-energy neutrons produced by the fusion reactions and achieve tritium self-sufficiency.

1. Introduction

The creation of a system code for the design-stage of a thermonuclear fusion reactor requires the creation of a neutronic module that performs calculations on the basic neutronic parameters and constraints. Within this context the utilization of neutronic models such as Monte Carlo or deterministic simulations is not foreseeable due to integration complexity and long computation times. It is therefore necessary to use a different method based on response functions that permits an easy integration and instant response.

The aim of the project is the creation of this parameterizable response function that given a certain Tokamak configuration, in terms of geometry, materials, and spatial disposition, is able to calculate some important and necessary parameters for the design stage of a Tokamak: the tritium breeding ratio (TBR), deposited energy and the fast neutron flux on the inboard magnet.

It should be pointed that the model developed here is only a pre-design tool and it should be used only in the design stage to prevent long design iterations involving different services, laboratories and teams. Therefore the program should not be used to make accurate and precise load but to get good-enough results that simplify the design stage of the different parts of the Tokamak.

The study has been performed in different stages that lead to the final response function that will be introduced in the system code. The steps involved in the creation of the response function are shown in Figure 1-1. After presenting the methodology and tools used during the project on chapter 2, creation and validation of physical models are done on chapters 3 and 4, plans of experience are detailed on chapter 5 and response functions are done on chapters 6 and 7. An environmental impact is also presented on chapter 8.

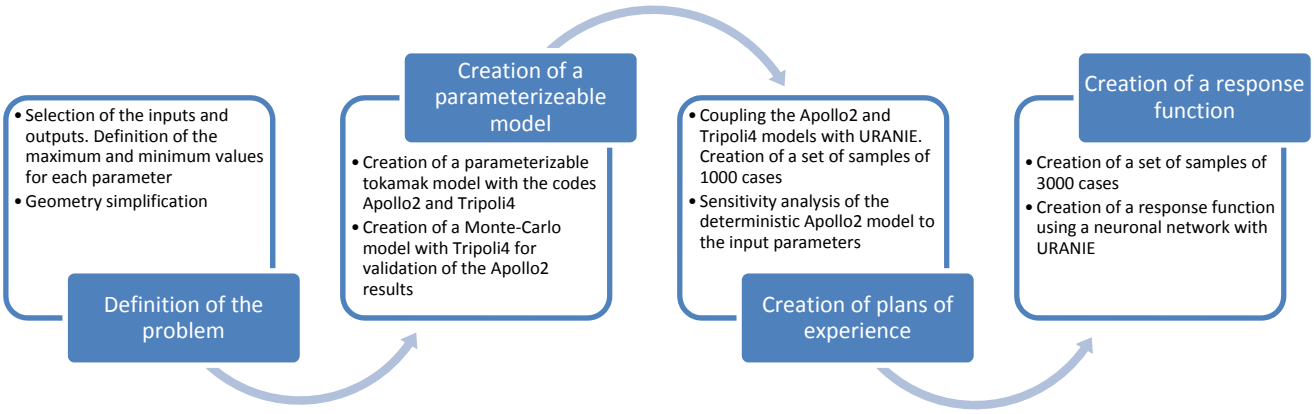

Figure 1-1 : Stages involved in the creation of a response function using a neuronal network

2. Methodology

In this section the methodology and steps followed to obtain a surrogate model will be presented. The approach will be first described referencing the programs and tools that have been used in our particular case to solve each of the steps, then a general description of the tools will be done.

2.1. Approach

The objective of the project being the creation of a neutronic module that can be easily integrated in a system code for the pre-design stage of a thermonuclear fusion reactor, a response function based on neural network has been created. Zooming out, this module needs to relate geometries, material compositions and plasma physics variables to key neutronic parameters. The ideal neural network should work as shown in Figure 2-1.

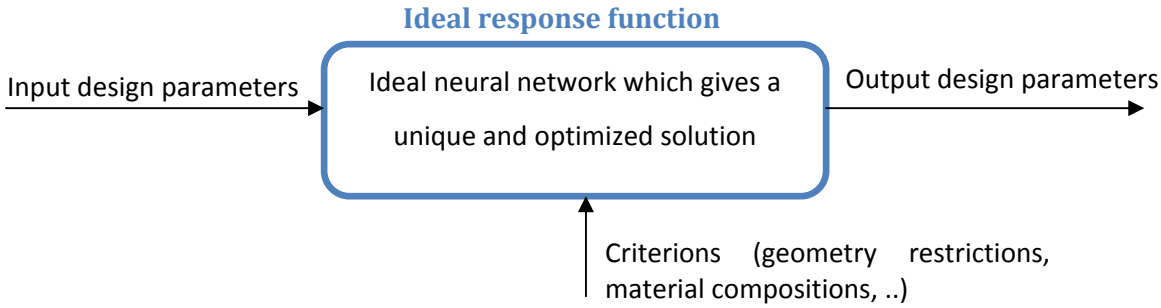

Figure 2-1 : Flowchart showing the ideal behavior of the response function

The process that allows us to obtain a response function consists on many different stages involving different programs, tools and competences. The steps followed in this study can be applied to almost any engineering problem with similar characteristics, the main restriction being the model that represents the physics of the problem.

2.1.1. Selection of a physical model for the proposed problem

In order to create a response function using neural networking it is imperative to possess a physical model that describes the studied model's physics. The calculation method used by the model, the physics behind it or the accuracy of the program are not relevant to the creation of a response function, the neural network will *copy* the results obtained by this physical model by creating a neural network that adapts itself to it. This physical model is then a black box that

gives us the answer to a given problem. The accuracy of the original program will be a characteristic of the created response function.

A representation of what this physical problem should do is done in Figure 2-2.

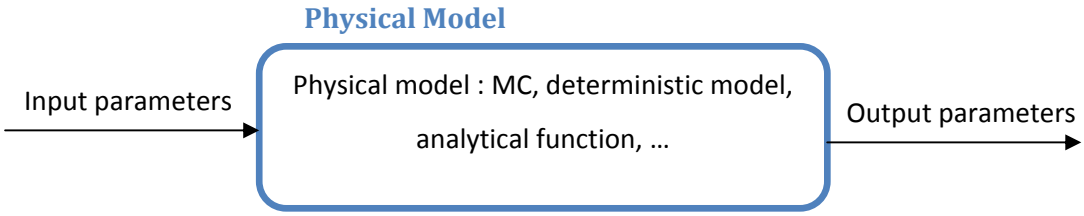

Figure 2-2 : Flowchart showing the behavior of the physical model that will be used

One could be skeptic about the necessity of a response function if a physical model represents the problem and gives us a more accurate result. Just as it is true that a physical model can be parameterized and is more accurate than a response function that adapts itself to a given model, the difficulty to integrate a physical model based on a complex scientific program in a system code and its long computation times makes it complicate and difficult to envisage this solution.

Nevertheless some conditions need to be fulfilled by the physical model: modifications have to be introduced to make it parameterizable, it needs to have reasonable calculation times in order to create a plan of experience of 1.000 to 10.000 cases and it needs to be based on a physical problem to be represented by a neural network.

In our case, previous studies (9) shown that an acceptable method to represent a Tokamak model given the imposed restrictions (parameterizability, calculation time, accuracy, …) is a deterministic model using a 1D or RZ geometries. This model will be created with the code Apollo2 (see section 2.2.1) and validated with the Monte-Carlo program Tripoli4 (see section 2.2.2). Another Monte Carlo Tripoli4 model will be also used to calculate the deposited energy on the tokamak's layers due to the restrictions imposed by the deterministic model. The creation of the physical models will be described in chapter 3.

2.1.2. Creation of a plan of experience

The next step after the creation and validation of the physical model is the creation of a plan of experience, or in other words, perform a large number of calculations varying the input parameters in order to study the impact on output parameters.

The first stage that will guide us to the creation of this set of samples is the definition of the operating window of each of the input parameters. The minimum and maximum values of each parameter need to be previously defined; in this case it has been done in collaboration with breeding blanket, plasma physics and coils experts to study a wide range of possible tokamak configurations. Discretization of the possible values in the space will be performed following the Uniform Law in order to cover the whole space between the variation limits. For example, the histogram for a given input variable that can oscillate between the limits $(-2,3)$ following a Uniform Law with 300 entries would look like the one shown in Figure 2-3. The main characteristic of this method is that each of the possible values of the variable has the same probability than the others, so we can evaluate the performance of our physical model within the whole space of phases.

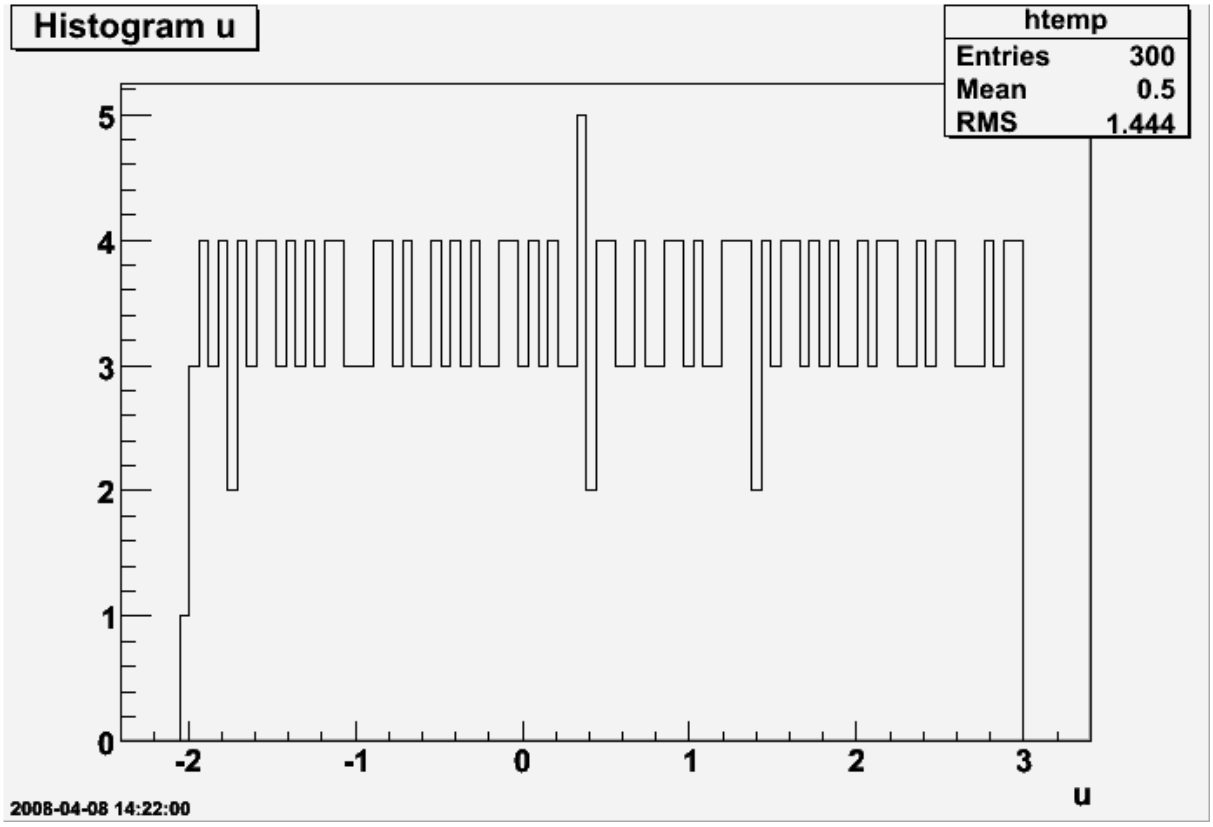

Figure 2-3 : LHS sampling with a size of 300 entries following a Uniform Law

It can be interesting to use other distribution laws such as the Normal Law in order to study the performance of the physical model in a given region of the space that has a greater probability than another. Our goal being the creation of a set of samples that covers the whole operating zone, the Uniform Law has been used.

Normally the physics involved in an engineering problem is complicated and depends on more than one parameter. This being the case in our problem, the strategy will be to create a set of

samples that covers the full space of phases following a Latin Hypercube Sampling (LHS) (10) technique that consists on applying a Uniform Law for each of the variables. For example in Figure 2-4, the two variables x and y are uniformly distributed in the space and cover the full space of possible solutions following a LHS distribution. The same approach needs to be followed but in a space of n dimensions, n being the number of input parameters.

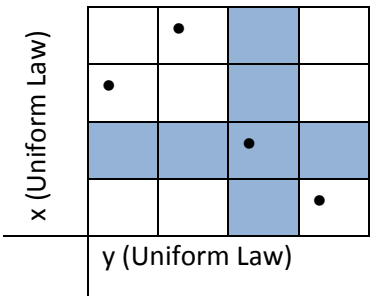

Figure 2-4 : Example of application of LHS application with two variables x and y following a Uniform Law

This large plan of experience of input parameters will be tested in the parameterized physical model and the results of each case will be collected and stored in the same database. The result is the creation of a set of samples, a large database where input and output variables are stored in columns and samples are stored in rows.

It is difficult to determine the number of cases needed to obtain a reliable plan of experience. It depends on the complexity of the physics, the variation limits and the reliability of the physical model. In our case we will be working with samples of 1.000 to 10.000 cases. Various tests have been performed and showed that these constitute indeed a good compromise between achieved accuracy and computation time.

In order to create this plan of experience we have used a tool called Uranie (see 2.2.3). This program allows to automatically create the set of samples, launch the physical model to perform the calculations, recuperate the values of the output parameters and store all these values in a database object called TData Server, an object that will be directly used to create the surrogate model.

2.1.3. Sensitivity analysis and creation of a response function

Once the plan of experience is created we have all necessary elements to create a surrogate model based on a neural network. Prior to that, and even if it is not imperative, it is useful to study the sensitivity of the output variables to the input parameters, or the variation of a certain output variable given a change in an input parameter. This will allow identifying those

parameters whose impact on output variables is negligible (at least in the considered operating window).

This sensitivity analysis can be done using different methods; in our case we will use a "Brute Force" method, in which a base case simulation is performed, and then the simulation is repeated using a change in some model input(11). The impact of each input parameter on each variable can be plotted as shown, e.g., in Figure 2-5. This kind of figure allows studying the physics behind the problem and verify expected trends; in this case, as expected, a reduction of the neutron flux in the external layers of the tokamak is observed when the thickness of a middle layer, the shield, is incremented. In order to compare the impact on the response of input parameter we will use the sensitivity indexes of each of the variables. Sensitivity indexes are compared to understand the implication of each variable on the result (Figure 2-6). In this case the analysis allows affirming that the thickness of the shield, the thickness of the vacuum vessel and the compositions of both the first wall and the breeding zone have a great impact on the estimation of the neutron flux on the toroidal field coils.

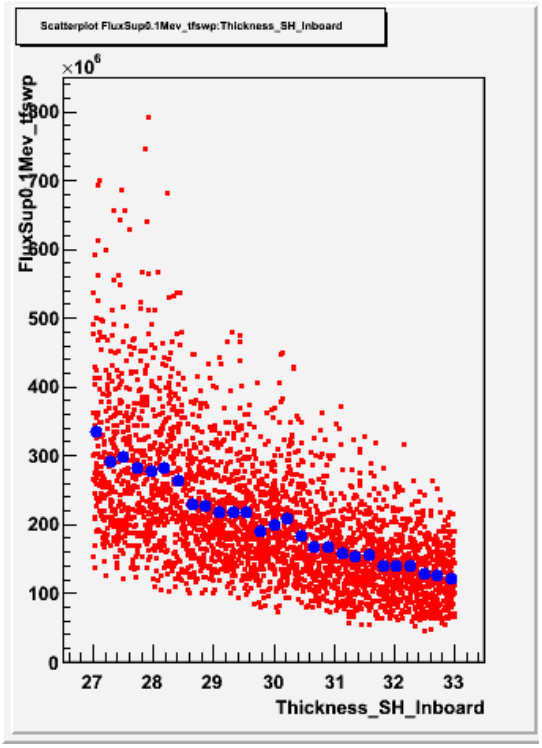

Figure 2-5 : Variation of the peak neutron flux as a function of the inboard shield thickness

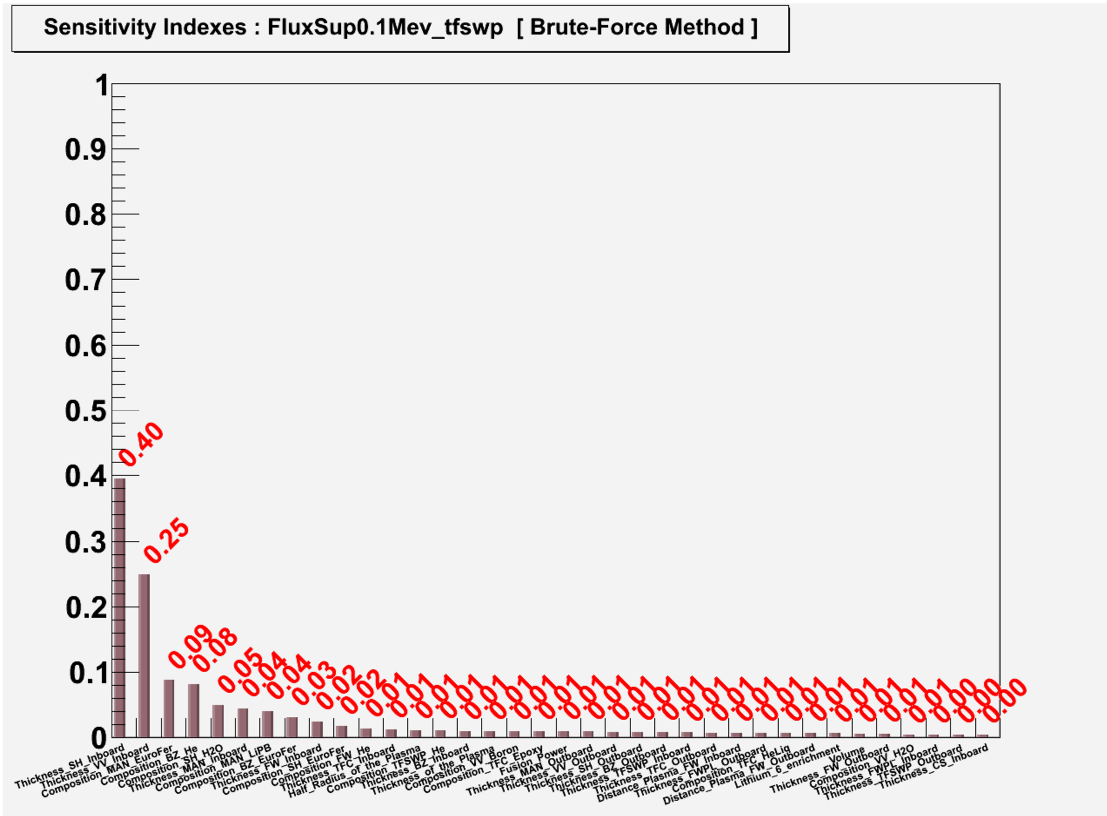

Figure 2-6 : Sensitivity indexes of input parameters on the neutron flux

After creating both neural networks with a reduced number of variables and with the whole set of variables, we decided to keep all the original input parameters in the creation of our neural network because the performance of the neural network is almost the same keeping all the variables in our final response function. This will avoid neglecting some of parameters which are "negligible" in the set of operating windows here considered, which could become relevant if operating windows were different.

The last stage of the approach is the creation of a response function based on a neural network. At this point it is imperative to use a program that allows us to create neural networks that are able to automatically *learn* and are capable of creating a response function for a given set of inputs and outputs. In our case we use the library Modeler of Uranie.

The plan of experience defined in 2.1.2 is recuperated and introduced into Uranie, where the neural network is created. The theory behind the neural network creation is behind the scope of this report and will not be repeated here, a short explanation can be found in chapter 6; one of main points to retain is that some hidden layers are introduced between the output variable and the input parameters, each layer having a defined number of neurons or points that try to define the physics that relate the inputs and outputs. It is necessary to try to prevent the overlearning

of the neural network, a common phenomenon that adapts the neural network to the given set of samples but does not learn the physics behind the problem. In order to avoid this situation, dozens of neural network need to be created, named trials, evaluating its performance against the original set of samples and another set of samples called “test”. This “test” set of samples is introduced in the neural network and estimations are benchmarked with the original results obtained with the physical model. Overlearning is avoided thanks to this methodology.

The result obtained with Uranie, and most of the programs used to create neural networks, is a program, such a C++ function, that can run in any computer. This program can easily be integrated in the reactor system code. It is important to note that one neural network will be identified for each variable, so we need to create as neural networks as output variables in the problem.

To evaluate the performance of the neural network some indicators have been selected, which give the “quality” of results obtained by the neural network with regard to those obtained by the original physical model. Those parameters are:

- Standard deviation between the physical model and the neural network
- Standard normalized deviation between the physical model and the neural network
- Average deviation between the physical model and the neural network
- Absolute average deviation between the physical model and the neural network
- Maximum deviation between the physical model and the neural network
- Maximum normalized deviation between the physical model and the neural network

Taking into account all these parameters, we need to select the best neural network. A graphic method can also be used which consist in plotting the results obtained with the neural network against the original physical problem. If the neural network represents accurately the physics of the problem the result would be a perfect line as shown in Figure 2-7.

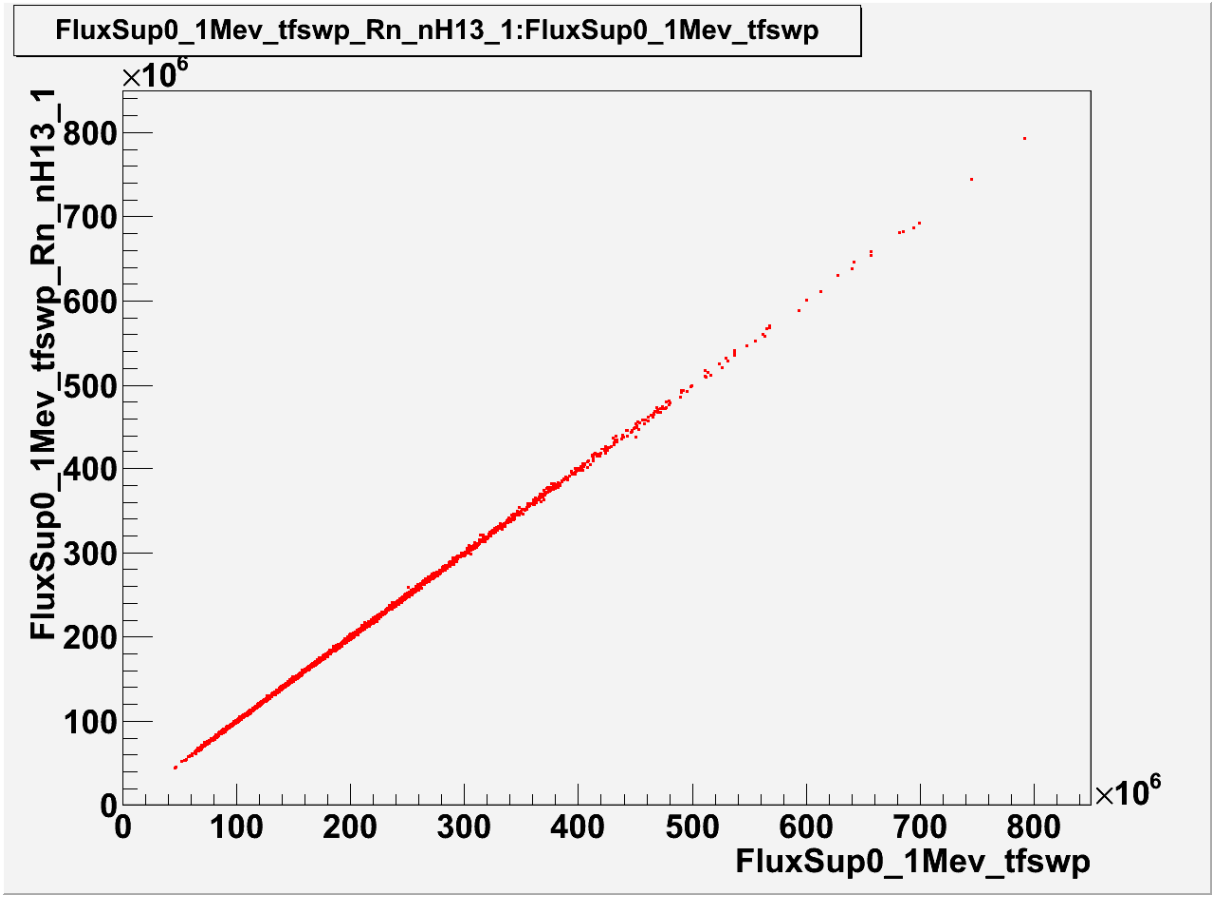

Figure 2-7 : Plot of the radial neutron flux obtained with the neural network against the radial neutronic flux obtained with the physical model

After following steps presented before, the result is a set of functions represented by C++ programs that given a certain configuration of our initial engineering problem give the output parameters defined in the first stage. These programs run fast and in any up-to-date computer, and are easy to integrate in any system code. The performance of the response function depends on the neural network (standard deviation, average deviation, …) and the performance of the original physical model used to build the neural network.

2.2. Presentation of the codes and tools

Different codes and tools were used during the project to attain the expected results. These programs are developed by the CEA DM2S teams, thus permit us to be in direct touch with the developers and allows us to have access to all the documentation and previous works performed with these codes. A brief presentation of the codes is done in this section but each of the programs will be further presented during the report as they are used to resolve our particular problem.

2.2.1. Apollo2

In a certain physical medium, the angular neutron flux $\psi(\vec{r}, E, \vec{\Omega})$ of energy E located at a given position $\vec{r}$ and directed along the angle $\vec{\Omega}$ obeys the Boltzmann equation:

$$\vec{\Omega}\vec{\nabla}\psi(\vec{r}, E, \vec{\Omega}) + \Sigma_t(\vec{r}, E)\psi(\vec{r}, E, \vec{\Omega}) = S(\vec{r}, E, \vec{\Omega}) + \int_{4\pi} d\vec{\Omega}' \int_0^{\infty} dE' \Sigma_s(\vec{r}, E' \to E, \vec{\Omega}' \to \vec{\Omega})\psi(\vec{r}, E, \vec{\Omega})$$

where $\Sigma_t(\vec{r}, E)$ is the macroscopic cross section of reactions on $\vec{r}$ involving neutrons of energy E, $S(\vec{r}, E, \vec{\Omega})$ is the source term, and $\Sigma_s(\vec{r}, E' \to E, \vec{\Omega}' \to \vec{\Omega})$ is the macroscopic cross section of reactions on $\vec{r}$ which produce neutrons of energy E directed along $\vec{\Omega}$ from neutrons of energy E' and directed along $\vec{\Omega}'$.

APOLLO-2 (12) solves the Boltzmann equation numerically, using discretization in space, energy and solid angle. We will come back on this last particular discretization which involves cutting the energy continuum in a number of groups and define the average cross sections for each reaction. The values of these average cross sections are grouped in libraries.

APOLLO-2 calculations reported hereafter were performed using the SN discrete ordinates solver, with an angular order S8 and an anisotropy order P3.

2.2.2. Tripoli4

Tripoli-4 (13) code is a three-dimensional, continuous energy computer code for particle transport based on the Monte-Carlo method. The code currently treats neutrons, photons, electrons, and positrons. Few physical simplifications are done as it uses the statistical-based Monte-Carlo method.

Monte Carlo (14) can be used to duplicate theoretically a statistical process (such as the interaction of nuclear particles with materials) and is particularly useful for complex problems that cannot be modeled by computer codes that use deterministic methods. The individual probabilistic events that comprise a process are simulated sequentially. The probability distributions governing these events are statistically sampled to describe the total phenomenon. In general, the simulation is performed on a digital computer because the number of trials necessary to adequately describe the phenomenon is usually quite large. The statistical sampling process is based on the selection of random numbers—analogous to throwing dice in a gambling casino—hence the name “Monte Carlo.” In particle transport, the Monte Carlo technique is pre-

eminently realistic (a numerical experiment). It consists of actually following each of many particles from a source throughout its life to its death in some terminal category (absorption, escape, etc.). Probability distributions are randomly sampled using transport data to determine the outcome at each step of its life.

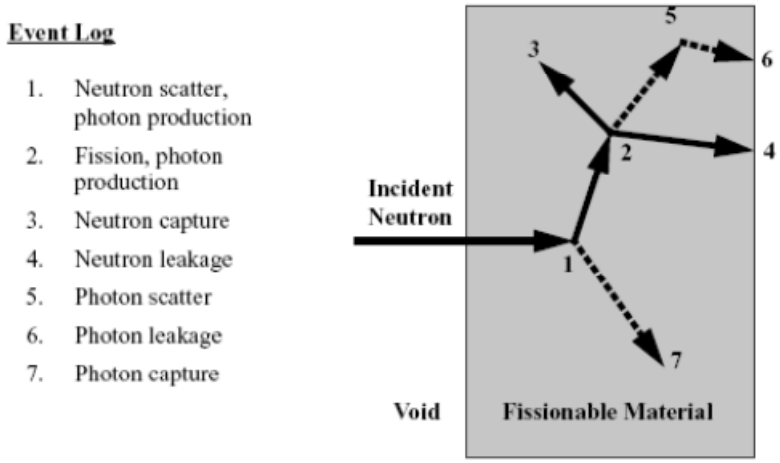

Figure 2-8 : Random history of a neutron incident on a slab of material that can undergo fission

Once the particle history (i.e. Figure 2-8) is complete Monte Carlo methode records some aspects (tallies) of its average behavior. As more and more such histories are followed, the neutron and photon distributions become better known. The quantities of interest (whatever the user requests) are tallied, along with estimates of the statistical precision (uncertainty) of the results.

2.2.3. Uranie

Uranie (15) is the uncertainty platform of the CEA/DEN. It allows for studies of propagation of uncertainty, sensitivity analysis and calibration of computer code in an integrated environment. It is based on the framework Root (Version v5.18) developed by CERN for particle physics (analysis of data generated by the LHC ("Large Hadron Collider “)) whose website is root.cern.ch. Thus, Uranie has many features offered by Root, and in particular:

- A C++ interpreter;
- Access to the database like SQL;
- Advanced data visualization;

It consists of a set of libraries, called libraries *“métiers*” (Figure 2-9), each addressing a specific task to take into account the uncertainties or the calibration of computer code.

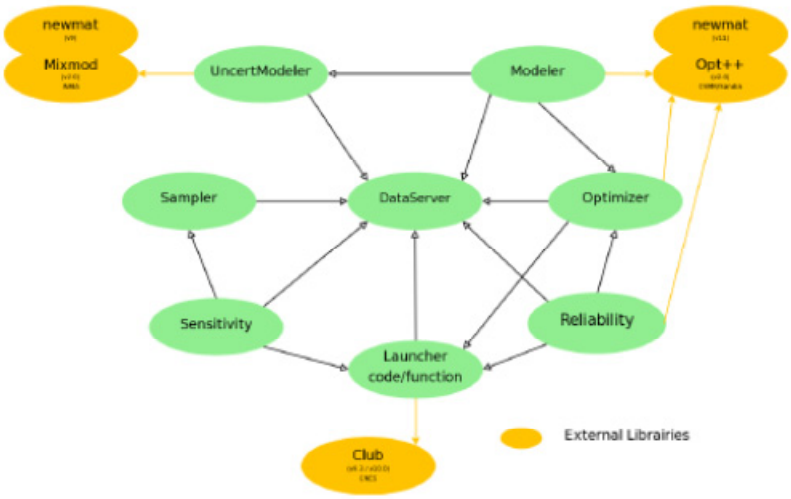

Figure 2-9 : Functional diagram of the libraries *métiers*

The central library is the library DataServer and contains the central object of Uranie: the TDATA-Server. This object contains all information required to describe variables (i.e. name, units, laws of probability index in which it is located, etc.) of a problem and it is this object that will "navigate" through the other libraries "*métiers*".

The library Sampler is used to create a set of samples with the attributes of the TDataServer that are random variables. The aim of the library Launcher is to evaluate a computer code or an analytic function for all the elements of a TDataServer. These elements can come either from a set of samples or an external database (ASCII file, SQL, etc.). The construction of a response surface ("surrogate model") between the "variables of interest y" and the "predictors x" is provided by the library Modeler which are polynomial models, neural networks, etc.

For the Launcher module, Uranie is based on the library Club (version v9.3) developed by CNES regarding the substitution of parameters in files.

3. Creation of a parameterized physical model describing the neutronic behaviors of a thermonuclear fusion reactor

As mentioned in previous section (2.1.1) it is necessary to develop a physical model that will be used to create a response function. In our case, one (or more if needed) physical model representing a thermonuclear fusion reactor will be created and validated. This(ese) model(s) needs to be completely parameterized, so that the values of the key input parameters can be easily changed.

Four neutronic parameters need to be estimated:

- TBR (see appendix A.5) : The number of tritium isotopes created for each fusion reaction that takes place in the plasma
- M_E (power multiplication factor) (see appendix A.5): total deposited energy on the tokamak for each neutron created of 14,07 MeV.
- DE (Deposited energy): deposited energy on each of the tokamak layers. In this case the peak deposited energy is calculated: 1D models overestimate the energy deposition (see 4.3.2).
- Fast neutron flux radial profile (Neutron Flux). In this case the peak neutron flux is calculated: 1D models overestimate the neutron flux (see 4.3.2).

The complexity of the tokamak's geometry, represented on Figure 0-2, forces us to develop a simplified model. The simplification that has been used is based on previous studies that show that local parameters, such as peak fluxes or deposited energy, can be represented with an infinite cylindrical geometry while integral parameters, such as the tritium breeding ratio, need to be represented with a more complex two-dimension geometry that takes into account the surfaces and volumes of the original tokamak(9). Keeping this in mind, two models have been built: one model based on concentric one-dimension infinite cylinders and a second model based on a R-Z with closed volumes that conserve the original surfaces of the tokamak. Both models will be used afterwards for the creation of the neural networks.

Apollo2, a deterministic code, has been used for neutronic analysis chosen for the rapidity of execution. Apollo2 was developed for fission reactors, nonetheless its suitability for fusion has been proven provided that some necessary corrections to the energy deposition. Tripoli4 is also used both for the validation and creation of plans of experience, see section 4.3.

3.1. Parameterization of the Apollo2 model

The first condition imposed for the creation of the physical model is the parameterization of this model for all the input parameters. In order to do so, chosen input parameters need to be declared in a certain way so that they can easily be changed, both by the user and Uranie. The declaration is done as shown in Code 3-1. It is also important to give the output results in a certain way so that Uranie can read them, an example of this special writing is given in Code 3-2.

```
dr_fw_ib = VALUE
```

Code 3-1 : Declaration of the input parameters on the Apollo2 code

```
Flux_TFSWP_ib = VALUE
```

Code 3-2 : Writing the output variables by the Apollo2 code

3.2. Geometry definition of the Apollo2 model

As mentioned before, two geometries will be used to represent the original tokamak. They will be based on geometrical parameters described in (16). Obtained results will be therefore directly compared with those presented in the report in terms of peak neutron flux and TBR.

Before the creation of the models it is imperative to define all the input parameters and the operating windows. The results of this study are shown in appendix A.1, where each parameter is defined and named.

3.2.1. 1-Dimension Cylindrical Geometry

This model will be used to calculate the peak neutron flux in the different layers or materials of the Tokamak. The neutron flux in the winding package of the inboard coils is one of the key parameters in the design of a thermonuclear fusion reactor and the optimization of this parameter will drive the performance studies.

A first Apollo2 model was developed using the geometry shown in Figure 3-1. In the model, the different components from the first wall to the coils are represented as homogeneous layers. Thicknesses of layers as well as their material composition are variable parameters.

The one dimension model represents a cylindrical geometry, with a height of 1 centimeter. The flux is calculated both volume integrated and per unit of volume.

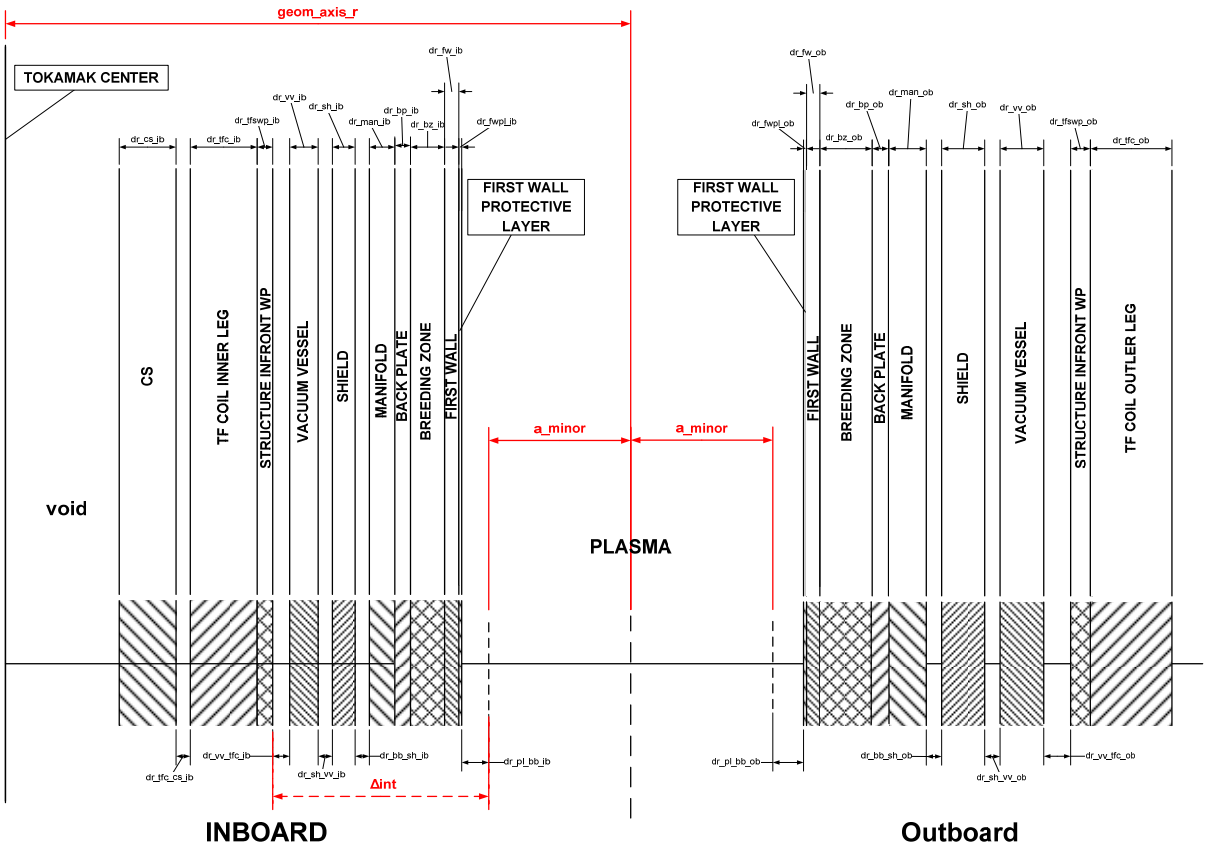

Figure 3-1 : Geometry represented in the Apollo2 cylindrical model

All layers of the tokamak radial build are identified in this model, including the gaps between layers and the gap between the plasma and the first wall protective layer.

It is also important to note that all output parameters will be scaled in order to obtain the relevant values. The calculated flux, namely, will be normalized to the fusion power, which is also an input variable, and the energy deposition will be converted to $\frac{MW}{m^3}$ from the original $\frac{MeV}{cm^3}$ calculated by Apollo2.

3.2.2. R-Z Square-Based Geometry

The second model is used for the calculation of integral parameters such as the TBR or the energy multiplication factor. It represents a vertical section of the tokamak from his axis to the toroidal field coils outer leg.

Apollo2 presents some restrictions on the creation of complex geometries, keeping this in mind, the geometry used is an R-Z model based on squares that are rotated according to the central axis of the tokamak. The geometry described before is represented on Figure 3-2. Previous studies have shown that the most suitable method to guarantee the equivalence between this

"squared" geometry ant the real ones is to keep surfaces equivalences between the two geometries.

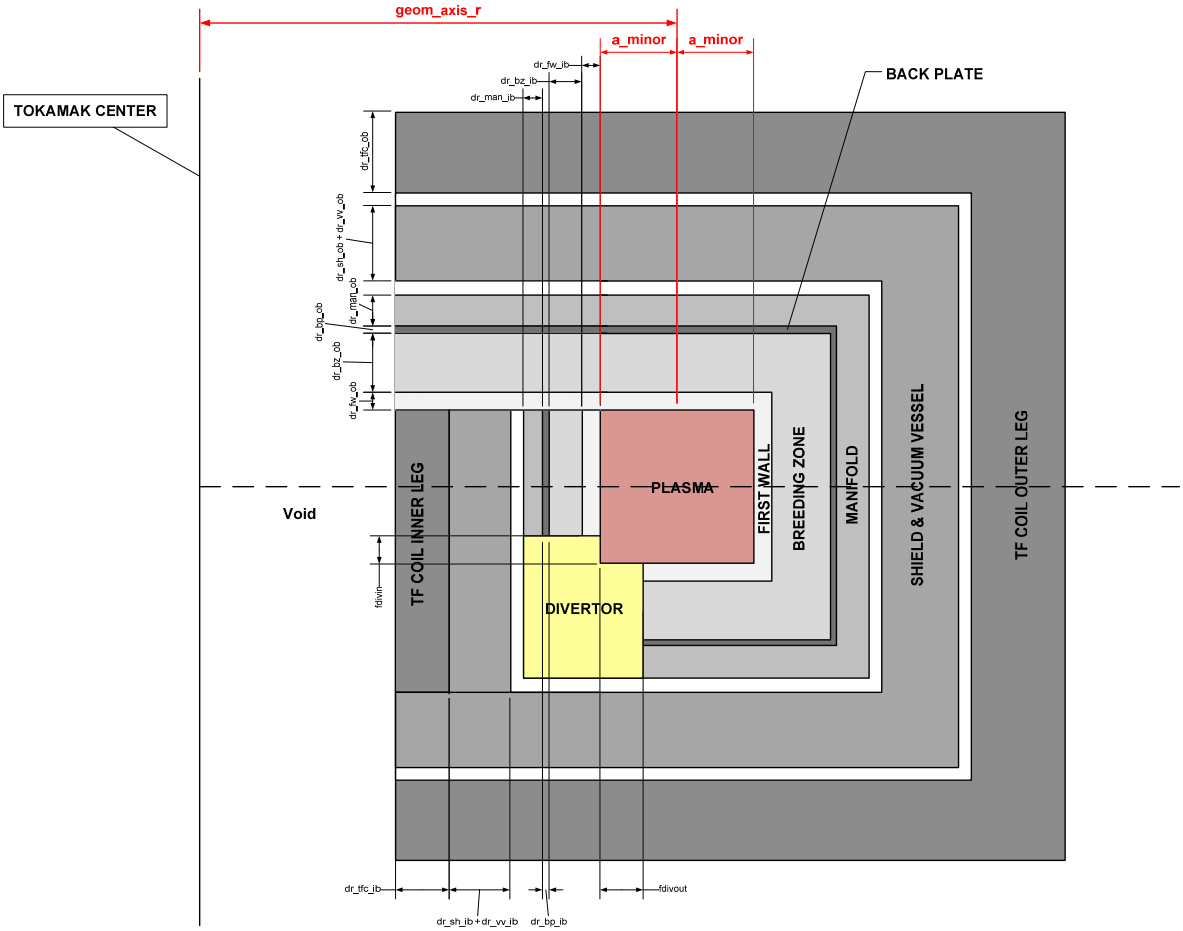

Figure 3-2 : Geometry of the tokamak used in the Apollo2 R-Z model

This geometry presents some big challenges, the greatest one being the transformation of the plasma chamber into a square and the positioning of the divertor regarding the plasma chamber. To solve this problem a program that calculates the width and the length of the square plasma chamber maintaining the original plasma chamber surface and the surface of the divertor that covers the plasma chamber in the inboard and outboard is created. This program takes into account the surface of the divertor in each side and the plasma parameters such as: triangularity (δ), elongation (El), major and minor radii (R0) and (a) of the original plasma chamber. These parameters are used to automatically create the model.

As observed in Figure 3-2 the model does not detail all tokamak's layers. The objective of this model is to calculate the TBR and the energy multiplication factor; therefore layers beyond the manifold can be simplified because there is no tritium generation in these external layers, even if

they need to be represented to maintain the neutron reflections. This will allow to considerably reduce the calculation time.

3.3. Materials' compositions and definitions

After the definition of the geometries it is necessary to identify the different materials. In this case material compositions have been parameterized so that the effect of the variation of the material's composition (due, e.g., to geometry variations) can be observed in the output variables. Both the 1D model and the RZ model will use the exact same compositions for each layer except for the shield and vacuum vessel in the RZ model, where a mixture of 50% of both compositions is used on the shield-vv layer.

The strategy followed to identify the materials was to create some basic compounds that afterwards will be combined to create the mixtures and alloys of each layer. In this case we used as reference the same compounds as in (16), in order to easily compare, as mentioned before, obtained results.

The basic compounds, Table 3-1, have been defined with great accuracy, using the chemical composition of each material, after having defined each chemical element according to its natural isotopic abundance.

Symbol	Definition
void	Void
eufer	Eurofer
lipb	Lithium-Plomb
ss316	Stainless steel 316
w	Tungsten
wc	Tungsten Carbide
h2o	Water
he	Helium
boron	Boron
cu	Copper
bronze	Bronze
nb3sn	Niobiun-tin
epoxy	Epoxy
heliq	Liquid Helium

Table 3-1 : Basic compounds used in the creation of the tokamak's materials

For each of mixtures and alloys the maximum and minimum values of the percentage in volume of each basic material have been defined, these being the input parameters. Reference values are summarized on Table 3-2, the detailed table of values and names can be found on appendix A.2.

Layer	Composition definition
First Wall Protective Layer	100% W
First Wall	70% Eurofer, 30%He
Breeding Zone	80% LiPb, 10% Eurofer, 10%He
Back Plate	67%He, 28% Eurofer, 5% LiPb
Manifold	67%He, 28% Eurofer, 5% LiPb
Shield	65% WC, 25% H2O, 10%Eurofer
Vacuum Vessel	61% SS316, 37% He, 2% Boron
Toroidal field structure in front of the winding package	95%Eurofer, 5% He
Toroidal field coil	43% SS316, 18% Epoxy, 17%LiqHe, 12% Cu, 7% Bronze, 3%Nb3Sn
Central Solenoid	43% SS316, 18% Epoxy, 17%LiqHe, 12% Cu, 7% Bronze, 3%Nb3Sn

Table 3-2 : Materials' compositions for each of Tokamak's layers

The composition for the central solenoid is not yet clear, but it has no repercussion on the calculations that will be performed as they are beyond the coils in the inboard side.

The percentage of minority compounds is explicitly defined, determining the percentage of the most common compound for each layer by substraction, i.e.: in the case of the breeding zone the percentage of both Eurofer and helium is defined and parameterizable while the percentage of lithium-lead is automatically calculated.

3.4. Source definition

One of the key aspects that affect the performance of the Apollo2 model is the definition of the source (17). Energy of neutrons created on a fusion reaction follows a Gaussian distribution centered on $14{,}07\ MeV$. Different energy grid will be used and tested in order to asses the impact on obtained results. Apollo2 does not allow to define a continuous-energy source,

instead a meshing of the neutron source needs to be performed. The source used will have a power of $1\frac{neutron}{second}$.

It is important to keep in mind that the objective is to find a compromise between the performance of the code and the calculation time. In regard of that, the objective will be to use lowest number of meshes to define the source keeping accurate results.

3.4.1. Energy spectrum

Based on the original Gaussian distribution of the neutron source we consider here four energy grids: ecco1968, RNR1200, RNR600 and RNR300. Those energy grids have 1968, 1200, 600 and 300 groups respectively. These meshes were originally defined for the study of fast neutron reactors (FNR) (18); the energy groups present fine discretizations from energies close to $14{,}07\ MeV$ to $0{,}1\ MeV$, which allows a better energy distribution and a better representation of physic phenomenas such as neutron slow down or threshold reaction. From those energy grids, the energy groups covering the energies under the Gaussian distribution for the fusion neutrons are chosen. The chosen groups are presented in Table 3-3.

Energy grid	Scope of the group (MeV)	Energy groups chosen
RNR300	12,944357 - 15,255644	4 to 5
RNR600	12,2957759 - 15,3880675	8 to 14
RNR1200	12,7037249 - 15,3880675	13 to 22
Ecco1968	12,5 - 15,30	32 to 50

Table 3-3 : Selected groups of each energy grid for source definition

When passing from an energy mesh to another less fine, two effects are taken into account: the first is the spectral broadening of the source and the second is the fineness of the mesh itself, namely the impact of averaging coarser mesh on the calculation algorithm. These two effects are shown on Figure 3-3.

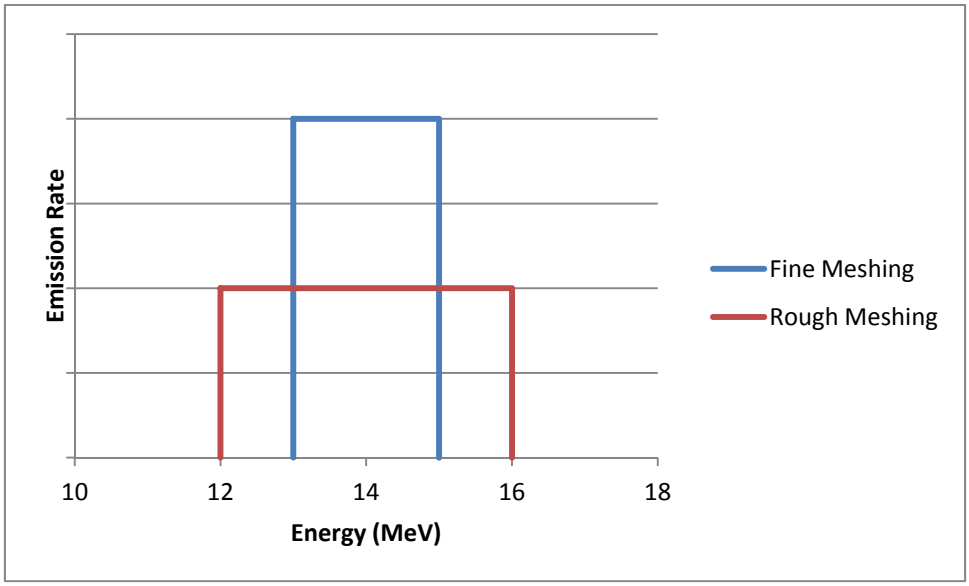

Figure 3-3: Spectral broadening of a source centered on 14,07 MeV

Energy grids only provide information regarding the division of the source in energy groups, but in order to create an energy spectrum it is necessary to define the emission rate of each of those groups. The calculation of the emission rate for each of the concerned energy groups of each energy grid is done based on a prior work(19) that defined precisely the energy spectrum emitted by a fusion reactor. A python program has been created to calculate these emission rates; based on the reference Gaussian-distributed energy spectrum the program weights the original emission rates to the energy grids considered here calculating the emission rates for each energy group.

Energy spectra of the source for each of energy grids have been plotted on Figure 3-4, Figure 3-5, Figure 3-6 and Figure 3-7, where they are compared to the Gaussian distribution of the fusion neutrons. These figures give a visual idea of the lost information when using rough grids.

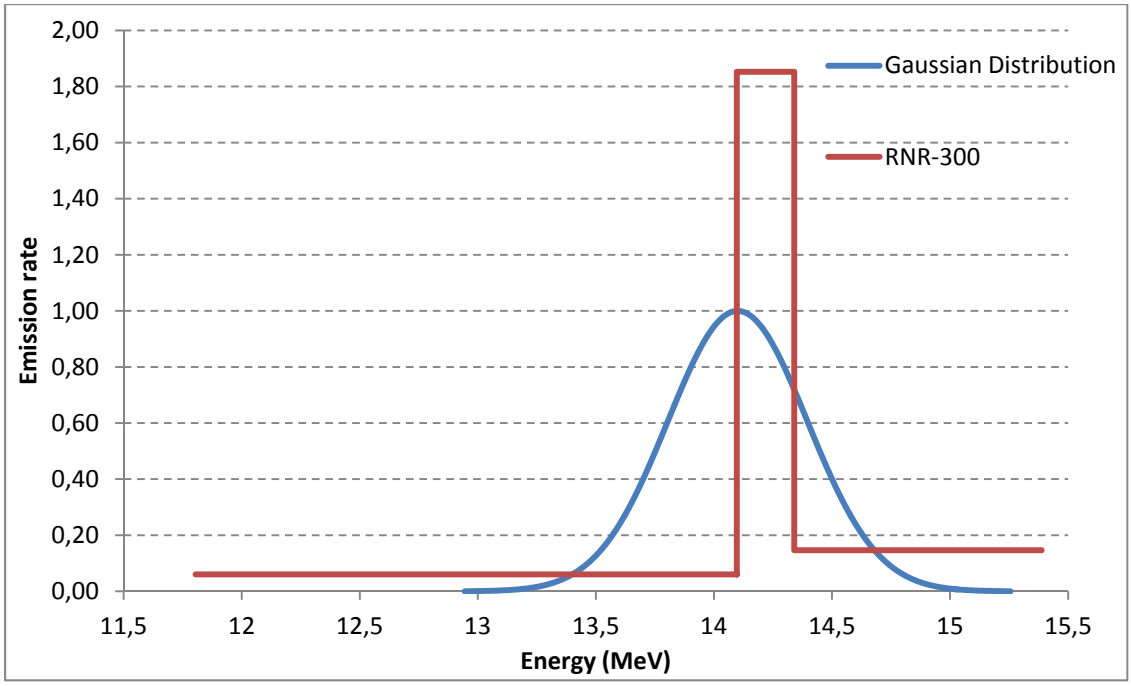

Figure 3-4 : Emission spectrum of the source for RNR300 energy grid. A correction on the emission rate has been performed in order to assure the value of the integrate emission rate

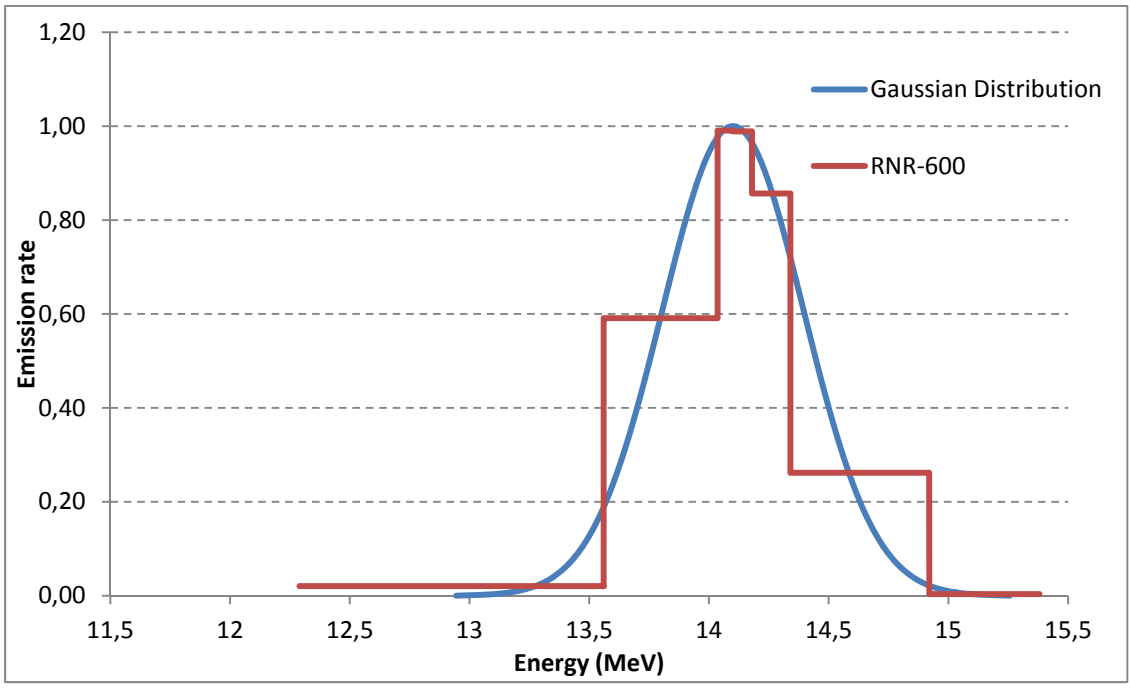

Figure 3-5 : Emission spectrum of the source for RNR600 energy grid

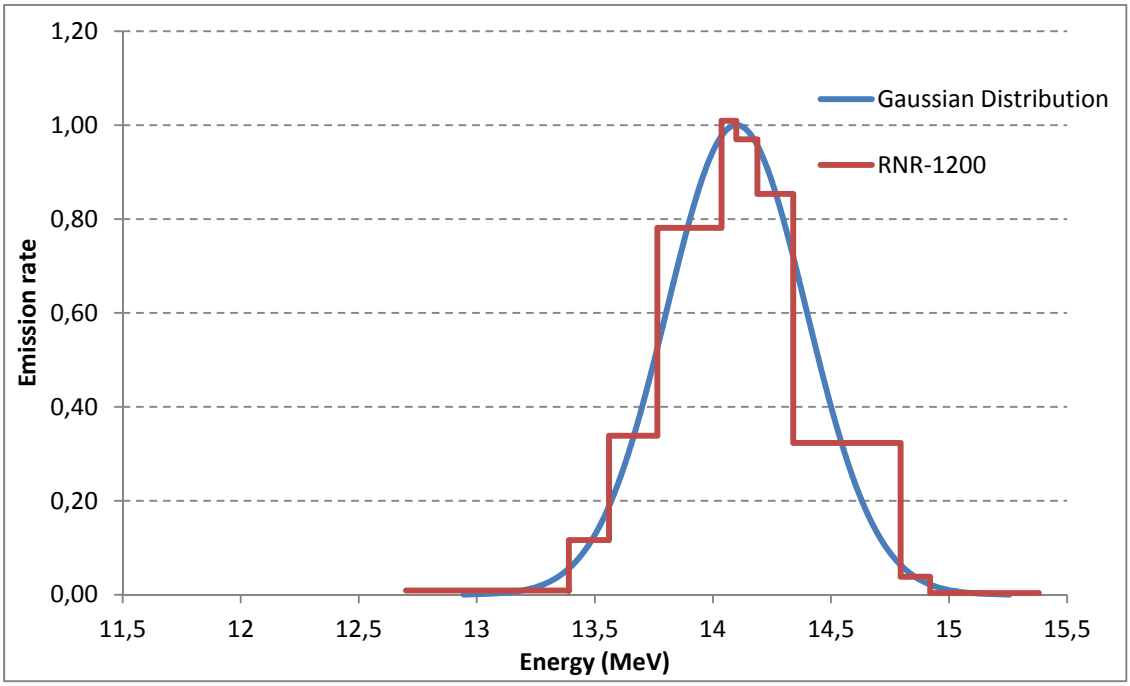

Figure 3-6 : Emission spectrum of the source for RNR1200 energy grid

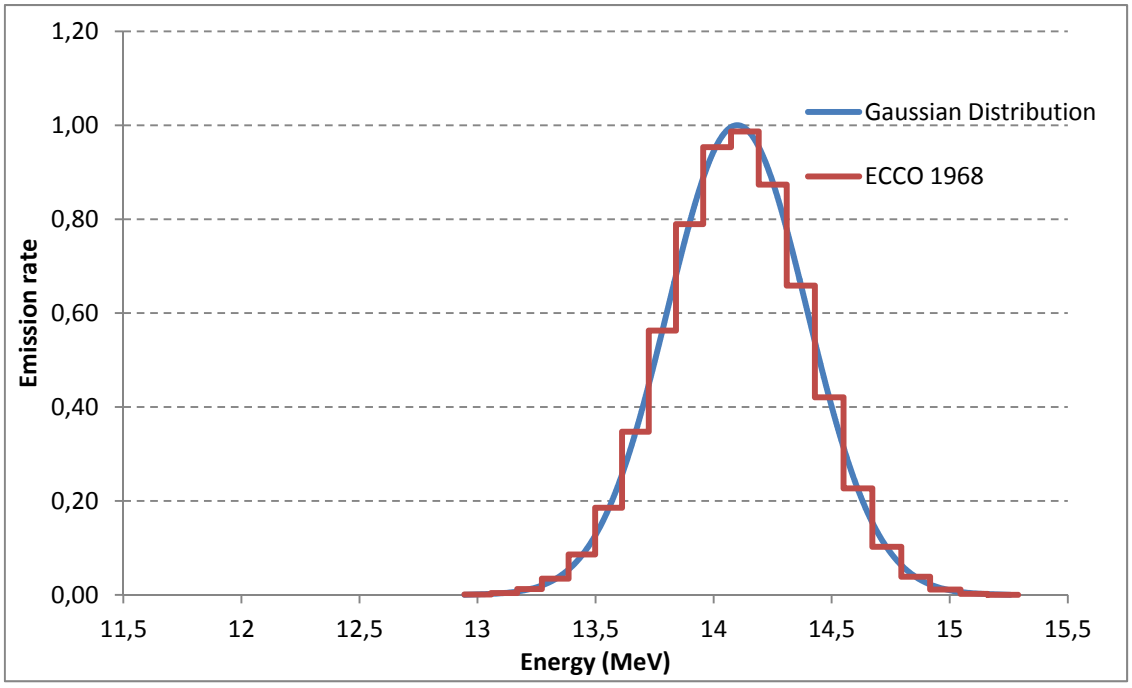

Figure 3-7 : Emission spectrum of the source for ECCO1968 energy grid

3.4.2. Spatial Spectrum

In addition to the energy spectrum, it is important to study the influence of the spatial distribution of the source. The neutron source intensity will be higher at the center of the plasma, so we should design a source of stronger emission rate in the center of the fusion chamber. Nevertheless, previous studies (17)(20) show that the difference in terms of TBR between a homogeneous source and a spatial distributed source are in the range of 1%. Nevertheless the spatial distribution of the source has greater impact on local parameters such as deposited energy or neutron flux, because the poloidal distribution of the energy is not taken into account. As the peak neutron flux and peak deposited energy are present on the middle plane of a 3D tokamak, neutron flux and deposited energy estimated on this project represent the highest values achieved on a tokamak. Homogeneous spatial-distributed sources seem therefore adequate for this study.

3.5. Energy corrections and gamma transport

Because of the deterministic code Apollo2, the cross-sections libraries are designed to work in the range of fission energy neutrons. This characteristic poses some problems when performing calculations on deposited energy. Some manual corrections will be done on the calculated deposited energy.

Apollo2 considers that when a neutron experiences a nuclear reaction in a given material, it deposes all its energy on this material. However this is not true in the case of endoenergetic reactions suffered by the neutrons. This kind of reaction consumes energy and therefore decreases the deposited energy in the tokamak. The deposited energy due to neutron reactions in each layer of the tokamak, will be therefore corrected to take into account this issue for some neutronic reactions such as $(n, 2n)$, (n, α), and (n, p). In addition, the gamma transport is not considered, meaning that a gamma created on a layer will deposit all its energy in this layer, when in many cases this gamma ray can travel through the tokamak and interact somewhere else (see later section 4.4).

3.6. Scores and result post-treatment

Once the parameterized geometry and material compositions are defined and the source is defined it is necessary to create the scores, Apollo2 results. These scores are not always calculated in the expected units, and some post-treatment is needed. Score definition and post-treatment for each variable are presented below.

3.6.1. 1D Model

The 1D model is used for calculation of local phenomena, the deposited energy and the local radial flux. These two parameters need to be normalized to the real fusion power of the tokamak. Apollo2 model calculates variables for a source of 1 $\frac{neutron}{second \times VolFusion\ Chamber1D}$, so it is imperative to apply a normalization factor, the number of neutrons for the given fusion energy of the reactor, to calculated results, as detailed on Equation 3-1. This normalization is done outside Apollo2, so that the fusion power is not a parameter of the program and is not taken into account in the creation of neural networks.

$$Normalization\ Factor\ \left[\frac{n}{s}\right] = FusionPower[MW] \times \frac{10^6 W}{1MW} \times \frac{1MeV}{e} \times \frac{1neutron}{E_{fusion}} \times \frac{VolFusionChamber1DModel}{VolFusionChamber3DOriginal}$$

$$e = 1{,}602144 \times 10^{-13} MeV/J$$

$$E_{fusion} = 17{,}6\ MeV$$

Equation 3-1 : Normalization factor applied to the deposited energy and neutron flux

Deposited energy: The deposited energy is a parameter directly calculated by Apollo2. This deposited energy will be differentially calculated, meaning that the result is not dependant on the volume of the layer. In our case we decided that the output must be expressed on $\frac{MW}{m^3}$ from the original $\frac{MeV}{cm^3}$ calculated by Apollo2; the change of units is detailed on Equation 3-2.

$$DE\left[\frac{MW}{m^3}\right] = DE\left[\frac{MeV}{cm^3}\right] \times \frac{1{,}602144 \times 10^{-13} MW/m^3}{1MeV/cm^3}$$

Equation 3-2 : Change of units applied to the deposited energy

Neutron flux : the neutron flux is directly calculated by Apollo2. The score is obtained directly in differential form in $\frac{neutron}{cm^2 \times s}$. No special post-treatment is needed for the radial flux calculation beyond the application of the normalization factor. Neutron flux on the inboard toroidal fields is a critic measurement for a thermonuclear reactor due to important impact of high neutron fluxes on physical properties of the superconducting materials used on the coils. Obtaining a good neutron flux resolution on the inboard coils guides then the selection of the model.

3.6.2. RZ Model

This Apollo2 model is used for the calculation of integral parameters such as the tritium breeding ratio and the multiplication factor. The scores leading to these two magnitudes are presented below.

Tritium breeding ratio (see Appendix A.5): the tritium breeding ratio is defined as the number of tritium isotopes created on the breeding zone for each tritium consumed on a fusion reaction. The score that permits the calculation of the tritium production on Apollo2 is defined as the rate of nuclear reactions between neutrons and lithium on the breeding zone. As the source is defined as 1 neutron per second and each neutron comes from the fusion of a tritium and deuterium, the interaction rate obtained from the Apollo2 simulation is the tritium breeding ratio.

Multiplication factor (see Appendix A.5): The multiplication factor is defined as the total deposited energy by the neutrons on the tokamak due to nuclear interactions divided by the energy of a neutron released in a fusion nuclear reaction. The total deposed energy on the tokamak (corrected for certain isotopes as presented on section 3.5) is divided by 14,07MeV, the typical energy of a neutron released on a fusion reaction between tritium and deuterium. Again, as for the tritium breeding ratio, the total deposited energy is calculated for 1 neutron, so it is not necessary to normalize the results to the source.

Two parametrizable deterministic Apollo2 models have been created. Those models are capable of calculating the “characteristic” neutronic parameters of a thermonuclear fusion reactor such as the TBR, multiplication factor, deposited energy and the neutron flux. The performances of these models are studied on chapter 4, where a comparison between the different energy meshes will be done. A reference Monte Carlo model will be furthermore used to compare Apollo2 results to those obtained by TRIPOLI4.8 reference model.

4. Validation of the Apollo2 model

4.1. Comparison between different Apollo2 energy grids

After creating the Apollo2 models it is necessary to compare the performances of the models for the different energy grids presented on 3.4.1. These comparisons are not going to define which of the energy grids will be used to create the plans of experience; this will be done by comparing the Apollo2 models to the Tripoli4 reference model. Nevertheless, it is important to study the performances of each of the energy grids to understand the behavior of the model. The study will be done for the 1D model because due to long calculation times the RZ model is limited to the 300 group energy grid.

4.1.1. 1D Apollo2 model

This cylindrical one-dimension model is studied for the energy grids Ecco1968(21), RNR1200 and RNR600 (18). Comparisons are done for the neutron flux profile and deposited energy.

The first analysis is done for the neutron flux in the inboard side of the tokamak. It is important to note that the objective is to obtain a good resolution of the neutron flux in the inboard coils, leaving the rest of the fluxes in a secondary plane. A table containing the fast and slow neutron fluxes is presented on appendix B.1.

It is interesting to study deviations due to different energy grids compared to the calculation time. This is done in Table 4-1. The neutron flux that will be used from now on is the flux calculated in the first centimeter of each layer. The peak neutron flux in the inboard coils is marked in red in Table 4-1, the peak neutron flux in the toroidal field structure in front of the winding package. Small deviations are observed between different energy grids until the first centimeters of the inboard coils, those are due to the smallest resolution obtained when using less energy groups. Nevertheless, when using large energy grids some convergence problems appear, a performance study will be done comparing those results to the ones obtained with a reference Monte Carlo model to choose the best energy grid in terms of calculation time and performance. The results obtained with Apollo2 models are plotted on Figure 4-1, a figure that shows that deviations due to different energy grids are depreciable when represented in a logarithmic scale.

	Peak Neutron Flux for E_n> 0,1MeV			
	Distance to plasma (cm)	ΔFastFlux 1968 vs 1200	ΔFastFlux 1968 vs 600	ΔFastFlux 1200 vs 600
First Wall	0,2	0,10%	-0,25%	-0,34%
	1,7	0,10%	-0,25%	-0,34%
Breeding Zone	3,2	0,04%	-0,43%	-0,47%
	4,2	0,12%	-0,32%	-0,44%
	8,2	0,12%	-0,38%	-0,50%
	13,2	0,08%	-0,51%	-0,59%
	18,2	0,03%	-0,64%	-0,67%
	23,2	-0,03%	-0,78%	-0,75%
	28,2	-0,08%	-0,91%	-0,83%
	33,2	-0,18%	-1,09%	-0,91%
Back Plate	47,7	-0,34%	-1,28%	-0,95%
	48,7	-0,22%	-1,04%	-0,82%
	52,7	-0,14%	-0,90%	-0,77%
	57,7	-0,14%	-0,98%	-0,84%
MF	65,7	-0,21%	-1,18%	-0,97%
	66,7	-0,27%	-1,34%	-1,07%
	70,7	-0,44%	-1,73%	-1,30%
	75,7	-0,69%	-2,30%	-1,62%
	80,7	-1,05%	-3,07%	-2,04%
	85,7	-1,54%	-4,13%	-2,62%
	90,7	-2,29%	-5,73%	-3,51%
Shield	105,7	-2,85%	-6,80%	-4,07%
	106,7	-3,08%	-6,90%	-3,94%
	110,7	-3,46%	-7,09%	-3,76%
	115,7	-3,65%	-7,01%	-3,49%
	120,7	-3,52%	-6,52%	-3,11%
	125,7	-3,06%	-5,63%	-2,65%
	130,7	-2,35%	-4,51%	-2,21%
VV	145,7	-1,81%	-3,70%	-1,93%
	146,7	-1,55%	-3,40%	-1,88%
	150,7	-1,18%	-3,07%	-1,91%
	155,7	-0,92%	-2,88%	-1,98%
	160,7	-0,77%	-2,84%	-2,08%
	165,7	-0,70%	-2,89%	-2,21%
	170,7	-0,67%	-3,01%	-2,35%
	175,7	-0,66%	-3,15%	-2,50%
TFCS	**190,7**	-0,65%	-3,21%	-2,57%
	191,7	-0,65%	-3,23%	-2,59%
	192,7	-0,70%	-3,34%	-2,67%
	194,7	-0,83%	-3,69%	-2,88%
TFC	196,7	-0,96%	-3,99%	-3,06%
	197,7	-0,91%	-3,94%	-3,05%
	206,7	-0,83%	-4,14%	-3,34%
	216,7	-0,82%	-4,62%	-3,83%
	226,7	-0,89%	-5,20%	-4,35%
	236,7	-0,93%	-5,49%	-4,60%
	246,7	-2,62%	-15,81%	-13,55%
	256,7	-2,82%	-14,32%	-11,83%

Table 4-1 : Deviation of the peak neutron fluxes obtained with the 3 Apollo2 models

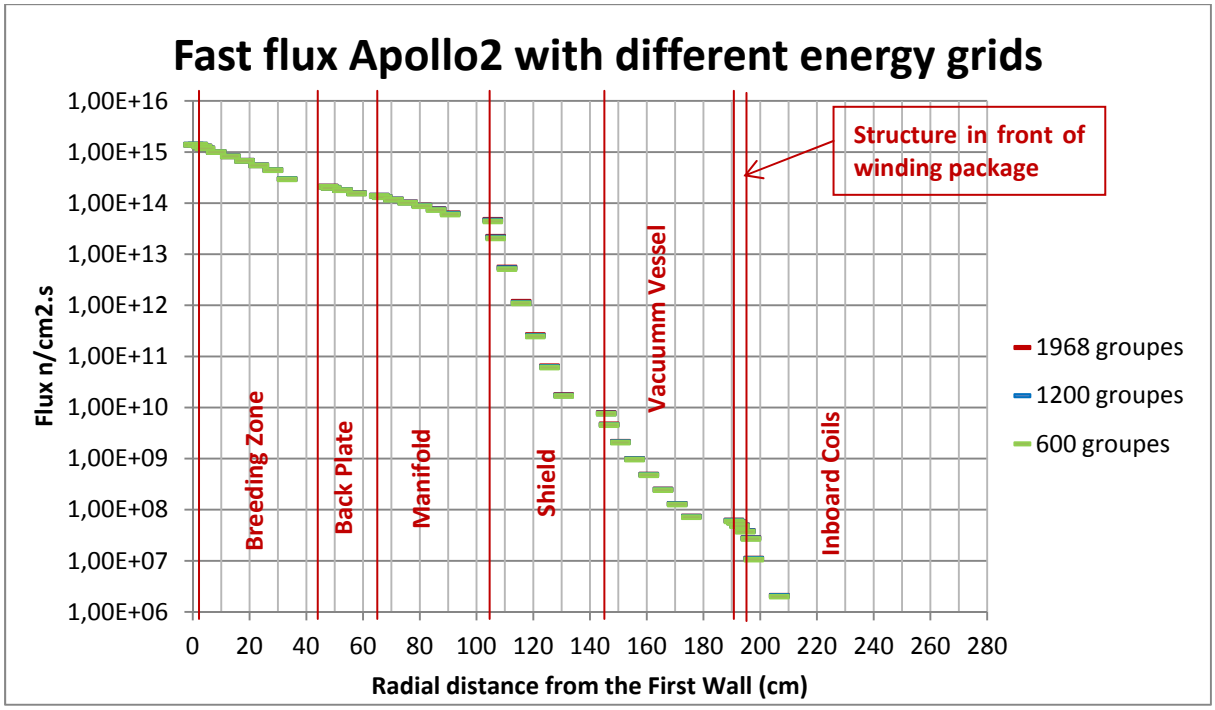

Figure 4-1 : Radial profile of the peak neutron flux across the inboard estimated with different energy grids

Once the study of the deviation in the radial flux deviation is done it is necessary to study the performance of the Apollo2 model in terms of deposited energy. The deposited energy is defined as the average deposited energy in each of the tokamak's layers per unit of volume.

		Total Neutron Deposited Energy			
		Distance to plasma	ΔDepositedE 1968 vs 1200	ΔDepositedE 1968 vs 600	ΔDepositedE 1200vs 600
Inboard	First Wall	0,2	0,71%	0,41%	-0,30%
	Breeding Zone 10 cm	3,2	-0,06%	-0,04%	0,05%
	Breeding zone	13,2	-0,09%	0,06%	0,11%
	Back Plate	47,7	0,66%	-1,03%	-1,70%
	Manifold	65,7	3,67%	5,59%	2,00%
	Shield	105,7	-0,44%	1,55%	1,98%
	Vacuum Vessel	145,7	9,66%	16,75%	7,85%
	Toroidail field structure in front of winding package	190,7	1,66%	4,57%	2,96%
	Toroidal field coils	196,7	-3,29%	0,13%	3,31%
Outboard	FW	0,2	0,68%	0,35%	-0,33%
	BZ 10 cm	3,2	0,07%	0,09%	0,11%
	BZ	13,2	-0,02%	0,30%	0,23%
	BP	80,7	0,76%	-1,27%	-2,05%
	MF	98,7	2,57%	3,31%	0,77%
	Shield	158,7	0,74%	4,63%	3,92%
	VV	218,7	69,04%	82,78%	44,40%
	TFCS	308,7	11,75%	8,82%	-3,32%
	TFC	316,7	-2,32%	3,89%	6,08%

Table 4-2 : Apollo2 deposited energy deviations for each of the energy grids

As shown in Table 4-2 (more detailed on appendix B.2) deviations due to different energy grids are not constant and as predictable as for the neutron flux. The reason for this random behavior is bad convergence of Apollo2 for regions with a high percentage of void, such as the vacuum vessel. The conclusion in this case is the same as for the neutron flux calculation, it is necessary to compare this model to a Monte Carlo reference model. It is important to point that a calculation of the deposited energy has been done for the first 10 cm of the breeding zone in order to obtain the maximum deposited energy deposited in the breeding zone to make thermo-hydraulic calculations.

4.2. Development of a Monte-Carlo model using Tripoli4

In order to validate the Apollo2 model a numeric benchmark using Monte Carlo models has been performed. It would be suitable to develop a 3D parameterizable tokamak Tripoli4 model featuring the "real" DEMO geometry. Nevertheless, due to the complexity of this geometry this is difficult. Instead, a 3D Tripoli4 Monte Carlo DEMO model previously developed by (22) is used. A second 1D-geometry Tripoli4 model is developed specially to compare neutron flux results. These two models are described below.

4.2.1. 3D Geometry Tripoli4

A model developed in the frame of previous DEMO studies will be used as reference model. This model has been built appropriately importing and modifying a CAD model and it is therefore not entirely parameterizable; only some minor modifications are feasible so the available points for the validation of the APOLLO2 model are limited. The model represents a DEMO thermonuclear fusion reactor with a helium cooled lithium lead breeding zone as conceived on 2007.

This model is a very accurate representation of the tokamak, including the divertor, blanket modules and shields, and relevant material compositions. A vertical section view is provided on Figure 4-2, while the original CAD 3D model view is available on Figure 4-3 as represented by(20).

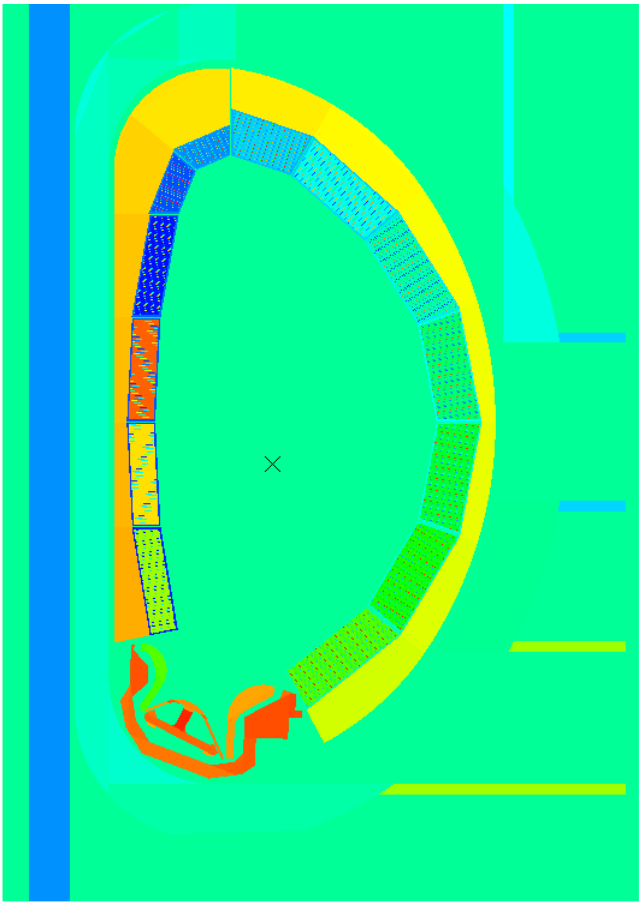

Figure 4-2 : Tripoli4 HCLL 2007 DEMO reactor model vertical section view

Starting from the original Tripoli4 3D model, 6 different geometry configurations and 3 different lithium-6 enrichment (for the original geometry) have been assessed. The characteristics of these geometries are summarized on Table 4-3. The main difference is the thickness of the breeding zone, a key parameter for the neutronic calculations as the creation of tritium is done on this layer. The Apollo2 model performances are compared to these models..

To have more than one validation point the tokamak is divided in 13 sections on the poloidal direction, of 11,25 degrees each. The M_E and neutron flux are estimated on each of these sections and the highest value is retained in order to assure that the studied fluxes and deposited energies correspond to the peak ones.

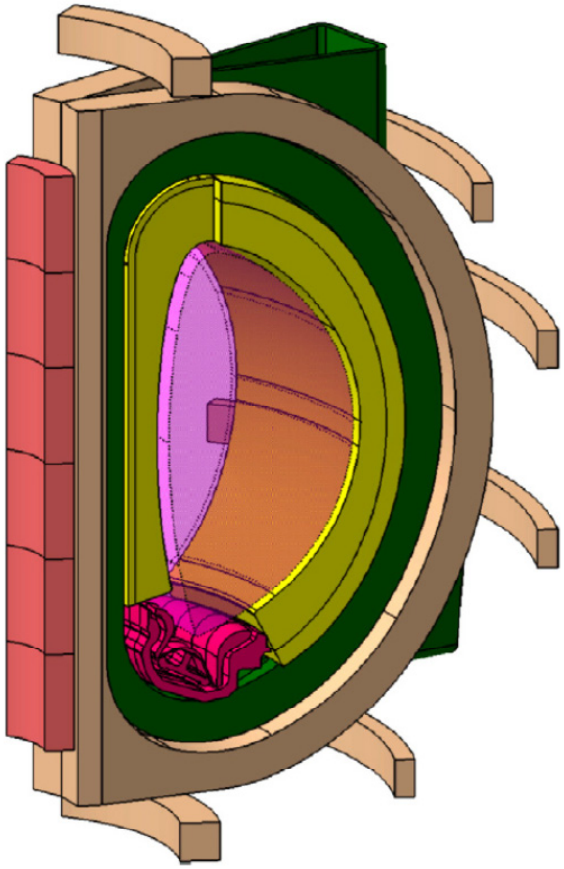

Figure 4-3 : Generic CAD model of DEMO (22.5◦ torus sector) constructed with CATIA V5

Model	Breeding Zone Inboard thickness (cm)	Breeding Zone Outboard thickness (cm)	Manifold Inboard thickness (cm)	Manifold Outboard thickness (cm)	Lithium 6 enrichment (%)
Reference	47,3	77,3	20,0	25,0	90%
IBminus10	37,3	77,3	30,0	25,0	90%
IBMinus20	27,3	77,3	40,0	25,0	90%
OBminus10	47,3	67,3	20,0	35,0	90%
OBminus20	47,3	57,3	20,0	45,0	90%
OBIBminus10	37,3	67,3	30,0	35,0	90%
OBIBminus20	27,3	57,3	40,0	45,0	90%
RefLi75	47,3	77,3	20,0	25,0	75%
RefLi60	47,3	77,3	20,0	25,0	60%
RefLi45	47,3	77,3	20,0	25,0	45%

Table 4-3 : Tripoli4 HCLL 2007 DEMO reactor model assessed configurations

This Tripoli4 model uses the original Gaussian-distributed source, directly using the results provided in (19). The source presents both an energy distribution and a spatial distribution (corresponding to H-mode plasma), as shown on Figure 4-4, which makes it the realest model

available. Nevertheless, as the source will be defined for $1\frac{neutron}{second}$ a normalization factor for the differential variables will be again used, as it is defined on Equation 3-1.

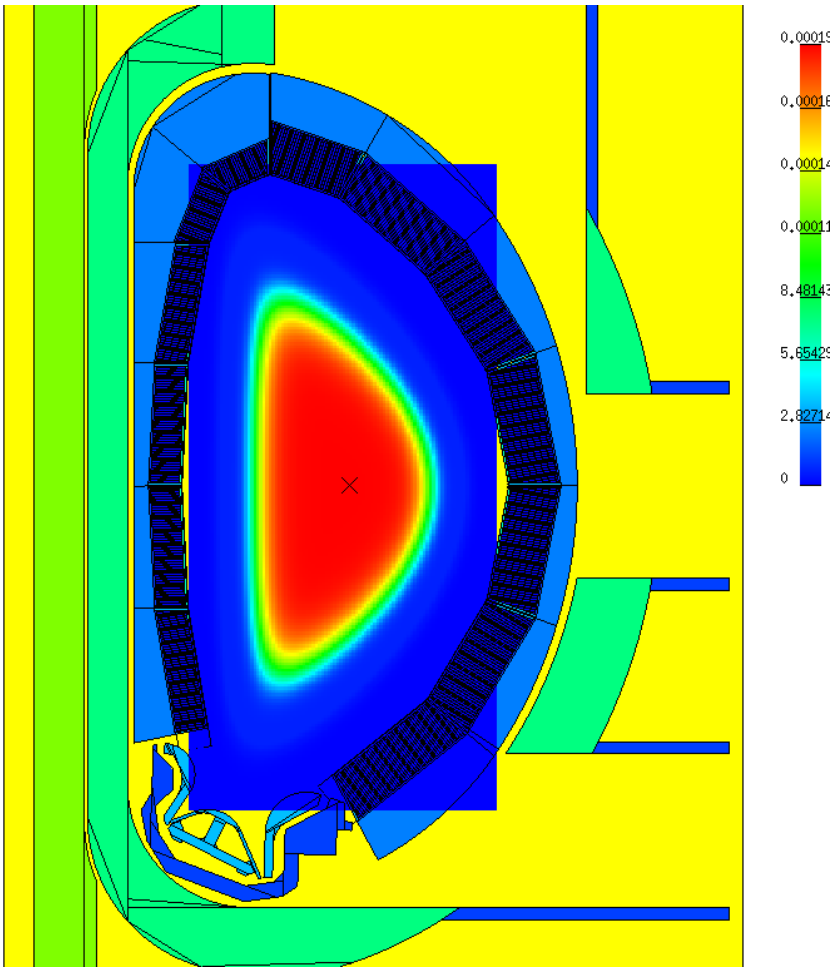

Figure 4-4 : H-mode spatial distribution of the neutron source density

4.2.2. 1D Geometry Tripoli4

The Tripoli4 3D model presented before is a good reference model but presents some restrictions due to its unparameterizable character. In order to validate the Apollo2 model within larger operating windows a one-dimension cylindrical Tripoli4 model is developed which represents the horizontal section of the tokamak at the equatorial plane . The geometry used to create the Tripoli4 model is the same as in Figure 3-1, except for the height of the cylinders which in this case will be fixed to 200 cm. The scores are calculated as in the Apollo2 model.

As for the one-dimension deterministic model, this kind of model is not suitable to calculate integral parameters such as the TBR and the multiplication factor. This model will be used to compare differential variables, in particular the peak neutron flux and the deposited energy. The

normalization factor used in this case is the same as used by the Apollo2 model, shown in Equation 3-1.

The representation of this Tripoli4 model is shown in Figure 4-5, where all tokamak's layers are represented in different colors, the blue represents void while yellow represents the plasma chamber. This model is fully parameterizable in terms of geometry, the material compositions are parameterized using python scripts and Apollo2.

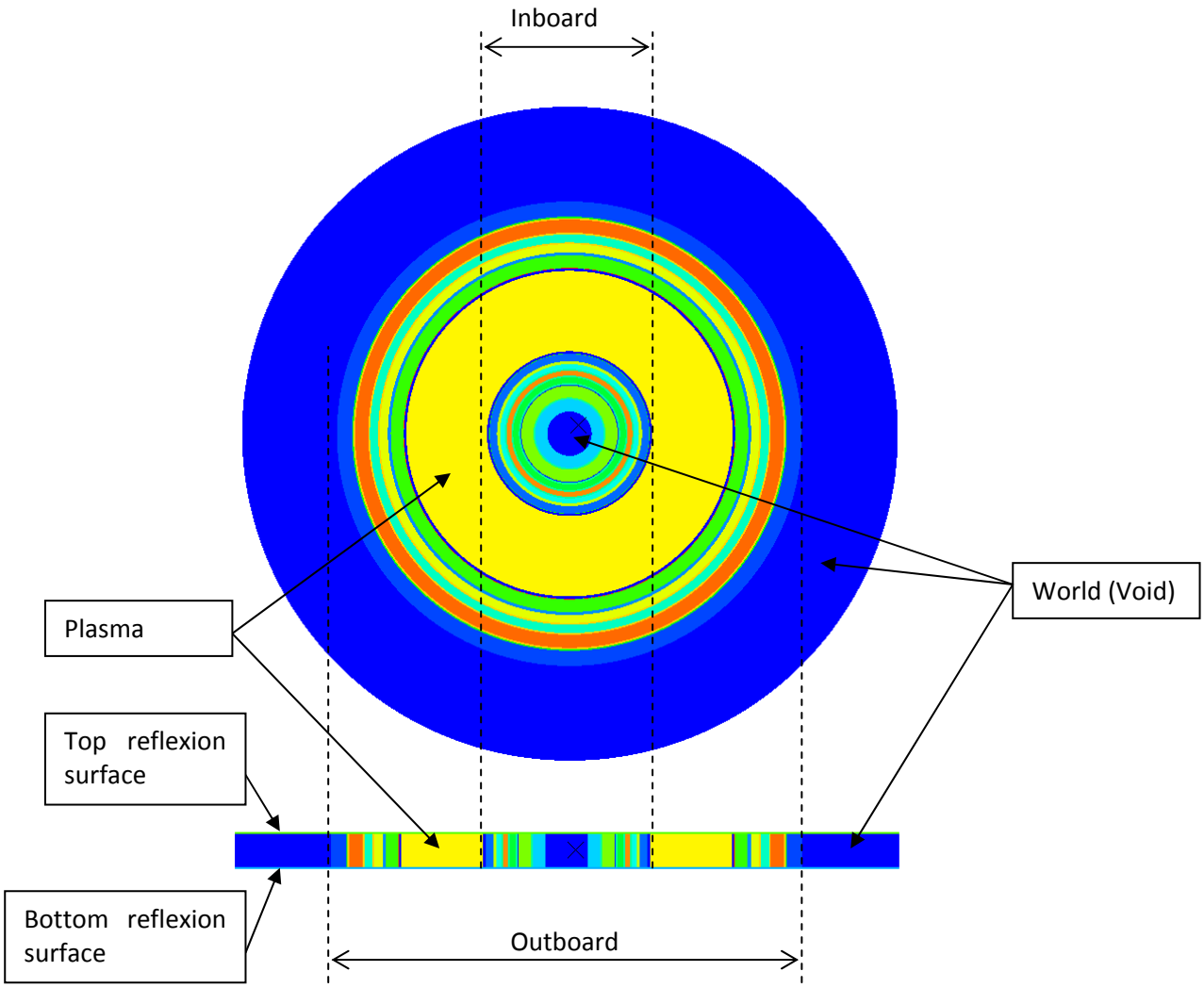

Figure 4-5 : Tripoli4 1D geometry model representation

4.2.3. Neutron and Neutron-Photon simulations

Tripoli4 simulates the neutron flux and energy deposition, but it also secondary photons created by nuclear reactions. This option gives more accurate results in terms of deposited energy profile. In this study the two simulations will be done, studying the performance of Apollo2 against a neutron-only simulation or a neutron-photon simulation.

Nuclear reactions producing photons are important because they introduce a different distribution of the deposited energy: using the neutron-only simulation when a neutron suffers a nuclear reaction in, for example, the breeding zone, it deposites all the energy in the breeding zone; using the neutron-photon simulation when a neutron suffers a nuclear reaction it can create secondary photons capable of traveling through the different layers of the tokamak depositing its energy in the more external layers. Figure 4-6 represents the track of a neutron using a neutron-only simulation, the neutron suffers scattering until it reacts and it deposited all its energy. Figure 4-7 represents a neutron track using a neutron-photon simulation; the neutron suffers a nuclear reaction creating a very energetic photon that travels through the tokamak depositing its energy in deeper zones. Figure 4-8 shows the Tripoli4 behavior with neutron-photon simulations; red tracks represent neutron trajectories while yellow tracks represent photon's ones, blue points represent neutron collision sites, the length of the track represents the distance travelled by each particle, concluding that the photons have greater speeds than the neutrons, which confirms that photons are more penetrating than neutrons.

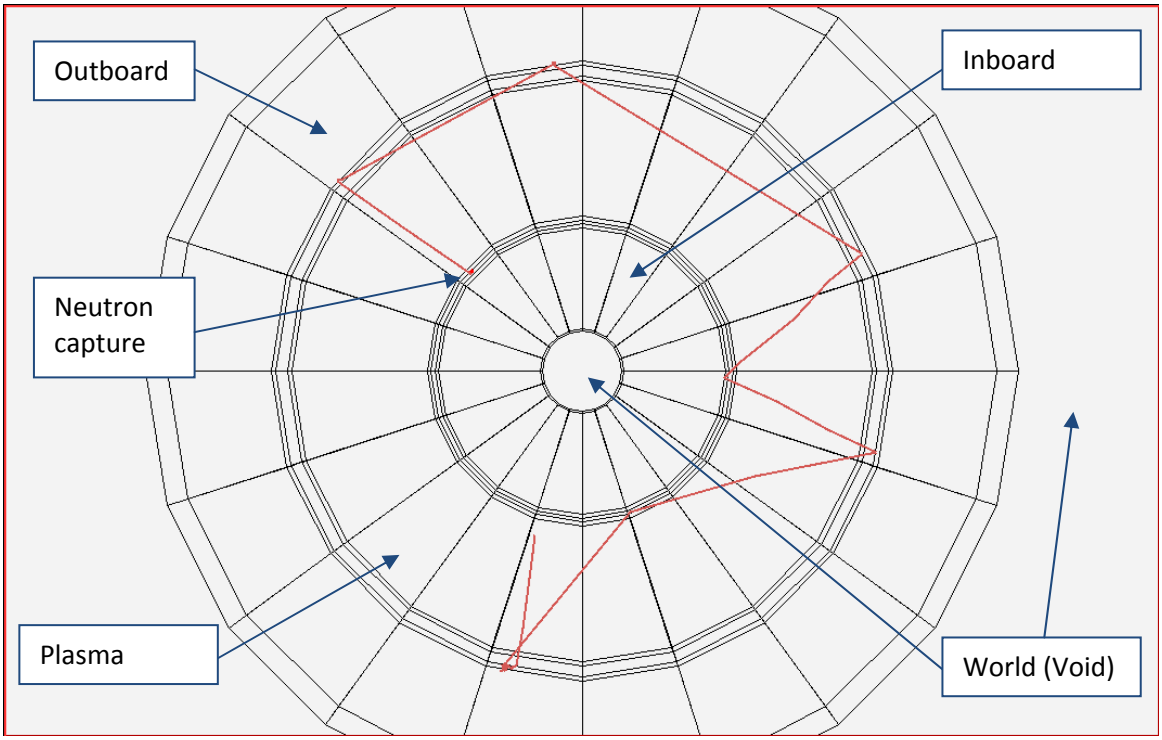

Figure 4-6 : One neutron track simulation in the tokamak (neutron simulation)

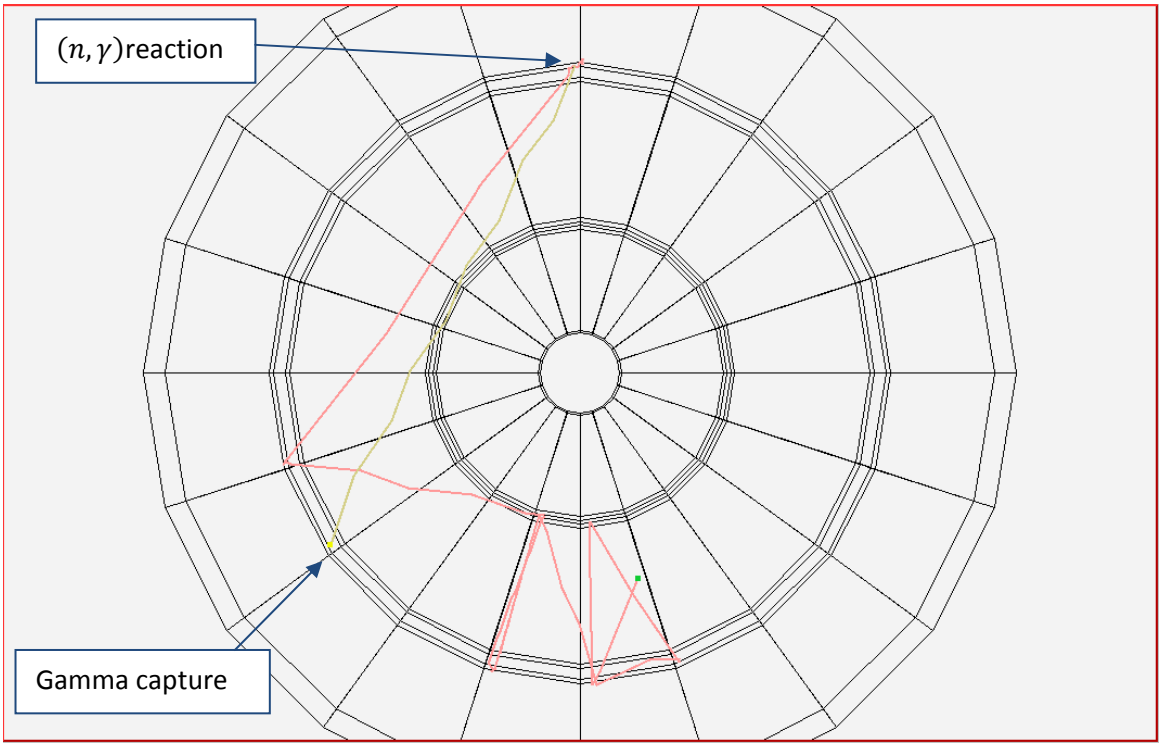

Figure 4-7 : Secondary photon track simulation in the tokamak (neutron-photon simulation).

***Neutron and photon desviations inside the plasma chamber are due to reflections with both top and bottom reflection surfaces.**

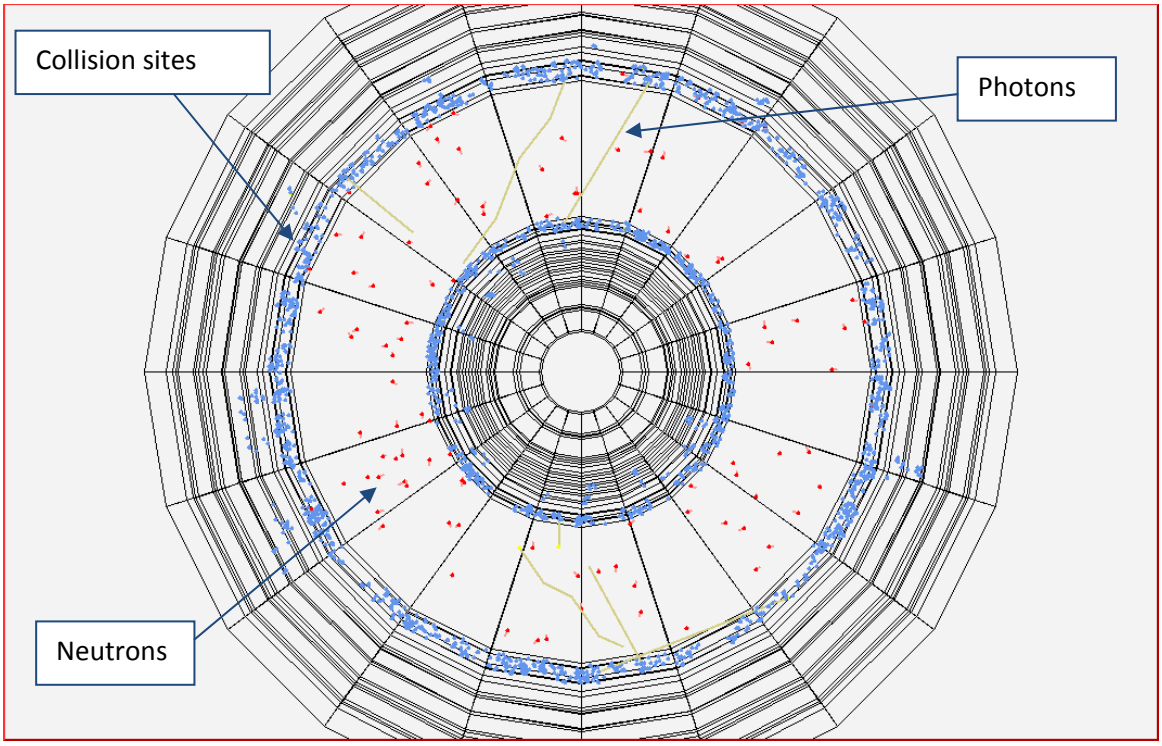

Figure 4-8 : Neutron and photon tracks in a 10ms time window (neutron-photon simulation)

4.3. Validation of the Apollo2 model with Tripoli4

4.3.1. RZ geometry model

The first validation stage is based on the RZ square-based model presented on section 3.2.2. Estimated variables by this model are the TBR and multiplication factor, two integral parameters that depend on the volume of the different tokamak layers; thus the three-dimension DEMO HCLL Tripoli4 reference model is used to validate the results.

A benchmark has been done using the different geometries and compositions introduced on Table 4-3. The results are summarized on Table 4-4, where the deviations between Apollo2 and Tripoli4 are presented. A more detailed table summarizing obtained absolute values is provided on appendix B.3.

	ΔTBR (%)	ΔTBR Inboard (%)	ΔTBR Outboard (%)	ΔMultiplication Factor (%)
Reference	-1,29	-0,81	-1,43	1,92
RefLi75	-1,15	-0,49	-1,35	2,02
RefLi60	-0,99	0,09	-1,32	2,08
RefLi45	-0,75	0,79	-1,2	2,21
IBminus10	-0,84	1,65	-1,52	2,09
IBMinus20	-0,45	4,65	-1,62	2,26
OBminus10	-0,56	-0,92	-0,44	2,11
OBminus20	0,34	-1,04	0,81	2,34
OBIBminus10	-0,1	1,45	-0,54	2,24
OBIBminus20	1,42	4,5	0,65	2,63

Table 4-4 : Deviations between RZ Apollo2 model and 3D Tripoli4 model

The RZ square-based geometry presents a very accurate performance both for the TBR and the multiplication factor. The worst deviation is obtained for OBIBminus20 case, the smallest breeding zone both on the inboard and outboard; the TBR presents a deviation of 1,42% and the multiplication factor is overestimated by a factor of 2,63%. These deviations are negligible when compared to typical uncertainties related to physical quantities: nuclear data for certain isotopes present incertitudes of up to 2% (23) or average difference between simulated TBR and experimental TBR up to 14% (20).

It can be concluded that the RZ model is suitable to compute integral parameters, i.e. the TBR and the energy multiplication factor. Maximumdiscrepancies between APOLLO2 and TRIPOLI-4 models will be used afterwards to correct the values calculated with Apollo2 (see section 6.2).

4.3.2. 1D geometry model

Following the results obtained in (24), instead of directly comparing the results between the 3D Tripoli4 reference model and Apollo2 the strategy followed in this study is to develop a Tripoli4 one-dimension geometry model with the same parameters as the Apollo2. This 1D Tripoli4 model will be validated with the 3D Tripoli4 DEMO model for the first tokamak layers. Results obtained with Apollo2 will be compared to the 1D Tripoli4 model.

4.3.2.1 1D Tripoli4 model validation

This model has been described on 4.2.2 and, as mentioned above, it will be used as reference model to validate the Apollo2 1D model. Performance of this 1D Tripoli4 model has been tested against 3D DEMO model on test cases described before, comparing the radial profile neutron flux and the deposited energy in the first wall, breeding zone and back plate. Obtained deviations are summarized on Table 4-5. A detailed table of absolute values is provided on appendix B.4.

	Ref		IBminus10		IBminus20	
	Deposited energy Tripoli 3D vs 1D	**Peak flux Tripoli 3D vs 1D**	**Deposited energy Tripoli 3D vs 1D**	**Peak flux Tripoli 3D vs 1D**	**Deposited energy Tripoli 3D vs 1D**	**Peak flux Tripoli 3D vs 1D**
FW Ib	54,55%	55,32%	53,14%	55,04%	54,92%	55,25%
FW Ob	90,20%	64,88%	89,26%	64,97%	90,97%	65,19%
BZ Ib	20,38%	36,21%	21,40%	37,81%	22,90%	40,34%
BZ Ob	43,33%	50,55%	43,30%	50,61%	43,32%	50,55%
BP I	8,81%	10,99%	5,84%	22,42%	4,33%	29,67%
BP O	4,92%	13,77%	3,36%	14,67%	6,66%	14,45%

	OBminus10		OBminus20	
	Deposited energy Tripoli 3D vs 1D	**Peak flux Tripoli 3D vs 1D**	**Deposited energy Tripoli 3D vs 1D**	**Peak flux Tripoli 3D vs 1D**
FW Ib	53,55%	55,27%	54,12%	55,37%
FW Ob	90,81%	65,16%	89,96%	65,18%
BZ Ib	21,00%	36,53%	21,00%	36,58%
BZ Ob	42,64%	50,07%	41,74%	49,79%
BP I	9,09%	10,82%	9,79%	11,29%
BP O	12,05%	24,21%	18,97%	33,15%

	IBOBminus10		IBOBminus20	
	Deposited energy Tripoli 3D vs 1D	**Peak flux Tripoli 3D vs 1D**	**Deposited energy Tripoli 3D vs 1D**	**Peak flux Tripoli 3D vs 1D**
FW Ib	54,19%	55,34%	54,23%	55,23%
FW Ob	90,54%	65,28%	90,60%	65,15%
BZ Ib	21,73%	38,18%	23,12%	40,48%
BZ Ob	42,53%	50,04%	41,90%	49,77%
BP I	3,01%	22,43%	5,96%	29,39%
BP O	11,30%	24,22%	16,30%	33,10%

	RefLi75		RefLi60		RefLi45	
	Deposited energy Tripoli 3D vs 1D	**Peak flux Tripoli 3D vs 1D**	**Deposited energy Tripoli 3D vs 1D**	**Peak flux Tripoli 3D vs 1D**	**Deposited energy Tripoli 3D vs 1D**	**Peak flux Tripoli 3D vs 1D**
FW Ib	53,70%	57,06%	53,11%	59,33%	52,91%	62,46%
FW Ob	89,94%	66,57%	88,18%	68,55%	88,34%	71,41%
BZ Ib	21,80%	38,52%	22,69%	41,09%	24,20%	44,52%
BZ Ob	44,05%	52,17%	45,31%	54,20%	46,60%	56,90%
BP I	9,88%	13,81%	13,93%	16,75%	17,01%	20,41%
BP O	9,06%	17,71%	15,24%	21,36%	20,76%	26,77%

Table 4-5 : Deviations between 3D DEMO Tripoli4 model and 1D Tripoli4 model.

As predicted by (24), obtained deviations show an overestimation of the deposited energy and the peak neutron flux. Beginning in the first wall, the deposited energy is overestimated in all layers, but an amelioration of deviations is observed in deeper (farer from the plasma) layers. This behavior is partly due to the presence of the divertor in the 3D DEMO model; previous studies (20) have indeed shown that 10 to 20% of the neutron flux is lost in the divertor, reducing the deposited energy in the first wall and the first layers of the tokamak.

It is important to remark that this study has been done using neutron-photon Monte Carlo simulation, which takes into account the possibility of creating secondary photons due to nuclear interactions of neutrons. The peak neutron flux is studied for both fast and slow neutrons.

Both the deposited energy and neutron flux are overestimated but are within reasonable deviation windows: an overestimation factor of ~200% is typically used on neutron fluxes, normally studied on a logarithmical scale a ~90% deviation represents a small deviation from the main value. Given the goal of creating a pre-design tool, a decision is taken to embrace the results obtained by the 1D geometry Tripoli4 model. Given this fact, Apollo2 calculations will be directly compared to 1D Monte Carlo Model.

4.3.2.2 1D Apollo2 model peak fast neutron flux

The deposited energy and peak neutron fast flux are calculated using the 1D geometry deterministic Apollo2 model introduced on section 3.2.1. The validation of this model will be done comparing it to the Monte Carlo 1D Tripoli4 model introduced on section 4.2.2, studying the performances for each energy grid.

The deterministic calculation is done for a neutron-only simulation. Simulations with neutron-only model and neutron-photon model will be carried out with Tripoli4. Actually this comparison has no sense when studying the peak neutron flux because the creation of secondary photons does not affect the neutron fluxes. The results of this benchmark for the peak neutron fast flux on the inboard are presented on Table 4-6. A more detailed table is provided on appendix B.5.

Peak Neutron Flux for E_n> 0,1MeV				
	Distance to Plasma (cm)	ΔFastFlux Tripoli vs 1968	ΔFastFlux Tripoli vs 1200	ΔFastFlux Tripoli vs 600
First Wall	0,2	-4,45%	-4,36%	-4,69%
	1,7	1,33%	1,43%	1,09%
BZ	3,2	-2,43%	-2,38%	-2,84%
	4,2	-1,65%	-1,53%	-1,96%
	8,2	-1,24%	-1,12%	-1,61%
	13,2	-1,10%	-1,02%	-1,60%
	18,2	-1,09%	-1,06%	-1,73%
	23,2	-1,15%	-1,17%	-1,91%
	28,2	-1,24%	-1,32%	-2,13%
	33,2	-1,39%	-1,57%	-2,47%
BP	47,7	-1,71%	-2,04%	-2,97%
	48,7	-1,61%	-1,83%	-2,64%
	52,7	-1,64%	-1,78%	-2,53%
	57,7	-2,10%	-2,24%	-3,06%
MF	65,7	-2,56%	-2,76%	-3,70%
	66,7	-2,84%	-3,10%	-4,14%
	70,7	-3,40%	-3,83%	-5,07%
	75,7	-4,15%	-4,81%	-6,35%
	80,7	-5,06%	-6,05%	-7,97%
	85,7	-6,23%	-7,67%	-10,10%
	90,7	-7,99%	-10,10%	-13,26%
Shield	105,7	-8,68%	-11,28%	-14,89%
	106,7	-10,24%	-13,00%	-16,43%
	110,7	-11,76%	-14,82%	-18,02%
	115,7	-12,59%	-15,77%	-18,71%
	120,7	-12,10%	-15,19%	-17,83%
	125,7	-10,12%	-12,87%	-15,18%
	130,7	-7,52%	-9,70%	-11,70%
VV	145,7	-2,85%	-4,60%	-6,44%
	146,7	-2,68%	-4,19%	-5,99%
	150,7	0,25%	-0,93%	-2,82%
	155,7	2,48%	1,54%	-0,47%
	160,7	0,70%	-0,07%	-2,16%
	165,7	1,80%	1,09%	-1,14%
	170,7	-4,63%	-5,28%	-7,50%
	175,7	-9,81%	-10,41%	-12,65%
TFCS	190,7	-9,76%	-10,35%	-12,66%
	191,7	-9,67%	-10,26%	-12,59%
	192,7	-10,23%	-10,86%	-13,24%
	194,7	-10,37%	-11,12%	-13,68%
TFC	196,7	-21,53%	-22,28%	-24,67%
	197,7	-16,36%	-17,12%	-19,65%
	206,7	-34,80%	-35,34%	-37,50%
	216,7	-62,99%	-63,29%	-64,70%
	226,7	-88,28%	-88,38%	-88,89%
	236,7	-97,13%	-97,15%	-97,29%
	246,7	-99,90%	-99,90%	-99,91%
	256,7	-99,99%	-99,99%	-99,99%

Table 4-6 : Deviations between Apollo2 and Tripoli4 on peak fast flux

The relative difference between Monte Carlo and deterministic code results is shown on Figure 4-9. In the first centimeters of the tokamak's inboard layers the finest the energy grid is, the most accurate the results are. After reaching a maximum deviation in the manifold and shield, the Apollo2 600 groups model presents lower deviations in the first layers of the coils region. The important deviations observed on the deeper regions of the TFC are due to low precision of Tripoli4 calculations, for which relative standard deviations are near to 50%.

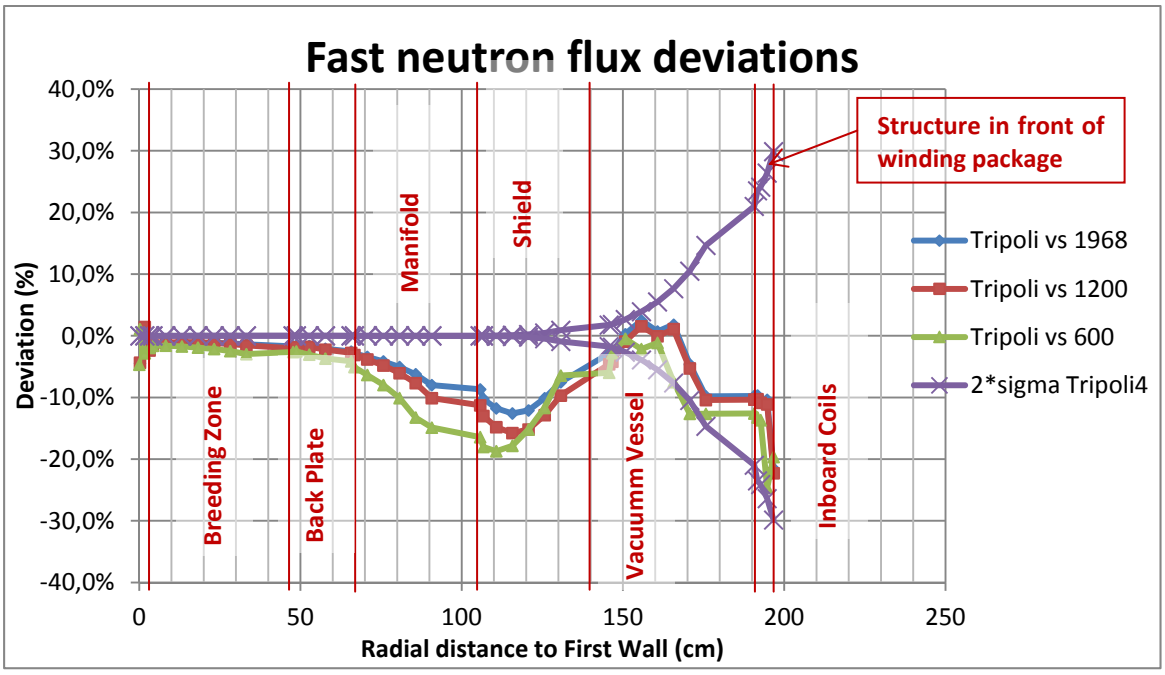

Figure 4-9 : Relative difference between Apollo2 and Tripoli4 results (on peak heat flux)

Deviations obtained between Tripoli4 and Apollo2 show that the deterministic model presents an accurate behavior for the estimation of the peak fast neutron flux. It is clear from these results that deviations from 3D TRIPOLI-4 model results in terms of peak neutron flux are not due to the deterministic model but due to the 1D geometry. Apollo2 is therefore selected to create the plan of experience afterwards; keeping in mind that the most restrictive parameter is the peak fast flux on the inboard coils, the Apollo2 600 groups energy grid model is chosen due to its low deviation for the peak radial flux on the toroidal field structure in front of the winding package and the vacuum vessel but mostly due to a lower calculation time, of about 100s in front of the 400s for the 1200 groups and 600s for the 1968 groups. These features make this model the best choice in terms of performance and CPU usage. A representation of the peak fast heat flux radial profile obtained with Tripoli4 and the Apollo2 600 is presented on Figure 4-10.

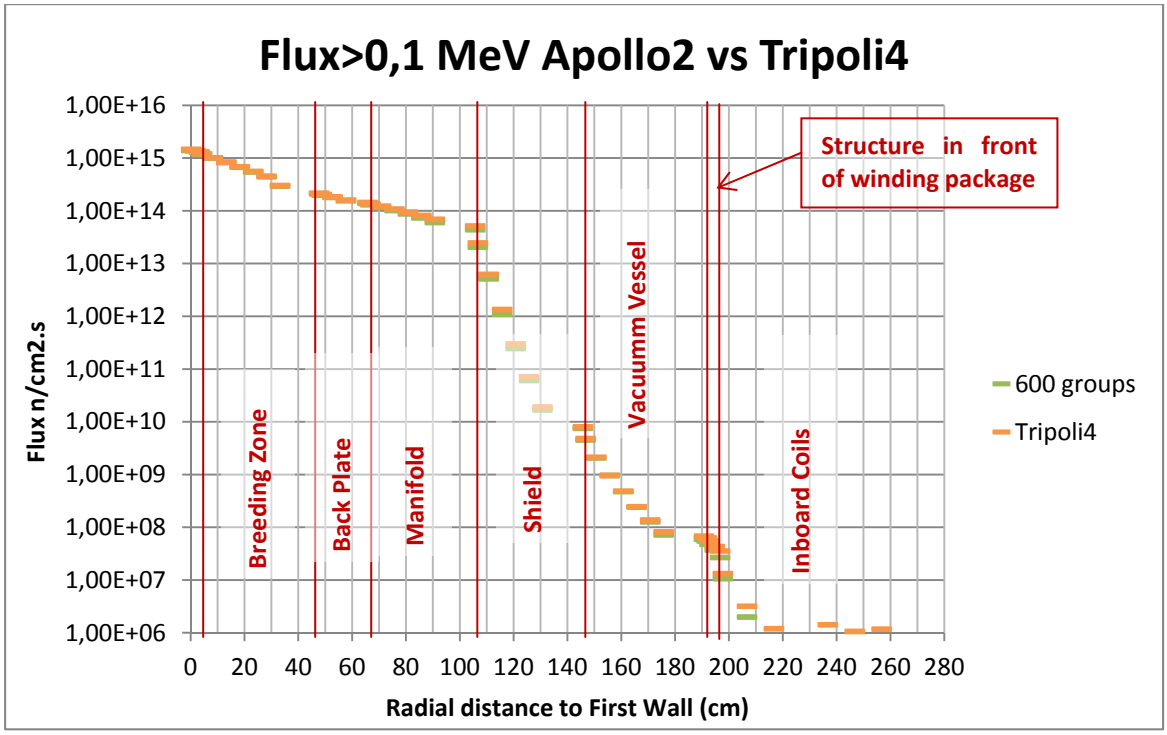

Figure 4-10 : Tripoli4 versus Apollo2 600 peak fast neutron flux profile

It is important to note that in all cases the peak flux obtained with Apollo2 underestimates the results derived from Tripoli4 in the first centimeters. This underestimation coupled with the overestimation committed by the Tripoli4 1D geometry model compared to the real 3D DEMO Tripoli4 model allows to affirm that Apollo2 overestimates of about 50% the fast heat flux in the first centimeters of the tokamak and of about 10% in deeper layers. Therefore, and given the accuracy expected from the pre-design tool and the principle of conservatism that guides this project, the fluxes calculated by the Apollo2 model won't be corrected when creating the plan of experience.

A last validation is done to this 1D geometry model: a comparison between the obtained results and the ones presented on (16). This is done by visually comparing the Figure 4-10 to the radial profile presented on Figure 4-12. The same geometry and composition is used, observing that the calculated peak fast neutron flux on the first centimeters of the inboard toroidal coils is just below the 10^8 decades in both cases. The 1D model is then validated against a reference model but also against studies performed by other teams.

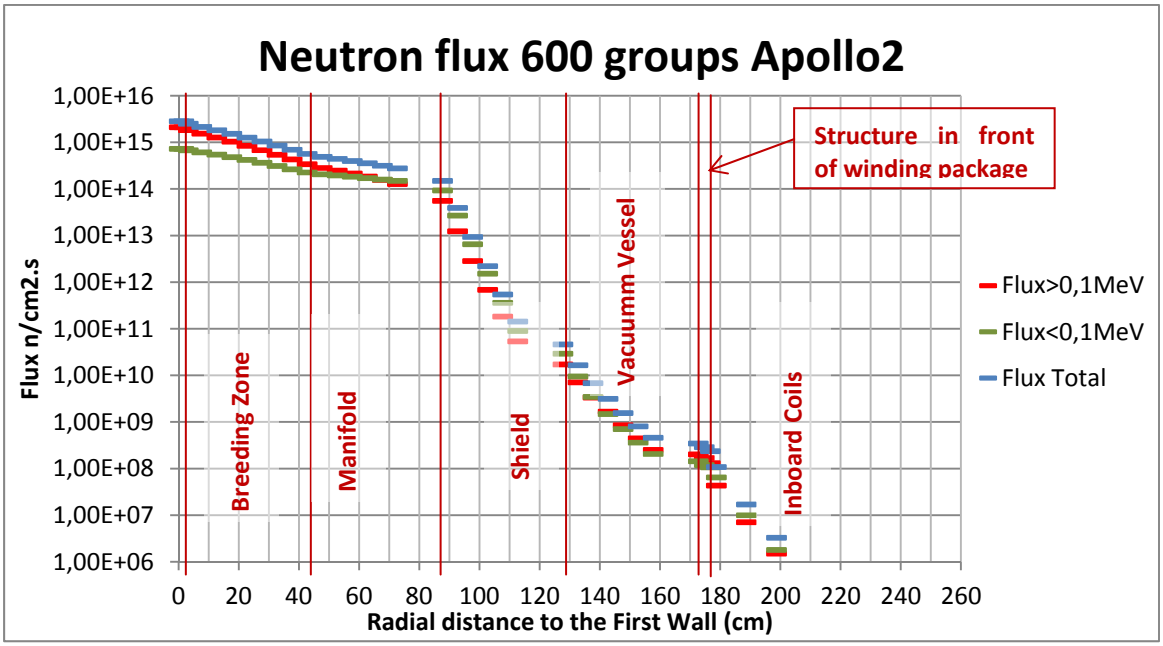

Figure 4-11 : Apollo2 600 neutron flux profile

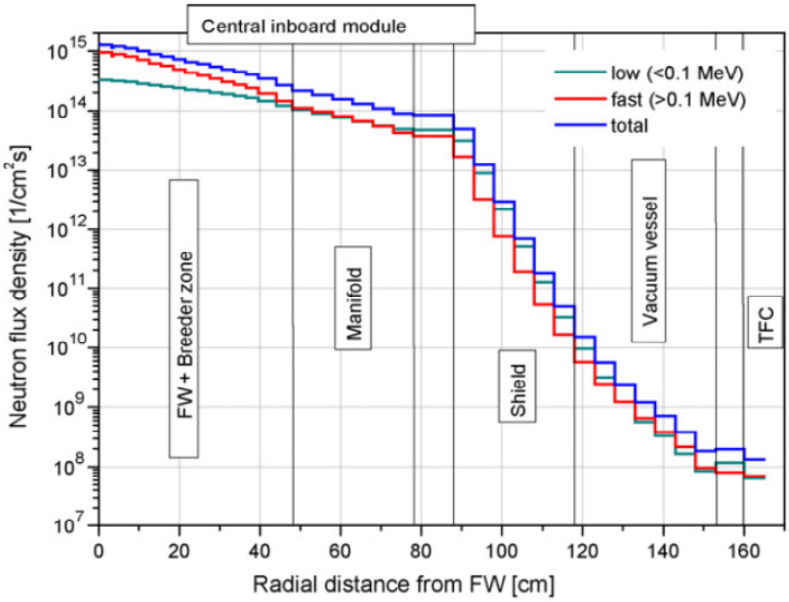

Figure 4-12 : Radial profiles of the neutron fluxes across the inboard torus mid-plane

4.3.2.3 1D Apollo2 model deposited energy

Deposited energy is the last of the studied neutronic variables to be validated. As introduced on 4.3.2.1 the performances study is done comparing the Apollo2 model to the 1D Tripoli4 model. In this case is important to compare the deposited energy derived from the deterministic code with Monte Carlo simulations both with neutron-only and neutron-photon simulations.

As shown in 4.1.1, the energy grid used for calculations on deposited energy is not relevant because deviations do not follow a pattern; the study will be done only with the 600 group

Apollo2 model because it presents the best performances and computation time in terms of peak neutron flux. summarizes the relative deviations on deposited energy Table 4-7. A more detailed table presenting absolurte values is provided on appendix B.6.

		Deviations on Total Deposited Energy					
		Distance to plasma	Apollo2 600 vs Tripoli4 N	Apollo2 600 vs Tripoli4 PN	Tripoli4 N vs Tripoli4 PN	Tripoli4 N sigma	Tripoli4 PN sigma
Inboard	FW	0,2	-2,82%	37,62%	41,61%	0,00	0,01
	BZ10	3,2	-1,66%	-16,38%	-14,96%	0,00	0,01
	BZ	13,2	-0,62%	-8,02%	-7,45%	0,00	0,00
	BP	47,7	9,08%	19,81%	9,84%	0,01	0,03
	MF	65,7	-2,67%	-20,42%	-18,24%	0,01	0,02
	Shield	105,7	-3,74%	4,33%	8,38%	0,01	0,01
	VV	145,7	-21,07%	-48,45%	-34,69%	0,40	0,82
	TFSWP	190,7	-6,44%	-38,14%	-33,88%	9,32	40,47
	TFC	196,7	-52,04%	-57,90%	-12,22%	7,29	14,68
Outboard	FW	0,2	3,49%	54,91%	-33,20%	0,00	0,01
	BZ10	3,2	-17,75%	-29,45%	16,58%	0,00	0,00
	BZ	13,2	-13,12%	-18,61%	6,74%	0,00	0,00
	BP	80,7	7,21%	19,70%	-10,44%	0,01	0,04
	MF	98,7	-2,02%	-11,77%	11,05%	0,01	0,03
	Shield	158,7	-10,80%	-2,89%	-8,14%	0,01	0,02
	VV	218,7	-63,78%	-64,83%	2,99%	5,97	16,12
	TFCS	308,7	-99,99%	-99,99%	-19,30%	29,67	68,08
	TFC	316,7	-100,00%	-100,00%	-42,06%	11,06	22,01

Table 4-7 : Apollo2 deposited energy deviations compared to Tripoli4 1D model

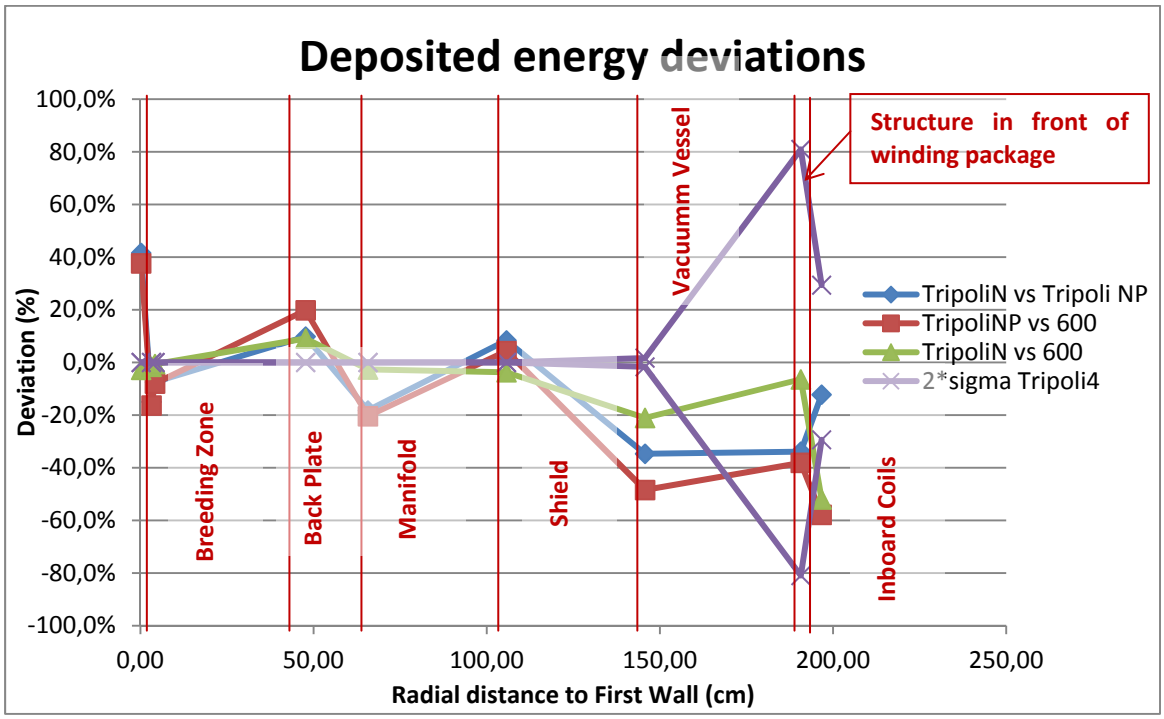

Figure 4-13 : Relative difference between Apollo2 and Tripoli4 results (on deposited energy)

While deviations between Apollo2 and Tripoli4 neutron simulations are within the expected values, study shows that the main error committed is due to neutron-only simulation:

differences between Tripoli4 neutron and neutron-photon simulations are very significant even in the first centimeters of the tokamak. This effect might be observed on Figure 4-13. In addition the committed error is an underestimation of the deposited energy, what might lead to problems with the principle of conservatism. For these reasons the 1D Apollo2 model cannot be used to estimate the deposited energy, at least in critic regions of the tokamak.

Instead, a decision is taken to use the 1D geometry Tripoli4 model to create the plan of experience for estimation of deposited energy in the first layers of the tokamak: first wall, breeding zone, back plate, manifold and shield. In these first tokamak layers calculation time is short enough (about 3000s) to create a plan of experience big enough to design neural networks. Deposited energy on vacuum vessel, TFCs and toroidal coils will be calculated using Apollo2 using a correcting factor that takes into account the deviation observed in Table 4-7 between Apollo2 and Tripoli4 neutron-photon simulation.

4.4. Selection of the final physical models: correcting factors

A benchmark study of each of the models used to calculate the different key neutronic parameters has been performed. Deviations arising from this study are used to define correcting factors used for each neutronic parameter. These correcting factors allow assuring that the results obtained by the physical models used to create neural networks are found within the limits of validity, and no parameter is underestimated or overestimated. All this information has been summarized on Table 4-8. It is important to remark that each neutronic parameter is corrected following the conservatism principle, i.e.: the TBR is underestimated while the peak flux is overestimated.

Neutronic parameters	Unit	Model	Minimum deviation	Maximum deviation	Estimation criteria	Correcting factor
TBR	N.A.	Apollo2 RZ	-1,29%	+1,42%	Underestimate	-1,42%
TBR Ib	N.A.	Apollo2 RZ	-0,92%	+4,65%	Underestimate	-4,65%
TBR Ob	N.A	Apollo2 RZ	-1,62%	+0,81%	Underestimate	-0,81%
Multiplication factor	N.A.	Apollo2 RZ	+1,92%	+2,63%	Underestimate	-2,63%
Peak neutron flux inboard	$\frac{1}{cm^2 \times s}$	Apollo2 1D	+10,82%	+71,41%	Overestimate	0,00%
Deposited energy (fw-sh)	$\frac{MW}{m^3}$	Tripoli4 1D neutron-photon	+3,01%	+90,97%	Overestimate	0,00%
Despoited energy (vv-tfc)	$\frac{MW}{m^3}$	Apollo2 1D	-48,33%	-57,70%	Overestimate	+200%

Table 4-8 : Physical model, deviation and correcting factor for each of the key neutronic parameters studied

Correcting factors calculated here will be used afterwards when creating the surrogate model

5. Coupling the physical model with URANIE

As exposed on methodology, section 2.1, after creating a physical model that represents the physics behind the problem is necessary to create a plan of experience, a big set of samples of input and output parameters. This data base is created with the tool URANIE. As already mentioned a set of input and output parameters is created using LHS method, physical model calculations are performed and results are recuperated and integrated on the plan of experience. A more detailed study is done for each of the physical models.

5.1. Plan of experience RZ geometry Apollo2 model

5.1.1. Creation

This model is used for the estimation of the TBR and deposited energy. An URANIE macro creates a TData Server (TDS), an output file containing the plan of experience. Steps taken to create this TDS are:

1. Creation of a sampler of input parameters.
2. Input parameters are introduced on *calcSurf.py*, the python program described on 3.2.2 that estimates internal parameters used by RZ Apollo2.
3. Input parameters are introduced on the RZ model.
4. Output variables are retrieved from the output Apollo2 file and added to TDS.
5. TDS is written on a file called *resultats.dat*

Given the calculation time for the RZ Apollo2 model of around 500s, a 5.000 samples plan of experience is created.

5.1.2. Evaluation

After creating the plan of experience it is necessary to evaluate its performances. The sensitivity of each parameter to the input variables is assessed and the histogram of the output variables checked. As an example on Figure 5-1 and Figure 5-2 the sensitivity of the TBR to each variable is studied, concluding that the TBR is very sensitive to variations of the BZ composition (a 10% variation on the Eurofer composition corresponds to a 10% variation on the TBR) as well as to the Lithium-6 enrichment and the thicknesses of both the shield and breeding zone. The histogram of the TBR, shown on Figure 5-3, provides information about the representation of all

the regions of the space by the model, in this case a correct distribution is observed, concluding that the plan of experience represents correctly all the possible TBR values.

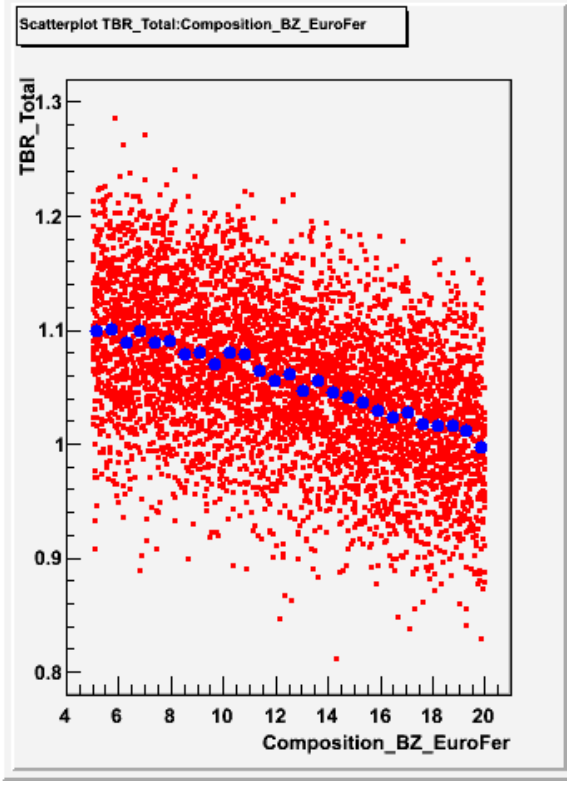

Figure 5-1 : TBR sensitivity to the composition of the Breeding Zone

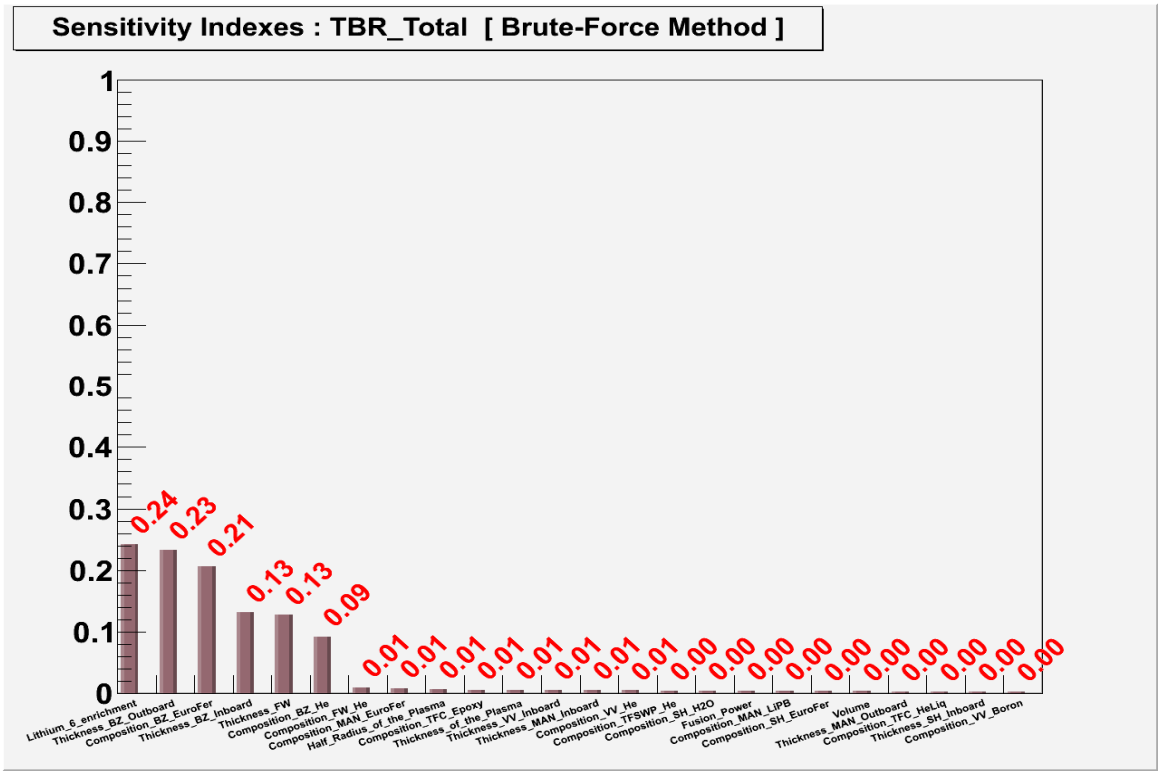

Figure 5-2 : Sensitivity indexes of the TBR

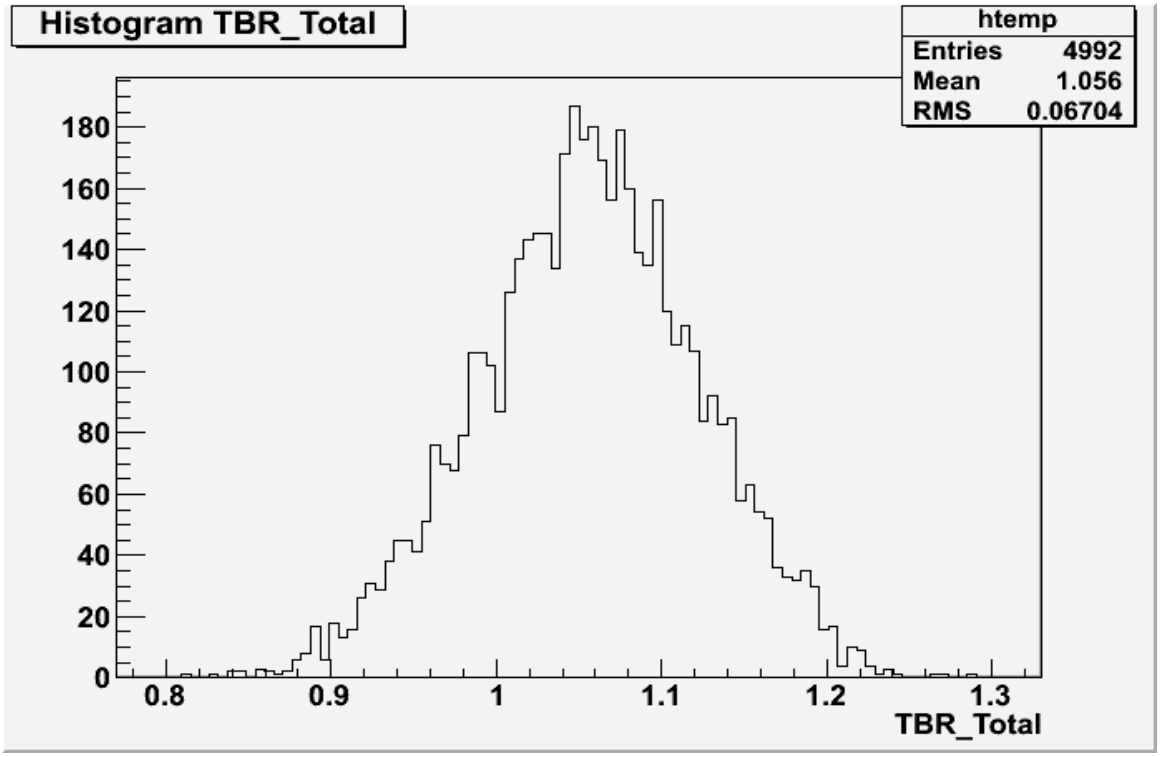

Figure 5-3 : Histogram of the TBR for the 5.000 samples

5.2. Plan of experience 1D geometry Apollo2 model

5.2.1. Creation

This model is used for the estimation of the peak fast neutron flux and deposited energy on the vacuum vessel, TFSWP and TFC. An URANIE macro creates a TData Server (TDS), an output file containing the plan of experience. Steps taken to create this TDS are:

1. Creation of a sampler of input parameters.
2. Input parameters are introduced on the 1D model.
3. Output variables are retrieved from the output Apollo2 file and added to TDS.
4. TDS is written on a file called *resultats.dat*

Given the calculation time for the 1D Apollo2 model of around 200s, a 10.000 samples plan of experience is created.

5.2.2. Evaluation

After early studies it is clear that because of the large variations of the neutron flux the plan of experience does no behave as expected. In this case it is observed that the large operating

windows of the breeding zone and shield cause important variations on the inboard neutron flux and are not suitable for neural network creation. The histogram on Figure 5-4 shows this poor behavior; a large variation zone is represented, two decades, while most of the cases are stuck in a small zone. This poor behavior of the plan of experience makes difficult difficulties the representation of all the space and can cause problems when creating the neural networks.

To solve this issue, the operating range is divided as specified on Figure 5-5.

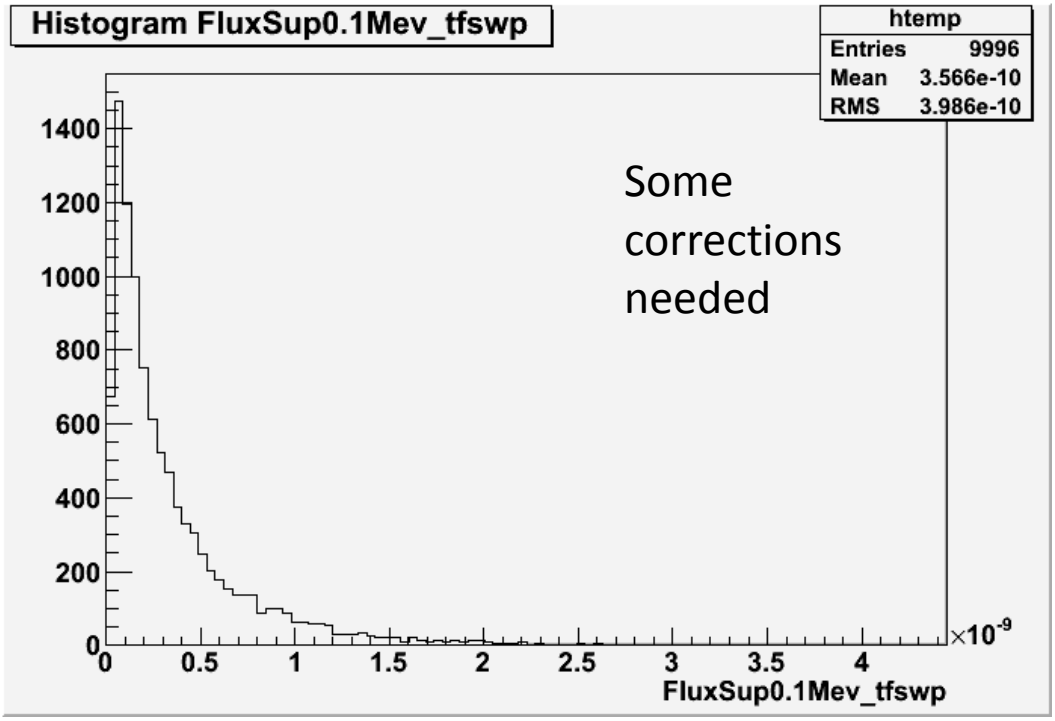

Figure 5-4 : Histogram of the peak neutron flux on the TFSWP

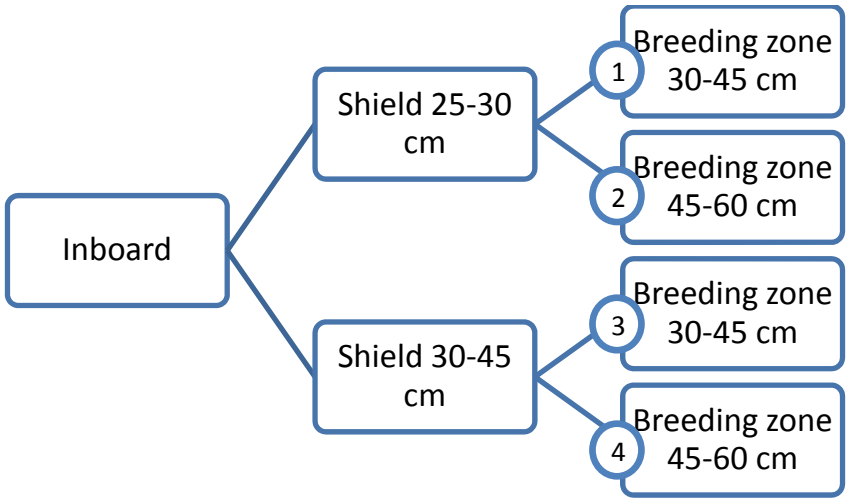

Figure 5-5 : Space phases division to improve neural network performances

After this space division four plans of experience are created for each operating zone, which allows to obtain a better representation of the phases space. Sensitivity indexes, Figure 5-6 and Figure 5-7, and histogram, Figure 5-8, for the 4th zone defined before show this performance amelioration. In the case of the sensitivity indexes it is clear that the division of the space allows a better representation of the physical phenomena, observing a correct response of the neutron flux to variations of the thickness of both the shield and breeding zone. In addition the histogram presents lower variation windows, and the estimated cases are better distributed in space, eliminated the stuck effect observed before. In this case, the most relevant variables when estimating the neutron flux are the thicknesses of shield, breeding zone and vacuum vessel as well as the composition of the breeding zone.

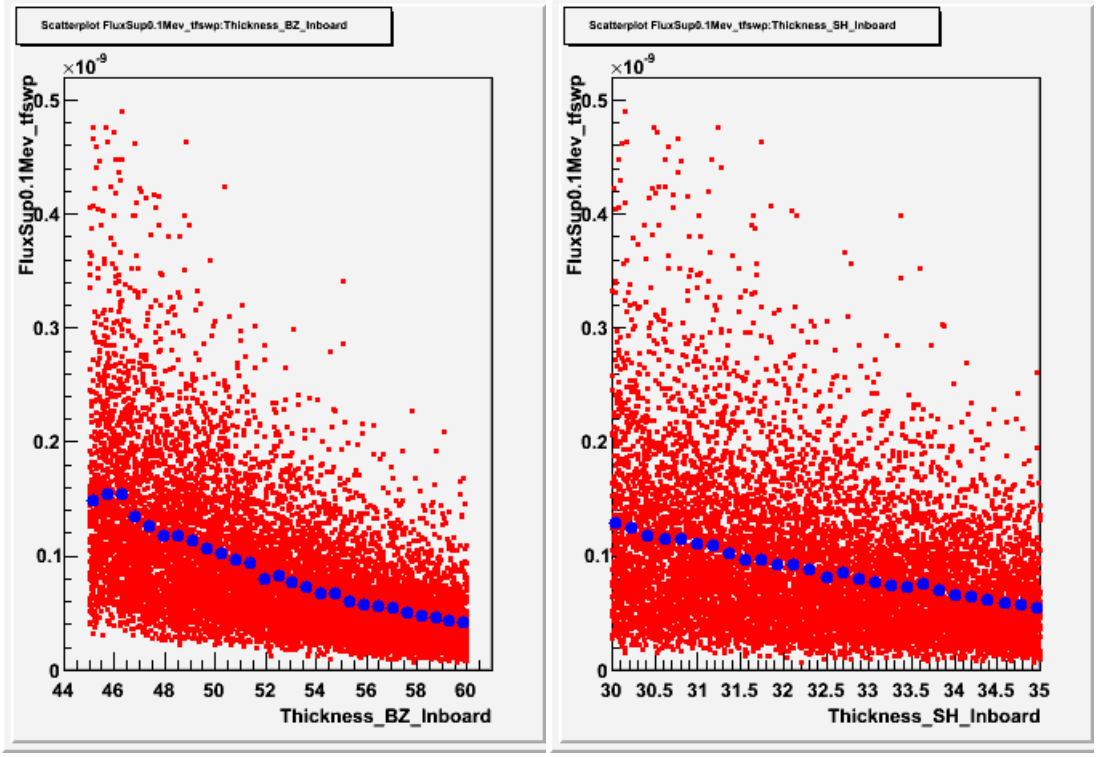

Figure 5-6 : Peak neutron flux on the TFSWP sensitivity to the thickness of the BZ and Shield

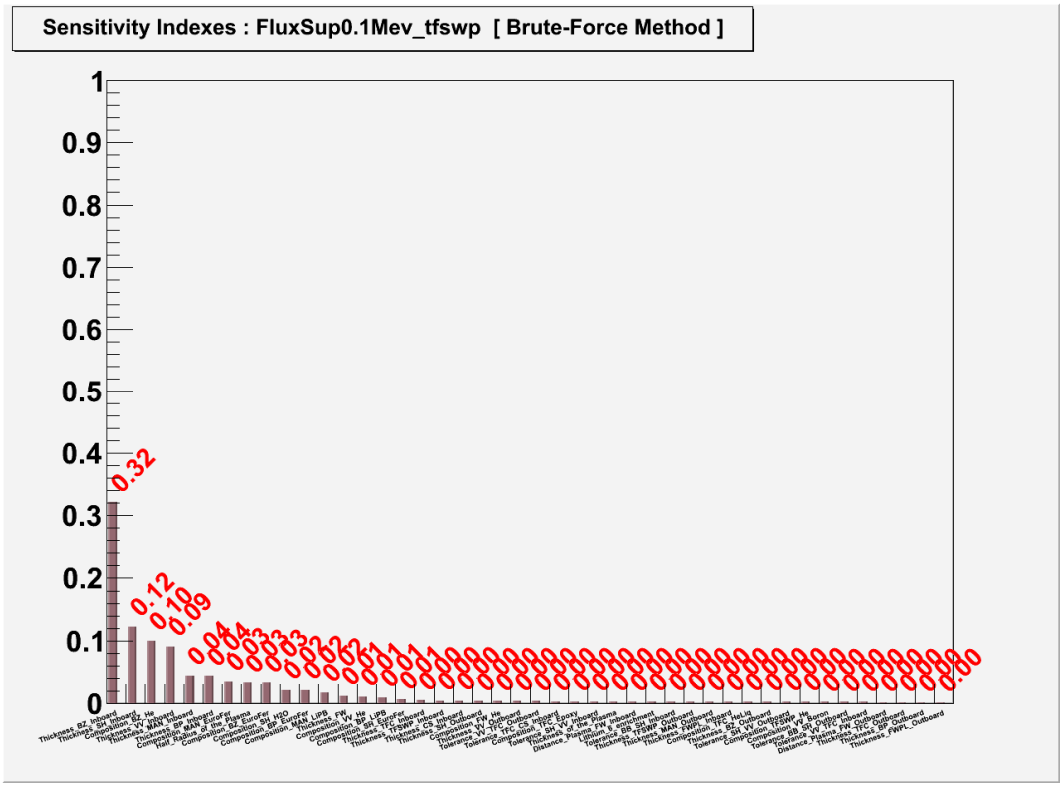

Figure 5-7 : Sensitivity indexes of the peak neutron flux on the TFSWP

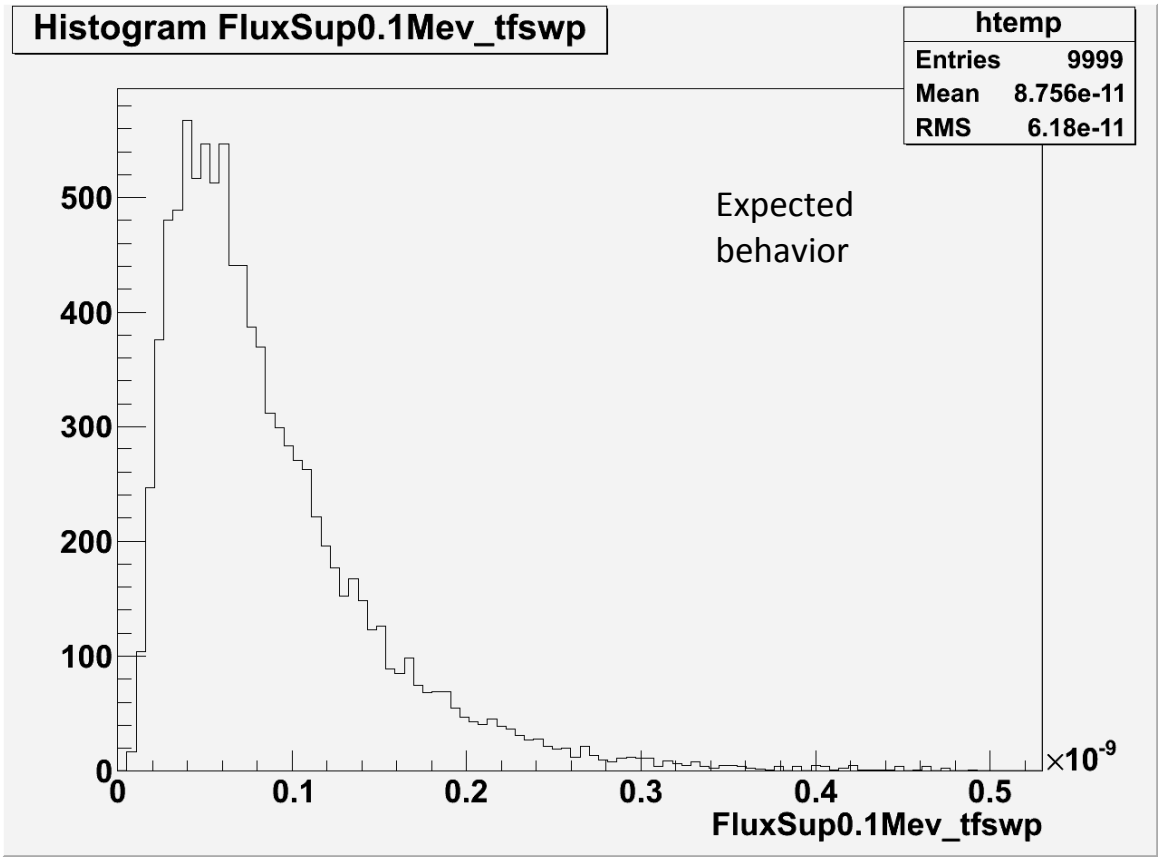

Figure 5-8 : Histogram of the peak neutron flux on the TFSWP for 10.000 samples

5.3. Plan of experience 1D geometry Tripoli4 model

5.3.1. Creation

This model is used for the estimation of the deposited energy on the First Wall, Breeding Zone, Back Plate, Manifold and Shield. To parameterize Tripoli4 for URANIE, python macros are created. In addition, isotopic material compositions are calculated with Apollo2 and embedded on Tripoli4.

An URANIE macro creates a TDS, an output file containing the plan of experience. Steps taken to create this TDS are:

1. Creation of a sampler of input parameters.
2. Input parameters are introduced on the file *param.py* and Apollo2 compositions model.
3. A CShell script called *launcherTripoli.sh* is launched by URANIE.
    a. Launch of the python macro *cylinder.py* that calculates the Tripoli4 geometry for the given inputs.
    b. The Apollo2 compositions model is launched and isotopic compositions are recuperated and embedded on Tripoli4 with the macro *preparation.py*.
    c. The Tripoli4 calculation is launched.
    d. The python macro *recup.py* reads the Tripoli4 output file, calculates the total deposited energy by adding the neutron and photon deposited energies and writes a file called *ouput.dat* that gets the results comprehensible for URANIE.
4. Output variables are retrieved from *output.dat* file and added to TDS.
5. TDS is written on a file called *resultats.dat*

Given the calculation time for the 1D Tripoli4 model of around 5000s, a 1.000 samples plan of experience is created.

5.3.2. Evaluation

The evaluation of the plan of experience is done as for the other models. In this case correct behavior in terms of distribution is observed, as shown in Figure 5-9 which represents the obtained histogram for the deposited energy. This histogram is correctly distributed in the whole variation window validating the plan of experience.

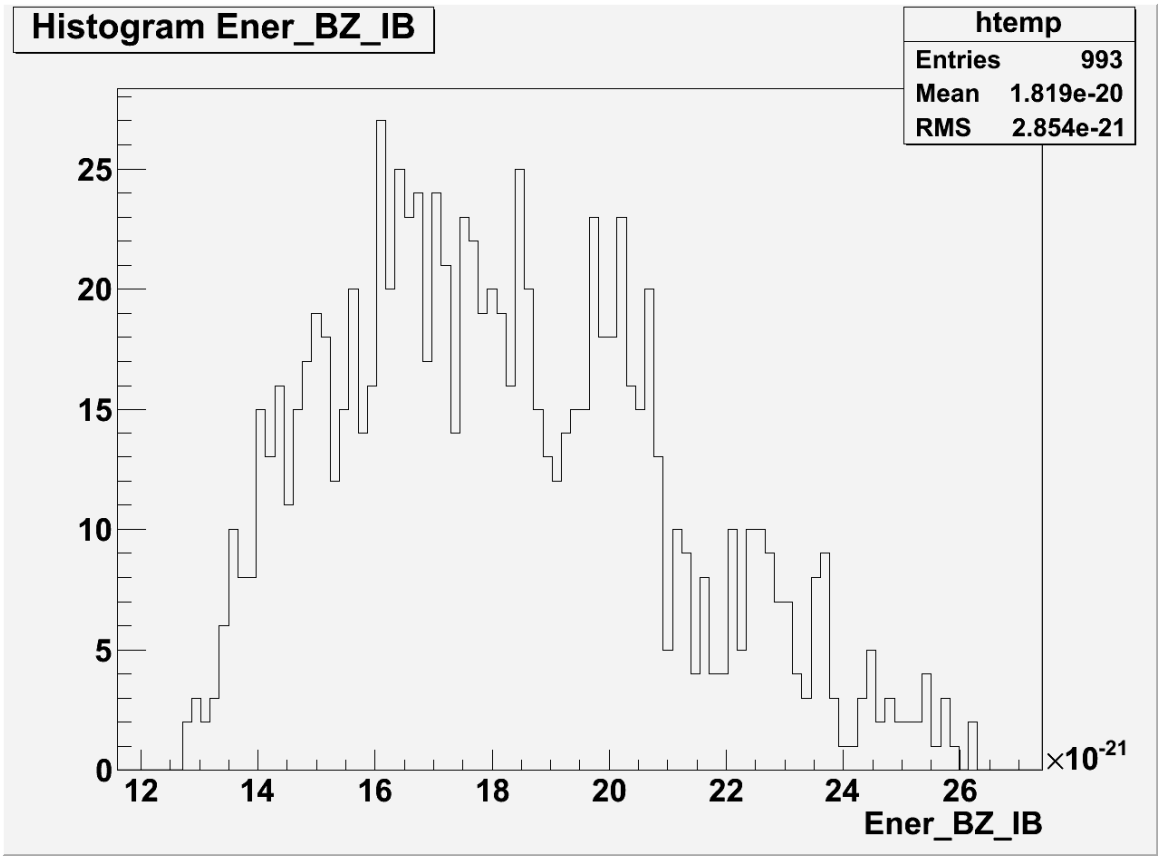

Figure 5-9 : Histogram of the deposited energy on the Breeding Zone inboard for 1.000 samples

5.4. Conclusions on plans of experience

Two plans of experience with the same characteristics have been created for each model, except for the 1D model where 10 plans of experience have been built due to the division of the input paramters operating window. The first plan of experience will be used as training base for the neutral network and the other one as test base.

The quality of obtained plans has been assessed and the 1D model has been modified in order to improve its behavior. The sensitivity of the output variables to the input parameters has also been checked giving the expected trends.

6. Creation of neural networks using URANIE

The creation of physical models describing the neutronic phenomena taking place in a thermonuclear reactor has been performed to create a surrogate model that allows the estimation of key neutronic parameters. Neural networks have been chosen to build this surrogate model. In this chapter the creation of neural networks will be described. The selection of the neural networks to be used by the surrogate model will also be specified.

6.1. Neural networks

6.1.1. Creation of neural networks

An introduction to neural networks (NN) has been done on 2.1.3 and will be extended here. The science behind the creation of NN is complex and is not the object of this study, nonetheless a short description is given hereafter for completeness. A neural network is a complex response function composed of interconnecting artificial neurons, programming constructors, which mimic the properties of a given physical model. The creation a neural network is then based on the *training* of the artificial networks to behave as predicted by a given physical model. In this case, the neural network is an adaptive system that changes its structure based on the information provided by a set of known cases that flows through the network during the learning phase. The neural network is then a non-linear statistical data modeling tool used to model complex relationships between inputs and outputs as shown on Figure 6-1.

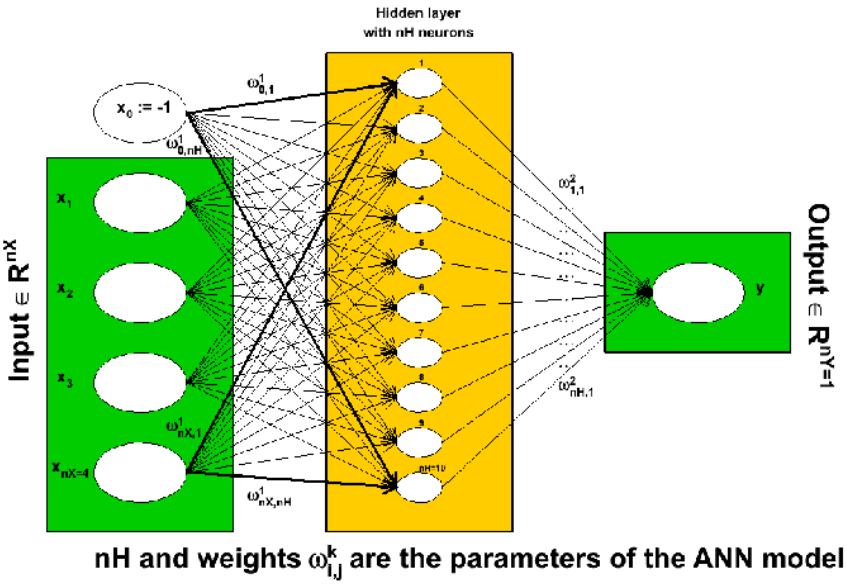

Figure 6-1 : Artificial neural network schema

The Uranie tool used to create plans of experience contains a module called *Modeler* that allows the creation of neural networks. This module allows creating neural networks with one hidden layer by defining the input parameters and the desired output variable of a given plan of experience created before. The number of neurons of the hidden layer needs to be also specified. The creation of the neural network is launched by using a specific Uranie macro called *TANNModeler*. The number of interconnections depends on the number of inputs, samples on the plan of experience and number of parameters used, and the number of neurons of the hidden layer.

The *TANNModeler* macro reads all the samples in the plan of experience, *base of training*, rearranges them randomly to avoid any dependence due to correlations present during the creation of the plan of experience and creates a neural network with the specified number of neurons on the hidden layer. The result is a C++ function that uses a pointer to an array of doubles as input and gives a pointer to an array of doubles as output, as shown on Code 6-1. The active function used by Uranie is the hyperbolic tangent, a function that allows the estimation of the output variable with each neuron of the hidden layer. An example of neural network estimating the TBR is provided on appendix B.7.

```
#define ActivationFunction(sum)          ( tanh(sum) )
void Fctener_man_ob_W_Rn_1_0(double *param, double *res)
```

Code 6-1 : Neural network C++ function header

6.1.2. Evaluation of neural networks

After creating a neural network its performances are evaluated. In order to do so two plans of experience are used: the same plan of experience used to create the neural network, or *base of training*, and a "virgin" plan of experience never seen by the neural network called *base of test.*

The evaluation of the neural networks is done by studying the differences between the output variables estimated by the neural networks and the original physical model. In this case the deviations studied are:

- Standard deviation between the physical model and the neural network
- Standard normalized deviation between the physical model and the neural network
- Average deviation between the physical model and the neural network
- Absolute average deviation between the physical model and the neural network
- Maximum deviation between the physical model and the neural network
- Maximum normalized deviation between the physical model and the neural network

These parameters allow to choose the optimal number neurons of the hidden layers for each output variable and are calculated for the two plans of experience: *base of training* and *base of test*. One might think that the larger the number of neurons on the hidden layers the more accurate the results are; however an overlearning phenomenon occurs during the creation of neural networks, causing the neural network to follow the plan of experience points more than the physical phenomena that links inputs to outputs, as shown, e.g., on Figure 6-2 and Figure 6-3. The utilization of the *base of test* seeks to avoid this phenomenon by evaluating the neural network with samples never evaluated. An example of the typical behavior of a neural network for different neurons of the hidden layer is provided on Figure 6-4, it is also important to remark that due to stochastical effects when creating neural networks it is important to create different trials with the same number of neurons on the hidden layer to obtain a performing neural network.

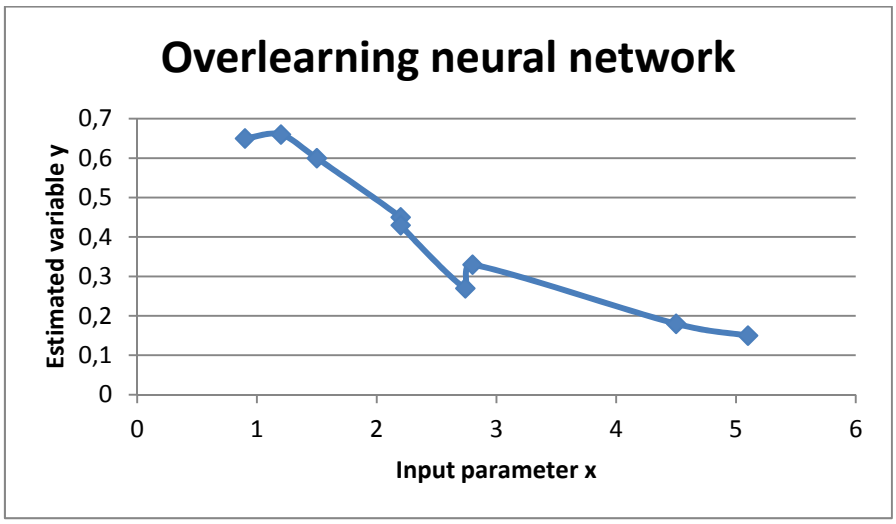

Figure 6-2 : Example of an overlearning neural network response

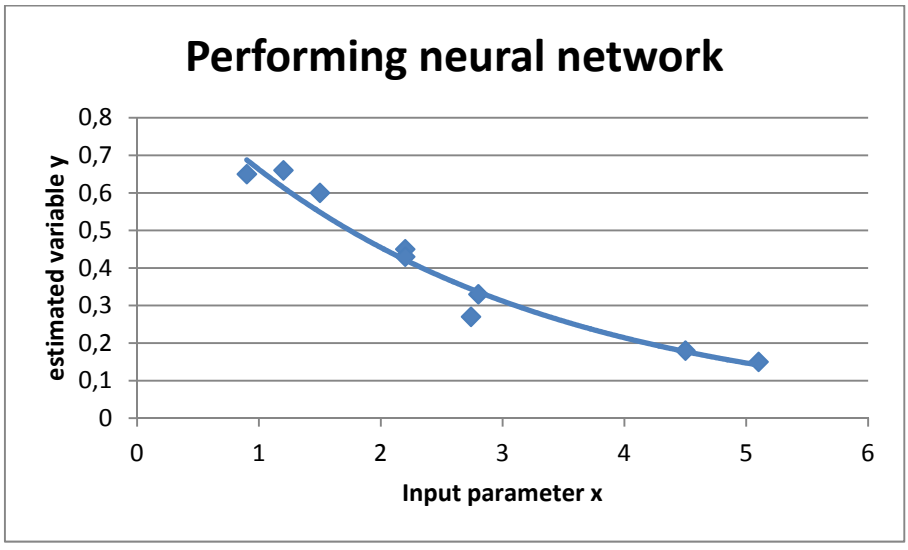

Figure 6-3 : Example of a performing neural network response

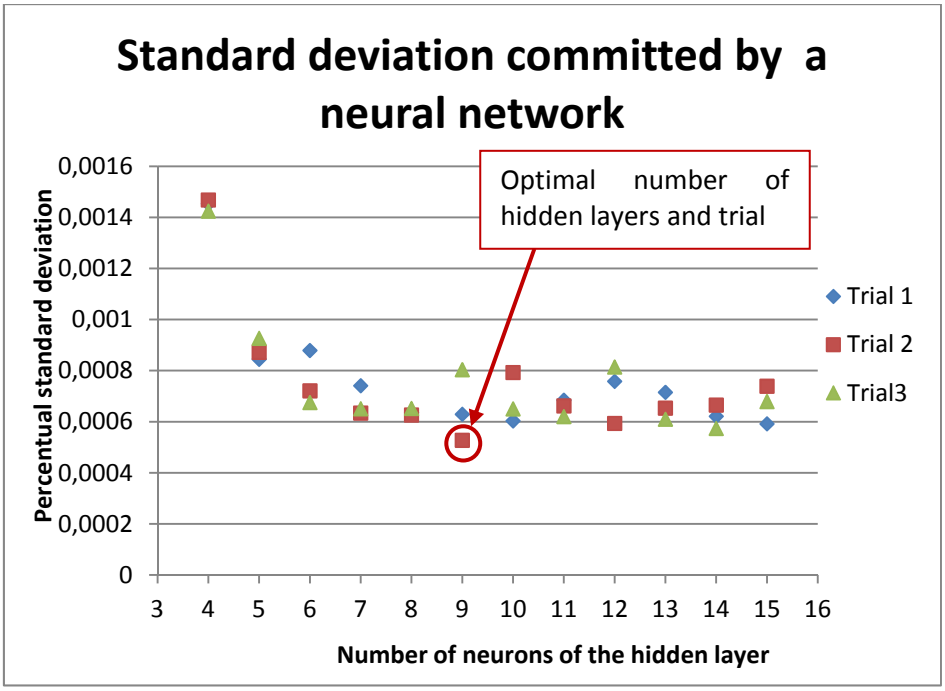

Figure 6-4 : Standard deviations observed for different NN depending on number of hidden layers for the total TBR

It is also possible to evaluate the performances of a neural network by plotting the results obtained with the neural network against the original values calculated with the reference physical model, an example for the TBR is provided on Figure 6-5. This analysis allows a visual study of the performances of a neural network and the localization of strange samples if they exist.

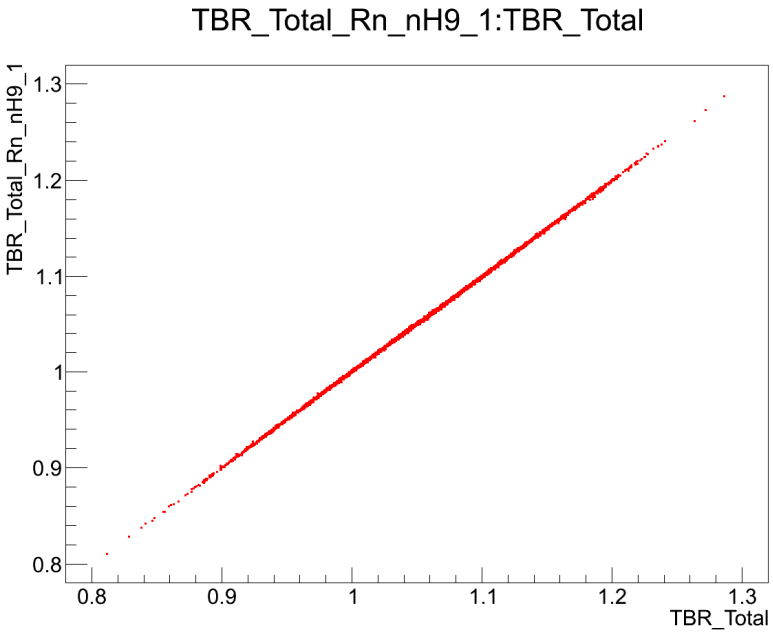

Figure 6-5 : Total TBR estimated with a neural network of 9 neurons against TBR estimated with Apollo2

Previous studies (25) concluded that for a non-linear artificial neural network the 95% of the estimated values are valid in a range of three sigma. Following this argument obtained results are corrected to overestimate or underestimate, following the principle of conservatism, three times the standard deviation obtained from the performance study of the neural network.

6.1.3. Automatization of the creation and evaluation of neural networks

Based on previous works (25) an Uranie macro that simplifies and automates the creation of neural networks is written. This macro creates a large number of neural networks within a previously defined window of possible neurons of the hidden layer, evaluates their behavior for the *base of traning* and the *base of test* and creates a file summarizing the errors and deviations observed. It is a fully parameterizable macro where input parameters and the desired output variable are defined as well as the names of the training and test bases. An example of the file created by this macro is reported on appendix B.8.

This macro gives a note to each neural network.. This note is calculated by weighting each of the deviations studied according to some predefined factors. The neural network with the lowest note is then chosen because it presents the lowest deviations.

6.2. Neural networks and correcting factors

Neural networks for each parameter are created using the plans of experience defined on chapter 5. All the neural networks created for each parameter are studied and evaluated and the most performing one is chosen to be used in the surrogate model. A detailed table containing the neural networks' characteristics as well as their performances is provided on appendix B.9.

At this point all the possible sources of error have been studied. Deviations due to the physical models have been studied on section 4.4 and those due to the neural networks have been studied on this section. With all this information a table summarizing the correcting factors applied to the estimated neutronic parameters is created and shown on Table 6-1. In this table the standard deviation between the neural network and the physical model and the percentual standard deviation, the percentual overestimation or underestimation comparing the NN and the reference code, as well as the three sigma correction applied to the obtained results and the correcting factor due to the physical model are reported.

Neutronic parameter	Standard deviation NN	3sigma (3*standard deviation)	Percentual standard deviation NN	Correcting factor due to physical model *
TBRTot	8,73E-04 (N.A.)	2,62E-03	0,05%	1,42%
TBRIb	3,19E-04 (N.A.)	9,57E-04	0,08%	4,65%
TBROb	8,70E-04 (N.A.)	2,61E-03	0,07%	0,81%
ME	1,39E-04 (N.A.)	4,16E-04	0,01%	2,63%
EnerFWIb	3,09E-22 (MW/m^3)	9,27E-22	0,40%	0,91%
EnerBZ10Ib	1,60E-22 (MW/m^3)	4,80E-22	0,25%	0,40%
EnerBZIb	7,24E-23 (MW/m^3)	2,17E-22	0,24%	0,31%
EnerBPIb	2,49E-23 (MW/m^3)	7,46E-23	1,39%	1,97%
EnerMANIb	2,59E-23 (MW/m^3)	7,76E-23	1,41%	1,54%
EnerSHIb	5,40E-23 (MW/m^3)	1,62E-22	1,00%	0,95%
EnerVVIb	3,95E-24 (MW/m^3)	1,19E-23	1,96%	200,00%
EnerTFSWPIb	5,72E-25 (MW/m^3)	1,72E-24	2,36%	200,00%
EnerTFCIb	1,10E-25 (MW/m^3)	3,31E-25	2,65%	200,00%
EnerFWOb	2,46E-22 (MW/m^3)	7,37E-22	0,24%	0,58%
EnerBZ10Ob	1,59E-22 (MW/m^3)	4,78E-22	0,21%	0,25%
EnerBZOb	5,07E-23 (MW/m^3)	1,52E-22	0,21%	0,18%
EnerBPOb	1,36E-23 (MW/m^3)	4,09E-23	2,36%	2,18%
EnerMANOb	1,08E-23 (MW/m^3)	3,23E-23	1,71%	1,43%
EnerSHOb	1,48E-23 (MW/m^3)	4,43E-23	1,67%	1,08%
EnerVVOb	2,34E-26 (MW/m^3)	7,03E-26	81,02%	200,00%
EnerTFSWPOb	9,22E-29 (MW/m^3)	2,77E-28	5,96%	200,00%
EnerTFCOb	1,07E-29 (MW/m^3)	3,20E-29	5,94%	200,00%
FluxFWIbsh1bz1	7,84E-07 (1/cm^{2}s)	2,35E-06	0,05%	0,00%
FluxBZIbsh1bz1	8,45E-07 (1/cm^{2}s)	2,54E-06	0,05%	0,00%
FluxBPIbsh1bz1	5,08E-07 (1/cm^{2}s)	1,52E-06	0,13%	0,00%
FluxMANIbsh1bz1	5,67E-07 (1/cm^{2}s)	1,70E-06	0,24%	0,00%
FluxSHIbsh1bz1	2,61E-07 (1/cm^{2}s)	7,84E-07	0,34%	0,00%
FluxVVIbsh1bz1	3,74E-10 (1/cm^{2}s)	1,12E-09	1,32%	0,00%
FluxTFSWPIbsh1bz1	1,99E-11 (1/cm^{2}s)	5,97E-11	1,53%	0,00%
FluxTFCIbsh1bz1	1,25E-11 (1/cm^{2}s)	3,75E-11	1,80%	0,00%
FluxFWIbsh1bz2	8,39E-07 (1/cm^{2}s)	2,52E-06	0,05%	0,00%
FluxBZIbsh1bz2	7,78E-07 (1/cm^{2}s)	2,33E-06	0,04%	0,00%
FluxBPIbsh1bz2	3,66E-07 (1/cm^{2}s)	1,10E-06	0,18%	0,00%
FluxMANIbsh1bz2	3,09E-07 (1/cm^{2}s)	9,28E-07	0,24%	0,00%
FluxSHIbsh1bz2	1,20E-07 (1/cm^{2}s)	3,61E-07	0,31%	0,00%
FluxVVIbsh1bz2	1,26E-10 (1/cm^{2}s)	3,79E-10	1,25%	0,00%
FluxTFSWPIbsh1bz2	5,35E-12 (1/cm^{2}s)	1,61E-11	1,39%	0,00%
FluxTFCIbsh1bz2	2,99E-12 (1/cm^{2}s)	8,96E-12	1,64%	0,00%
FluxFWIbsh2bz1	7,89E-07 (1/cm^{2}s)	2,37E-06	0,05%	0,00%
FluxBZIbsh2bz1	8,02E-07 (1/cm^{2}s)	2,41E-06	0,05%	0,00%
FluxBPIbsh2bz1	5,72E-07 (1/cm^{2}s)	1,72E-06	0,15%	0,00%
FluxMANIbsh2bz1	6,24E-07 (1/cm^{2}s)	1,87E-06	0,25%	0,00%
FluxSHIbsh2bz1	1,81E-07 (1/cm^{2}s)	5,42E-07	0,25%	0,00%
FluxVVIbsh2bz1	1,25E-10 (1/cm^{2}s)	3,76E-10	1,24%	0,00%
FluxTFSWPIbsh2bz1	7,57E-12 (1/cm^{2}s)	2,27E-11	1,23%	0,00%
FluxTFCIbsh2bz1	4,21E-12 (1/cm^{2}s)	1,26E-11	1,41%	0,00%
FluxFWIbsh2bz2	9,00E-07 (1/cm^{2}s)	2,70E-06	0,05%	0,00%

FluxBZIbsh2bz2	7,47E-07 (1/cm^{2}s)	2,24E-06	0,05%	0,00%
FluxBPIbsh2bz2	4,32E-07 (1/cm^{2}s)	1,30E-06	0,20%	0,00%
FluxMANIbsh2bz2	3,86E-07 (1/cm^{2}s)	1,16E-06	0,29%	0,00%
FluxSHIbsh2bz2	1,23E-07 (1/cm^{2}s)	3,70E-07	0,32%	0,00%
FluxVVIbsh2bz2	3,30E-11 (1/cm^{2}s)	9,91E-11	1,08%	0,00%
FluxTFSWPIbsh2bz2	2,12E-12 (1/cm^{2}s)	6,35E-12	1,34%	0,00%
FluxTFCIbsh2bz2	1,06E-12 (1/cm^{2}s)	3,18E-12	1,30%	0,00%

Table 6-1 : Correcting factors due to neural networks deviations and physical model

***For the deposited energy on FW, BZ, BP, MAN and SH this is the Tripoli4 uncertainty (sigma)**

7. Creation of the surrogate model

At this stage of the project a large number of functions, neural networks, capable of calculating key neutronic parameters of a thermonuclear fusion reactor have been created. It is now necessary to integrate all these neural networks in a program that treats input parameters, performs the geometry check, launches calculations with neural networks and presents the results in a suitable form. This program will practically represent the surrogate model, the main objective of the project.

This surrogate model will be integrated on SYCOMORE, a multiphysics platform that serves as basis for the thermonuclear fusion reactor system code. It is therefore necessary to meet certain requirements imposed by the platform:

1. The model could be written on python, C++, Matlab, Scilab, Fortran, xml, and should avoid to rely on any external software (Apollo, Tripoli or Uranie) in order to avoid any installation/compilation/licence issue.
2. It is suitable that it is self sufficient and contains all necessary modules to execute it on any machine.
3. External variables (input and output parameters) need to be declared on a specific way and accordingly to a nomenclature that has been chosen to declare them in specific SYCOMORE databases which represents Consistent Physical Objects (CPO), as e.g. the breeding blanket.

These restrictions imposed by the platform complicate the surrogate model creation. Steps taken to create the surrogate model are detailed in this chapter.

7.1. Coupling python and C++

The first step to integrate the surrogate model in SYCOMORE is the coupling of the neural networks written on C++ with python. Different macros and modules that allow python to directly call functions written on C++ (such as Swig) are considered, but those are refused due to their complexity and their non-standard character.

Instead, a less polyvalent but easier and more elegant solution is taken: the compilation of the C++ neural network programs into dynamic libraries easily callable from python with the standard module *ctypes* (26).

The compilation of a C++ program is an easy step, but in this case it is necessary to change the header of the program in order to make the function callable from external programs. The original header and the modified one are presented on Code 7-1 and Code 7-2 respectively.

```
#define ActivationFunction(sum)          ( tanh(sum) )
void Fctener_man_ob_W_Rn_1_0(double *param, double *res)
```

Code 7-1 : Neural network C++ function original header

```
#include <stdio.h>
#include <math.h>
#define ActivationFunction(sum)          ( tanh(sum) )
extern "C" void fct_nn (double *param, double *res)
```

Code 7-2 : Neural network C++ function lodified header

This modification of the header allows calling the function "fct_nn" from python using the *ctypes* module. It is important to keep in mind the kind of variables used by the C++ program, a pointer to an array of real both for the input and outputs. Once the header is modified the compilation of the C++ function is done, Code 7-3, creating a shared library ".so" callable from python. The code that allows charging the dynamic libraries from python and sends the input and output pointers is presented on Code 7-4.

```
g++ --shared my_NN.C -o my_NN.so
```

Code 7-3 : Compilation of a C++ function into a shared library

```
def load_nn(key,param,res):
      function = cdll.LoadLibrary(nn_files[LuT[key],2])
      return function.fct_nn(param.ctypes.data_as(c_void_p), byref(res))
```

Code 7-4 : Charging a C++ shared library from python

The neural network functions created on chapter 6 are now usable objects that a python program is capable of calling to estimate neutronic parameters.

7.2. The Neutronic Module

The neutronic surrogate model is now ready to plug it in SYCOMORE. It is written in the form of a universal python program that calls dynamic libraries to estimate the neutronic parameters defined at the beginning of the project. The structure used is detailed on Figure 7-1, the following structure of files can be found on the distribution package: (all files are available on appendix C.1)

- `launcher.py` – main python script file that launches the calculations
- `functions.py` – a python file containing support functions for the main script
- `neuralnetworks.py` – a python file containing the path to call the NN and their performances
- `inputs.py` – a python file containing the input parameters values

- `NN` – a folder containing the NN used by the model in form of dynamic libraries ".so"
- `HCLL_DEMO_NEUTRONIC_MODULE_ReleaseNotes.pdf` – a user manual

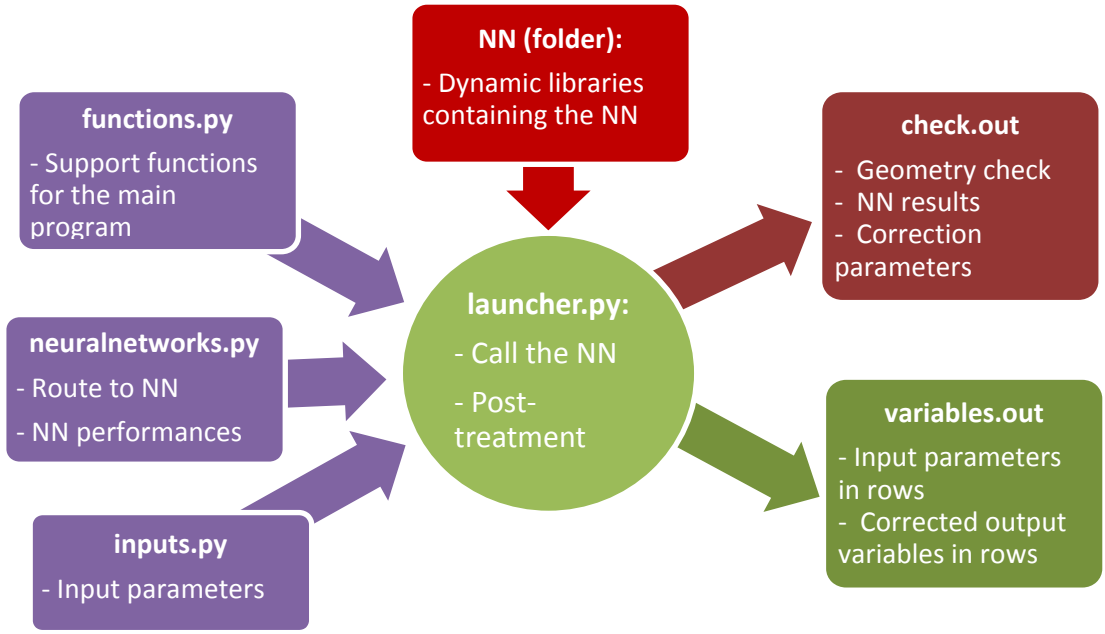

Figure 7-1 : structure of the python neutronic module

One of the restrictions imposed by SYCOMORE is the declaration of the input parameters. The *inputs.py* file is created following these guidelines and is shown on Code 7-5.

```
#Input parameters stored in rows

Fusion_Power = 2385                          # MW
Volume = 1870                                # m^3
Lithium_6_enrichment =    0.90               # %
Half_Radius_of_the_Plasma =  7.5000          # m
Thickness_of_the_Plasma =  2.4600            # m
Thickness_CS_Inboard =   0.7430              # m
Thickness_TFC_Inboard =   0.7400             # m
Thickness_TFSWP_Inboard =    0.0600          # m
Thickness_VV_Inboard =   0.3500              # m
Thickness_SH_Inboard =   0.3000              # m
Thickness_MAN_Inboard =   0.3000             # m
Thickness_BP_Inboard =   0.1800              # m
Thickness_BZ_Inboard =   0.4450              # m
Thickness_FW =    0.0300                     # m
Thickness_FWPL_Inboard =    0.0020           # m
Thickness_TFC_Outboard =   0.9300            # m
Thickness_TFSWP_Outboard =    0.0800         # m
Thickness_VV_Outboard =   0.8000             # m
Thickness_SH_Outboard =   0.5000             # m
Thickness_MAN_Outboard =   0.5000            # m
Thickness_BP_Outboard =   0.1800             # m
Thickness_BZ_Outboard =   0.7700             # m
Thickness_FWPL_Outboard =    0.0020          # m
Tolerance_TFC_CS_Inboard =   0.1000          # m
Tolerance_VV_TFC_Inboard =   0.1000          # m
```

```
Tolerance_SH_VV_Inboard =    0.1000          # m
Tolerance_BB_SH_Inboard =    0.1000          # m
Tolerance_VV_TFC_Outboard =    0.1000        # m
Tolerance_SH_VV_Outboard =    0.1000         # m
Tolerance_BB_SH_Outboard =    0.1000         # m
Distance_Plasma_FW_Inboard =    0.1300       # m
Distance_Plasma_FW_Outboard =    0.1500      # m
Composition_FW_He =    30.00                # %
Composition_BZ_EuroFer =    10.00           # %
Composition_BZ_He =    10.00                # %
Composition_BP_LiPB =     5.00              # %
Composition_BP_EuroFer =    28.00           # %
Composition_MAN_LiPB =     5.00             # %
Composition_MAN_EuroFer =    28.00          # %
Composition_SH_EuroFer =    10.00           # %
Composition_SH_H2O =    25.00               # %
Composition_VV_He =    37.00                # %
Composition_VV_Boron =     2.00             # %
Composition_TFSWP_He =     5.00             # %
Composition_TFC_Epoxy =    18.00            # %
Composition_TFC_HeLiq =    17.00            # %
Triangulation =     0.47                    # no unit
Elongation =     1.90                       # no unit
Surface_Div_Inboard =     5.50              # %
Surface_Div_Outboard =     6.50             # %
```

Code 7-5 : Declaration of the input variables in *inputs.py*

The *launch.py* file, the main program, reads the input parameters and checks that they are within the operating windows of the model, creates the arrays of parameters used by each neural network, charges the dynamic libraries, recuperates the estimated values, corrects them taking into account the corresiton factors presented on Table 6-1, normalizes them and creates two output text files.

The two output files containing detailed information about the steps followed by the program and the estimated parameters are simple text files that store information on rows. An example of these generated files is available on appendix C.1. The characteristics of the output files are:

- `check.out` :
  - Geometry check: checkup of the geometry consistency.
  - Creation: checkup of the creation of the variables arrays
  - Neural network calculations: writing of the calculated value, the correcting factors and the final estimated value derived corrected and normalised
- `variables.out` (see Code 7-6):
  - Input parameters: rewriting of the input parameters and dimensions
  - Normalization factor: writing of the normalization factors used by the program
  - Output variables: writing of the estimated neutronic parameters in rows. Dimensions are also specified.

```
TBRTot =  1.1164 no unit
TBRIb =  0.2768 no unit
TBROb =  0.8348 no unit
ME =  1.1534 no unit
EnerFWIb =   11.67 MW.m^-3
EnerBZ10Ib =   9.372 MW.m^-3
EnerBZIb =    4.36 MW.m^-3
EnerBPIb =  0.2578 MW.m^-3
EnerMANIb =  0.2887 MW.m^-3
EnerSHIb =  0.8013 MW.m^-3
EnerVVIb = 0.0003293 MW.m^-3
EnerTFSWPIb = 3.497e-05 MW.m^-3
EnerFWOb =   15.07 MW.m^-3
EnerBZ10Ob =   11.59 MW.m^-3
EnerBZOb =   3.194 MW.m^-3
EnerBPOb = 0.07182 MW.m^-3
EnerMANOb =   0.061 MW.m^-3
EnerSHOb = 0.08902 MW.m^-3
EnerVVOb = 1.366e-07 MW.m^-3
EnerTFSWPOb = 8.958e-10 MW.m^-3
FluxFWIb = 1.3989e+15 n.cm^-2.s^-1
FluxBZIb = 1.2861e+15 n.cm^-2.s^-1
FluxBPIb = 2.1098e+14 n.cm^-2.s^-1
FluxMANIb = 1.4107e+14 n.cm^-2.s^-1
FluxSHIb = 4.4966e+13 n.cm^-2.s^-1
FluxVVIb = 8.0649e+09 n.cm^-2.s^-1
FluxTFSWPIb = 3.9139e+08 n.cm^-2.s^-1
```

Code 7-6 *: variables.out* automatically generated file

The *variables.out* file contains the output parameters stored in rows in order to make them readable for the SYCOMORE code.

It should be emphasized that this neutronic module can be used individually without being integrated into SYCOMORE. The user only needs to edit the *inputs.py* file and change the variables for numeric values in the specified magnitudes.

8. Environmental impact

The ultimate goal of the SYCOMORE code is to perform optimization of the main parameters of a tokamak, in terms of geometries and material compositions, complying with a number of key parameters of the physic of plasmas and neutronics. A multi-criteria optimization is based on a large number of iterations around a base model that lead to an optimal model that meets the restrictions. The number of iterations can range from 1.000 to 10.000 or even 100.000 cases.

The neutronic module developed here performs one estimation of the neutronic parameters in about 0.1 seconds using one processor, while a Monte Carlo Tripoli-4 simulation, with uncertainty values similar to the ones obtained with the developed model, takes about 48 hours using 60 processors[1]. It is therefore clear that the developed model is able to save not only computation time but also electric energy.

The power consumption is calculated for the IBM x3755 M3 servers used by the CEA clusters, which uses a 1100W power supply. These servers feature 4 processors with 8-cores per processor, so 32 cores per server. The power consumption per core is 34.375 W.

Another source of power consumption is the large refrigeration systems needed to refrigerate those servers. A hypothesis is done here considering that all the power consumed by a processor is transformed into heat, therefore it is necessary to cool 34.375 W per core. Considering a 33% efficiency of the refrigeration systems the power consumed per core is 103.125 W per core.

The total consumption per core is estimated to be 137.5 W. The total energy consumptions for the 1.000 and 10.000 cases are estimated on Table 8-1. Energy savings are also detailed as well as the CO_2 emissions[2]. It is noted that the reduction in both electricity consumption and in emissions is substantial, involving reductions of almost 100% in power consumption and CO_2 emissions.

[1] Benchmark for a cluster using 8-core AMD Opteron 6200 @ 3.0GHz processor with 36Gb ram (30)
[2] As estimated by the French *Réseau de Transport d'Electricité* 83kg CO^2/MWh during 2011 (29)

	Item	Time per iteration per core	Energy (kWh)	CO^2 emissions (kg)
1.000 iterations	Neutronic module	$0{,}1\ \frac{s}{iter \times core}$	0,003819	3.17×10^{-3}
	Tripoli-4 simulation	$2880\ \frac{h}{iter \times core}$	396.00	32.87
	ENERGY & EMISSION SAVINGS		**~ 396.00 kWh**	**~ 32.87**

	Item	Time per iteration per core	Energy (kWh)	CO^2 emissions (kg)
10.000 iterations	Neutronic module	$0{,}1\ \frac{s}{iter \times core}$	38.19	3.17
	Tripoli-4 simulation	$2880\ \frac{h}{iter \times core}$	396.000.00	32.868.00
	ENERGY & EMISSION SAVINGS		**395.961.81**	**32.864.83**

Table 8-1 : Energy consumptions, CO_2 emissions and savings

Beyond the environmental impact that the project has in terms of energy consumption, the reduction of computation time and the development of a system code for fusion reactors facilitates research in this area, improving the long iterative processes of research and therefore shortening, slightly, the terms to create nuclear fusion reactors. An improvement in delays concerning the investigation of fusion energy has great depth both environmentally and socially, bringing a clean, safe and cheap energy to society.

Conclusions

The methodology, based on the utilization of neural networks for the creation of a surrogate model, has been validated. Deterministic fully-parameterizable 1D and RZ tokamak models have been created and validated against a Monte Carlo reference model. Correcting factors have been chosen to assure the compliance with the principle of conservatism. Large set of samples containing input and output parameters, called plans of experience, have been created using the tokamak model. Response functions estimating the neutronic parameters have been created using neural networks. A surrogate model for the HCLL-blanket thermonuclear-fusion-reactor neutronic-parameters estimation has been created following the guidelines imposed by SYCOMORE.

The tool estimates the neutronic parameters: TBR; multiplication factor (M_E); radial profile of the peak fast neutron flux and deposited energy on each layer of the tokamak. The calculations are valid within the operating windows of the surrogate model.

Compared to a Monte Carlo TRIPOLI-4 DEMO HCLL 3D reference model, deviations up to ~3% are observed for the TBR and the M_E, and can attain values as high as ~10% to ~50% for the peak neutron flux. Deviations on deposited energy for the first layers of the tokamak, from first wall to shield, range from ~1% to ~50%, while they can attain values as high as ~60% for the vacuum vessel and toroidal field coils a overestimation factor of 200% has been used on these layers. Obtained values are corrected with these deviations automatically.

The project's objective has been achieved, creating a parameterizable surrogate model that allows estimating key neutronic parameters of an HCLL-blanket thermonuclear fusion reactor with short computation times, of about 0.1 seconds, with acceptable performances for a pre-design tool.

Improvement in future stages of the project is to be had by ameliorating the physical model that represents the tokamak. A TRIPOLI-4 parameterizable model based on elliptic toroids could be used to improve results substantially in terms of TBR, M_E, peak neutron flux and deposited energy. Computation time of the surrogate model does not depend on the physical model but higher computation times to create the plans of experience should be expected when using Monte Carlo simulations as a physical model.

Budget

The project being a research work, associated costs to the development of the surrogate model are mostly due to codes and tools, access to scientific reports and previous knowledge, computational resources and the salary of a trained nuclear engineer. Following these premises, total costs that have allowed the development of the project and the creation of the program have been calculated. A table summarizing costs and revenues is available on Table 0-1.

Item	Cost per unit	Units	Cost (€)
Engineer salary [3]	150.000,00 €/year	6 months	75.000,00
Science papers and books [4]	~ 40€/book	3 books	120,00
Computational resources [5]	26.40 €/hour	320 hours	8.448,00
TRIPOLI v4.8 License [6]	0,00 €/license	1 license	0,00
Apollo v2.8.3 License [6]	0,00 €/license	1 license	0,00
URANIE v3.0.2 License [6]	0,00 €/license	1 license	0,00
PROJECT COST		**TOTAL:**	**83.568,00 €**

Table 0-1 : Project budget

It is important to stress that due to the complexity of computing the overall costs of a research institution as large as the CEA to a single project, the costs due to scientific sources and computational resources are estimated, but in all cases overestimated compared to the actual cost computed to the CEA.

With all this estimations the total cost of the project is 83.568€.

[3] As estimated by the CEA human resources
[4] Estimated price for (28) and other sources
[5] As estimated by the CEA technical and computational services
[6] Price of a licence for research objectives

Acknowledgments

I want to thank all those who have framed and helped me during these past 5 months internship at SERMA. I thank first of all my tutors, Antonella Li Puma and Jean Charles Jaboulay, for their enthusiasm, their patient, their explanations, their guidance and their invaluable advice and support. I also thank Javier Dies for his help and support from the UPC since the beginning of the project.

I particularly want to thank Pierre Lasseur and Karim Ammar for their availability and unwavering support dealing with problems and bugs. I also thank Clement Fausser for his teachings in nuclear fusion technologies, and other topics, and Celine Guenaut for her assistance with IT problems.

I also thank Patrick Blanc-Tranchant and Alain Aggery, officials SERMA and LPEC respectively, for welcoming me in the service and Jocelyne Corona and Jocelyne Sevilla for their help in the administrative field.

A big thank to students and PhD students of SERMA for their help and support on a daily basis, and the entire LPEC team.

Also give thanks to the international relations services of the UPC, especially to Jose Parra for his dedication and attention during this year and the previous ones, thanking them for the granted Erasmus internship scholarship.

Finally thank the indispensable help of all my family and friends throughout the project. Especially thank the unconditional support of my parents who have helped and encouraged me to the realization of this project.

Bibliography

1. **SOFT 2012.** *27th Symposium on Fusion Technology (SOFT).* [Online] 2012. http://www.soft2012.eu/.

2. **Fusion Engineering and Design.** Fusion Engineering and Design. *Elsevier.* [Online] 2012. http://www.journals.elsevier.com/fusion-engineering-and-design/.

3. **The European Atomic Energy Community .** *EURATOM.* [Online] 08 2012. http://www.euratom.org/.

4. **International Thermonuclear Experimental Reactor.** *ITER.* [Online] 08 2012. www.iter.org.

5. **Fusion for Energy.** F4E. [Online] 08 2012. http://fusionforenergy.europa.eu.

6. **European Fusion Development Agreement.** *EFDA.* [Online] 08 2012. http://www.efda.org.

7. **Comissariat à l'Energie Atomique.** *Tore Supra.* [Online] EURATOM-CEA, 2012. http://www-drfc.cea.fr/cea/ts/ts.htm.

8. **A. Li Puma, J. Bonnemason, L. Cachon, J.L. Duchateau, F. Gabriel.** Consistent integration in preparing the helium cooled lithium lead DEMO-2007 reactor. *Fusion Engineering and Design.* June 2009, Vol. 84, 7-11, pp. 1197-1205.

9. **Jordanova, Jordan.** *Evaluation of the volumetric heat distribution, shielding and tritium breeding capabilities of the HCLL DEMO breeder blanket.* Bulgaria : EFDA Technology Workprogramme 2004, 2005. FU06-CT-2004-00025.

10. **McKay, M. D. and Beckman, R. J.** *Technometrics.* Los Alamos : American Statistical Association, 1979.

11. **Chinnek, John W.** *Practical Optimization: A Gentle Introduction.* Ottawa, Canada : Carleton University, 2000.

12. **PROJET APOLLO2.** *APOLLO2: MANUEL DE REFERENCE DE LA VERSION 2.8-3.* Saclay : CEA, 2011. SERMA/LLPR/RT/11-5070/.

13. **TRIPOLI-4 Project Team.** *TRIPOLI-4 VERSION 8 USER GUIDE.* Saclay : CEA, 2011. SERMA/LTSD/RT/11-5185/A.

14. **X-5 Monte Carlo Team.** *MCNP — A General Monte Carlo N-Particle Transport Code, Version 5.* Los Alamos : Los Alamos National Laboratory, 2008. LA-UR-03-1987.

15. **Gaudier, Fabrice.** *User manual for Uranie.* Saclay : CEA DEN/DANS/DM2S/SFME/LGLS, 2012.

16. **U. Fischer, P. Pereslavtsev, D. Grosse, V. Weber, A. Li Puma, F. Gabriel.** Nuclear design analyses of the helium cooled lithium lead blanket for a fusion. *Fusion Engineering and Design.* Elsevier, 2010, Vol. 85, 1133-1138.

17. **VIGNITCHOUK, Ladislas.** *Modélisation d'une couverture tritigène et de son shield avec le code APOLLO-2.* Saclay : CEA, 2011.

18. **MOSCA, Pietro.** *Conception et développement d'un mailleur énergétique adaptatif pour la génération des bibliothèques multigroupes des codes de transport.* Saclay : CEA, 2010. CEA-R-6245.

19. **Fausser, Clément, et al.** *Tokamak D-T neutron source & transgen code.* Saclay : Commissariat à l'Energie Atomique, December 2010. DEN/DANS/DM2S/SERMA/LPEC/RT/10-4992.

20. **F.Gabriel, C. Fausser and.** *TRIPOLI-4 Validation & Use for Fusion Blankets.* Saclay : s.n., 2010. DEN/DANS/DM2S/SERMA/LPEC/RT/10-4993/A.

21. *Principes théoriques et méthodologie pour la validation de JEF2.2. Application à la réalisation d'ERALIB1, bibliothèque de données neutroniques pour le calcul des systèmes à spectre rapide.* **Fort, E., Assal, W., Rimpault, G., Rowlands, J., Smith, P., Soule, R.** Saclay : CEA, 2003.

22. **Fausser, Clement, et al.** *Tokamak D-T neutron source models for different plasma physics confinement modes.* Saclay : CEA, 2011.

23. **Fausser, Clément.** *Notice et outil de calcul pour tests d'échanges de données sans objectif de pré-dimensionnement.* Saclay : CEA DEN/DANS/DM2S/SERMA/LPEC, 2011. 11MMBV000049.

24. **Fischer, U.** *Multi-dimensional Neutronics Analysis of the "Canister Blanket" for NET.* Karlsruhe, Germany : Kernforschungszentrum Karlsruhe, 1987. KfK4255.

25. **Ammar, Karim.** *Mise en place d'une démarche de conception de cœur de RnR-Na par plan d'expérience* . Saclay : INSTN, 2010.

26. **Martelli, Alex, et al.** *Python par l'example.* s.l. : O'Reilly Editions, 2006. 2841773795 .

27. **U. Fischer, P. Pereslavtsev.** *Neutronic Analyses for the Conceptual Design of a HCLL Reactor.* Germany : Forschungszentrum Karlsruhe, March 2005. Final Report on task TW4-TRP-002.

28. **Stacey, Weston N.** *Fusion, An introduction to the Physics and Technology of Magnetic Confinement Fusion.* 2nd Edition. Atlanta : WILEY-VCH, 2011.

29. **Réseau de transport d'électricité.** *Bilan electrique.* La Defense : PARIMAGE, 2012.

30. **IBM.** IBM System X. *IBM smarter computing.* [Online] 2012. http://www-03.ibm.com/systems/x/.

Electronic version

Final Thesis
Industrial Engineer

Development of a surrogate model for simplified neutronic calculations involved in the design stage of a thermonuclear fusion reactor

Volume II

APPENDIX A: Parameters, geometries and definitions
APPENDIX B: Results
APPENDIX C: Programs and codes

Author:	Javier Martínez Arroyo
Thesis Director:	Antonella Li Puma
Thesis Co-Director:	Jean-Charles Jaboulay
University Director:	Javier Dies Llovera
Session:	September 2012

Commissariat à l'Energie Atomique
DEN/DANS/DM2S/SERMA/LPEC
Centre de Saclay

Escola Tècnica Superior
d'Enginyeria Industrial de Barcelona

Table of Contents

(Volume I)

Registration Sheet

Abstract

Glossary of signs, symbols, abbreviations, acronyms and terms 7

Preface 9

i. Context 9

ii. Organizations overview 9

iii. Thesis topic in the context 11

iv. Host organization 13

v. Brief introduction to fusion reactors 13

vi. Presentation of the HCLL DEMO thermonuclear reactor 14

1. Introduction 17

2. Methodology 19

2.1. Approach 19

2.1.1. Selection of a physical model for the proposed problem 19

Ideal response function 19

2.1.2. Creation of a plan of experience 20

Physical Model 20

2.1.3. Sensitivity analysis and creation of a response function 22

2.2. Presentation of the codes and tools 26

2.2.1. Apollo2 27

2.2.2. Tripoli4 27

2.2.3. Uranie 28

3. Creation of a parameterized physical model describing the neutronic behaviors of a thermonuclear fusion reactor 31

3.1. Parameterization of the Apollo2 model 32

3.2. Geometry definition of the Apollo2 model 32
3.2.1. 1-Dimension Cylindrical Geometry 32
3.2.2. R-Z Square-Based Geometry 33
3.3. Materials' compositions and definitions 35
3.4. Source definition 36
3.4.1. Energy spectrum 37
3.4.2. Spatial Spectrum 41
3.5. Energy corrections and gamma transport 41
3.6. Scores and result post-treatment 41
3.6.1. 1D Model 42
3.6.2. RZ Model 43
4. Validation of the Apollo2 model 45
4.1. Comparison between different Apollo2 energy grids 45
4.1.1. 1D Apollo2 model 45
4.2. Development of a Monte-Carlo model using Tripoli4 48
4.2.1. 3D Geometry Tripoli4 48
4.2.2. 1D Geometry Tripoli4 51
4.2.3. Neutron and Neutron-Photon simulations 52
4.3. Validation of the Apollo2 model with Tripoli4 55
4.3.1. RZ geometry model 55
4.3.2. 1D geometry model 56
4.3.2.1 1D Tripoli4 model validation 56
4.3.2.2 1D Apollo2 model peak fast neutron flux 58
4.3.2.3 1D Apollo2 model deposited energy 62
4.4. Selection of the final physical models: correcting factors 64
5. Coupling the physical model with URANIE 65
5.1. Plan of experience RZ geometry Apollo2 model 65

5.1.1. Creation 65
5.1.2. Evaluation 65
5.2. Plan of experience 1D geometry Apollo2 model 67
5.2.1. Creation 67
5.2.2. Evaluation 67
5.3. Plan of experience 1D geometry Tripoli4 model 71
5.3.1. Creation 71
5.3.2. Evaluation 71
5.4. Conclusions on plans of experience 72
6. Creation of neural networks using URANIE 73
6.1. Neural networks 73
6.1.1. Creation of neural networks 73
6.1.2. Evaluation of neural networks 74
6.1.3. Automatization of the creation and evaluation of neural networks 77
6.2. Neural networks and correcting factors 77
7. Creation of the surrogate model 81
7.1. Coupling python and C++ 81
7.2. The Neutronic Module 82
8. Environmental impact 87
Conclusions 89
Budget 91
Acknowledgments 93
Bibliography 95
Electronic version 99

(Volume II)

A. Appendix : Parameters, geometries and definitions 107
A.1. Input geometry parameters 107

A.2. Input materials' composition parameters 109

A.3. Other input parameters 111

A.4. Output variables 111

A.5. TBR and M_E definitions 113

A.6. 1-Dimension Cylindrical Geometry 115

A.7. RZ Square-Based Geometry 117

B. Apendix : Results 119

B.1. Apollo2 Peak Radial Flux Results 119

B.2. Apollo2 Energy Deposition Results 120

B.3. RZ Apollo2 performances 121

B.4. 1D Tripoli4 performances 122

B.5. 1D Apollo2 peak neutron flux performances 125

B.6. 1D Apollo2 deposited energy performances 128

B.7. Example of neural network 129

B.8. Neural network performances example 132

B.9. Chosen neural network performances 138

C. Apendix : Programs and Codes 149

C.1. Neutronic Module 149

A. Appendix : Parameters, geometries and definitions

A.1. Input geometry parameters

	Name	Type	Description	Unit	Mean value (Fischer 2010)	Maximum Value	Minumim Value
General	geom_axis_r	scal	Radius of the plasma from the center of the Tokamak	m	7,50E+00	9,00E+00	7,00E+00
	a_minor	scal	Radial thickness of the plasma. This parameter is common for both the inboard and outboard in the equatorial section	m	2,46E+00	2,60E+00	2,40E+00
	tria	scal	Tringularity of the plasma boundary		4,70E-01	7,00E-01	4,00E-01
	elongation	scal	Elongation of the plasma boundary		1,90E+00	2,20E+00	1,80E+00
	dr_pl_bb_ib	scal	Gap between the plasma and the first wall protective layer (inboard) in the equatorial section	m	1,30E-01	5,00E-02	1,50E-01
	dr_pl_bb_ob	scal	Gap between the plasma and the first wall protective layer (outboard) in the equatorial section	m	1,50E-01	5,00E-02	2,00E-01
	fdivin	scal	Percentage of the divertor in the inboard	%	5,50%	6,00%	5,00%
	fdivout	scal	Percentage of the divertor in the outboard	%	6,80%	7,00%	6,00%
Inboard	dr_fwpl_ib	scal	radial thickness of the FW Protective Layer (Inboard)	m	2,00E-03	3,00E-03	1,00E-03
	dr_fw_ib	scal	radial thickness of the FW (Inboard)	m	3,00E-02	4,00E-02	2,00E-02
	dr_bz_ib	scal	radial thickness of the BZ (between the FW wall and the 1st back plate wall)	m	4,45E-01	6,00E-01	3,00E-01
	dr_bp_ib	scal	radial thickness of the back plate (Inboard)	m	1,80E-01	2,50E-01	1,50E-01
	dr_man_ib	scal	radial thickness of the banana manifold common to all modules(Inboard)	m	3,00E-01	3,50E-01	2,50E-01
	dr_bb_sh_ib	scal	Gap between the breeding blanekt module and the shield (inboard) in the equatorial section	m	1,00E-01	1,20E-01	8,00E-02
	dr_sh_ib	scal	radial thickness of the shield (Inboard)	m	3,00E-01	3,50E-01	2,50E-01
	dr_sh_vv_ib	scal	Gap between the shield and the vacuum vessel (inboard) in the equatorial section	m	1,00E-01	1,20E-01	8,00E-02
	dr_vv_ib	scal	radial thickness of the vacuum vessel (Inboard)	m	3,50E-01	4,00E-01	3,00E-01
	dr_vv_tfc_ib	scal	Gap between the vacuum vessel and the toroidal field coils (inboard) in the equatorial section	m	1,00E-01	1,20E-01	8,00E-02
	dr_tfswp_ib	scal	radial thickness of the toroidal field structure infront of the winding package (Inboard)	m	6,00E-02	7,00E-02	5,00E-02
	dr_tfc_ib	scal	radial thickness of the toroidal field coils (Inboard)	m	7,40E-01	7,80E-01	7,00E-01
	dr_tfc_cs_ib	scal	Gap between the the toroidal field coils qnd the central selenoide (inboard) in the equatorial section	m	1,00E-01	1,20E-01	8,00E-02
	dr_cs_ib	scal	radial thickness of the central selenoide(Inboard)	m	7,43E-01	7,60E-01	7,20E-01
Outboard	dr_fwpl_ob	scal	radial thickness of the FW Protective Layer (outboard)	m	2,00E-03	3,00E-03	1,00E-03
	dr_fw_ob	scal	radial thickness of the FW (outboard)	m	3,00E-02	4,00E-02	2,00E-02
	dr_bz_ob	scal	radial thickness of the BZ (between the FW wall and the 1st back plate wall)	m	7,75E-01	9,00E-01	6,00E-01
	dr_bp_ob	scal	radial thickness of the back plate (outboard)	m	1,80E-01	2,50E-01	1,50E-01
	dr_man_ob	scal	radial thickness of the banana manifold common to all modules (outboard)	m	5,00E-01	5,50E-01	4,50E-01
	dr_bb_sh_ob	scal	Gap between the breeding blanekt module and the shield (outboard) in the equatorial section	m	1,00E-01	1,20E-01	8,00E-02
	dr_sh_ob	scal	radial thickness of the shield (outboard)	m	5,00E-01	5,50E-01	4,50E-01
	dr_sh_vv_ob	scal	Gap between the shield and the vacuum vessel (outboard) in the equatorial section	m	1,00E-01	1,20E-01	8,00E-02
	dr_vv_ob	scal	radial thickness of the vacuum vessel (outboard)	m	8,00E-01	8,30E-01	7,70E-01
	dr_vv_tfc_ob	scal	Gap between the vacuum vessel and the toroidal field coils (outboard) in the equatorial section	m	1,00E-01	1,20E-01	8,00E-02
	dr_tfswp_ob	scal	radial thickness of the toroidal field structure infront of the winding package (outboard)	m	8,00E-02	9,00E-02	7,00E-02
	dr_tfc_ob	scal	radial thickness of the toroidal field coils (outboard)	m	9,30E-01	9,60E-01	9,00E-01

A.2. Input materials' composition parameters

	Name	Type	Description	Unit	Mean value	Maximum Value	Minumim Value
FW protective layer	fwpl_w	scal	First wall protective layer % of Tungsten	%	100%		
FW	fw_eufer	scal	First wall % of EuroFer	%	Rest	Rest	Rest
	fw_he	scal	First wall % of Helium	%	30%	35%	25%
BZ	bz_lipb	scal	Breeding Zone % of LiPb	%	Rest	Rest	Rest
	bz_eufer	scal	Breeding Zone % of EuroFer	%	10%	20%	5%
	bz_he	scal	Breeding Zone % of Helium	%	10%	20%	5%
BP	man_lipb	scal	back plate % of LiPb	%	5%	10%	0%
	man_eufer	scal	back plate % of EuroFer	%	28%	35%	25%
	man_he	scal	back plate % of Helium	%	Rest	Rest	Rest
MAN	man_lipb	scal	manifold % of LiPb	%	5%	10%	0%
	man_eufer	scal	manifold % of EuroFer	%	28%	35%	25%
	man_he	scal	manifold % of Helium	%	Rest	Rest	Rest
SH	sh_eufer	scal	Shield % of EuroFer	%	10%	15%	5%
	sh_h2o	scal	Shield % of Water	%	25%	30%	20%
	sh_wc	scal	Shield % of Tungsten Carbide	%	Rest	Rest	Rest
VV	vv_ss316	scal	Vacuum vessel % of Stainless Steel 316	%	Rest	Rest	Rest
	vv_he	scal	Vacuum vessel % of Helium	%	37%	40%	35%
	vv_boron	scal	Vacuum vessel % of Boron	%	2%	3%	1%
TFSWP	tfswp_ss316	scal	Toroidal field structure infront of winding package % of Stainless Steel 316	%	Rest	Rest	Rest
	tfswp_he	scal	Toroidal field structure infront of winding package % of Helium	%	5%	10%	0%
TFC	tfc_ss316	scal	Toroidal field coil % of Stainless Steel 316	%	Rest	Rest	Rest
	tfc_heliq	scal	Toroidal field coil % of Liuid Helium	%	17%	20%	13%
	tfc_cu	scal	Toroidal field coil % of Copper	%	12%		
	tfc_bronze	scal	Toroidal field coil % of Bronze	%	7%		
	tfc_epoxy	scal	Toroidal field coil % of Epoxy	%	18%	25%	15%
	tfc_nb3sn	scal	Toroidal field coil % of Nb3Sn	%	3%		
CS	cs_ss316	scal	Central Selenoide % of Stainless Steel 316	%	Rest	Rest	Rest
	cs_he	scal	Central Selenoide % of Helium	%	17%	20%	13%
	cs_cu	scal	Central Selenoide % of Copper	%	12%		
	cs_bronze	scal	Central Selenoide % of Bronze	%	7%		
	cs_epoxy	scal	Central Selenoide % of Epoxy	%	18%	25%	15%
	cs_nb3sn	scal	Central Selenoide % of Nb3Sn	%	3%		

A.3. Other input parameters

	Name	Type	Description	Unit	Mean value	Maximum Value	Minumim Value
Enrichment	li6_enrich	scal	Lithium 6 enrichment (at%)	%	90%	99%	60%
Power	fus_powr	scal	Fusion Power of the reactor	MW	2385	N.A.	N.A.
Plasma volume	volume	scal	Total plasma volume	m^3	1,08E+03	N.A.	N.A.

A.4. Output variables

Name	Type	Description	Unit
tbr_res_bk	scal	resulting global breeding blanket tritium breeding ratio	no
tbr_ib_bk	scal	resulting inboard breeding blanket tritium breeding ratio	no
tbr_ob_bk	scal	resulting outboard breeding blanket tritium breeding ratio	no
me_bk	scal	energy multiplication factor in breeding blanket	no
ener_fw_ib	scal	Peak energy deposition in FW Inboard	MW.m^-3
ener_bz10_ib	scal	Peak energy deposition in first 10cm of ther Breeding Zone Inboard	MW.m^-3
ener_bz_ib	scal	Peak energy deposition in Breeding Zone Inboard	MW.m^-3
ener_bp_ib	scal	Peak energy deposition in Back Plates Inboard	MW.m^-3
ener_man_ib	scal	Peak energy deposition in Manifold Inboard	MW.m^-3
ener_sh_ib	scal	Peak energy deposition in Shield Inboard	MW.m^-3
ener_vv_ib	scal	Peak energy deposition in vacuum vessel inboard	MW.m^-3
ener_tfswp_ib	scal	Peak energy deposition in winding pack inboard	MW.m^-3
ener_fw_ob	scal	Peak energy deposition in FW Outboard	MW.m^-3
ener_bz10_ob	scal	Peak energy deposition in first 10cm of ther Breeding Zone Outboard	MW.m^-3
ener_bz_ob	scal	Peak energy deposition in Breeding Zone Outboard	MW.m^-3
ener_bp_ob	scal	Peak energy deposition in Back Plate Outboard	MW.m^-3
ener_man_ob	scal	Peak energy deposition in Manifold Outboard	MW.m^-3
ener_sh_ob	scal	Peak energy deposition in Shield Outboard	MW.m^-3

ener_vv_ob	scal	Peak energy deposition in vacuum vessel Outboard	MW.m^-3
ener_tfswp_ob	scal	Peak energy deposition in winding pack Outboard	MW.m^-3
FluxSup0.1Mev_fw	scal	Peak fast flux in FW Inboard	cm.-2.s-1
FluxSup0.1Mev_bz	scal	Peak fast flux in Breeding Zone Inboard	cm.-2.s-1
FluxSup0.1Mev_bp	scal	Peak fast flux in Back Plate Inboard	cm.-2.s-1
FluxSup0.1Mev_man	scal	Peak fast flux in Manifold Inboard	cm.-2.s-1
FluxSup0.1Mev_sh	scal	Peak fast flux in Shield Inboard	cm.-2.s-1
FluxSup0.1Mev_vv	scal	Peak fast flux in vacuum vessel inboard	cm.-2.s-1
FluxSup0.1Mev_tfswp	scal	Peak fast flux in winding pack inboard	cm.-2.s-1

A.5. TBR and M_E definitions

Definition of the TBR (20) :

$$TBR(t) = \int \frac{Tritium\ production\ rate\ in\ reactor\ (t)}{Tritium\ burning\ rate\ in\ plasma\ (t)}$$

$$TBR(t) = \frac{\iiint R_{6Li(n,\alpha)T}(\vec{r},t)d^3r + \iiint R_{7Li(n,n'\alpha)T}(\vec{r},t)d^3r}{S_{Fussion\ neutrons}(t)}$$

$$TBR(t) = \frac{\iiint \left[N_{6Li}(\vec{r}) \cdot \left(\int_0^\infty \left[\sigma_{6Li(n,\alpha)T}(E) \cdot \phi(\vec{r},E,t)\right]dE\right)\right]d^3r + \iiint \left[N_{7Li}(\vec{r}) \cdot \left(\int_0^\infty \left[\sigma_{7Li(n,n'\alpha)T}(E) \cdot \phi(\vec{r},E,t)\right]dE\right)\right]d^3r}{S_{Fussion\ neutrons}(t)}$$

Where:

- *t* is the time (in s) and is often omitted because of the usual steady-state assumption for *TBR*,
- *E* is the neutron energy (in MeV),
- $\vec{r}$ is the space vector defining the 3 coordinates in space (in cm),
- *R* are the local reaction rates (in $cm^{-3}.s^{-1}$),
- N_{6Li} and N_{7Li} are respectively the local atoms concentrations of ^{6}Li and ^{7}Li (in $atoms.cm^{-3}$),
- $S_{fusion\ neutrons}$ is the fusion neutron source (in $neutrons.s^{-1}$), which formulae are proposed in,
- $\sigma_{6Li(n,\alpha)T}$ and $\sigma_{7Li(n,n'\alpha)T}$ are the ^{6}Li and ^{7}Li cross-sections producing tritium (in cm2),
- $\phi(\vec{r},E,t)$ is called in neutronics the "scalar neutronic flux" (in $neutrons.cm^{-2}.s^{-1}.MeV^{-1}$). $\phi(\vec{r},E,t)$ is itself the integration for all solid angles $\vec{\Omega}$ (in steradian) of $\phi(\vec{r},E,\vec{\Omega},t)$ (in $neutrons.cm^{-2}.s^{-1}.MeV^{-1}.steradian^{-1}$). $\phi(\vec{r},E,\vec{\Omega},t)$is called in neutronics the "angular neutronic flux" and is defined as: $\boldsymbol{\phi(\vec{r},E,\vec{\Omega},t) = n(\vec{r},E,\vec{\Omega},t) \times v}$

  Where :

  - v is the speed of neutron ($cm.s_{-1}$)
  - $n(\vec{r},E,\vec{\Omega},t)$ (in $neutrons.cm^{-3}.^{s-1}.MeV^{-1}$) is the volumic density (in $neutron.cm^{-3}$) of the neutron population having the same energy E, i.e. the same speed $\boldsymbol{v}$, and the same solid angle $\vec{\Omega}$ at the time t.

The needed *TBRglobal*, average in time of *TBR(t)*, is design dependent. On the basis of that, the minimum *TBRglobal*, for a fusion reactor should be between 1.04 and 1.07 andmay be higher if a fast development of industrial tokamaks is wanted. Considering, furthermore,uncertainties due to 3D MC calculations including nuclear data ones, a value of *TBRglobal* = 1.10 is considered sufficient.

Definition of the multiplication facotr M_E (20) :

$$M_E(t) = \frac{Nuclear\ power\ generated\ in\ reactor\ (t)}{Fusion\ neutrons\ power\ (t)}$$

$$M_E(t) = \frac{Total\ energy\ deposition\ per\ source\ neutron(t)}{Average\ energy\ of\ a\ fusion\ neutron\ (t)}$$

Time is often omitted in M_E because of the usual steady-state assumption. M_E is typically between 1.1 and 1.3. Only a part of the deposited energy is recovered by energy conversion system and then useful in terms of electricity production (i.e. typically energy deposited into the vacuum vessel or into the coils is lost for electricity production).

A.6. 1-Dimension Cylindrical Geometry

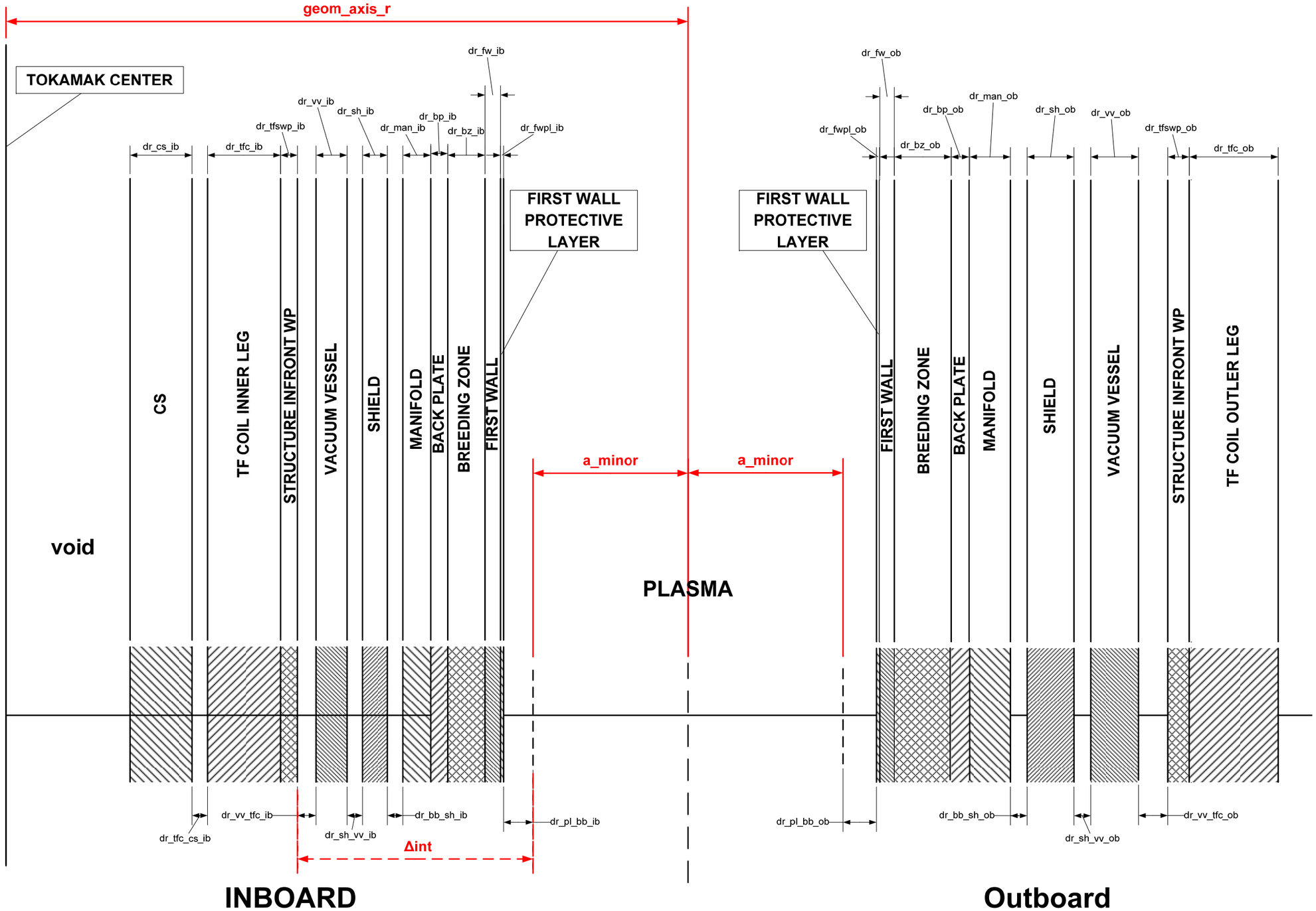

A.7. RZ Square-Based Geometry

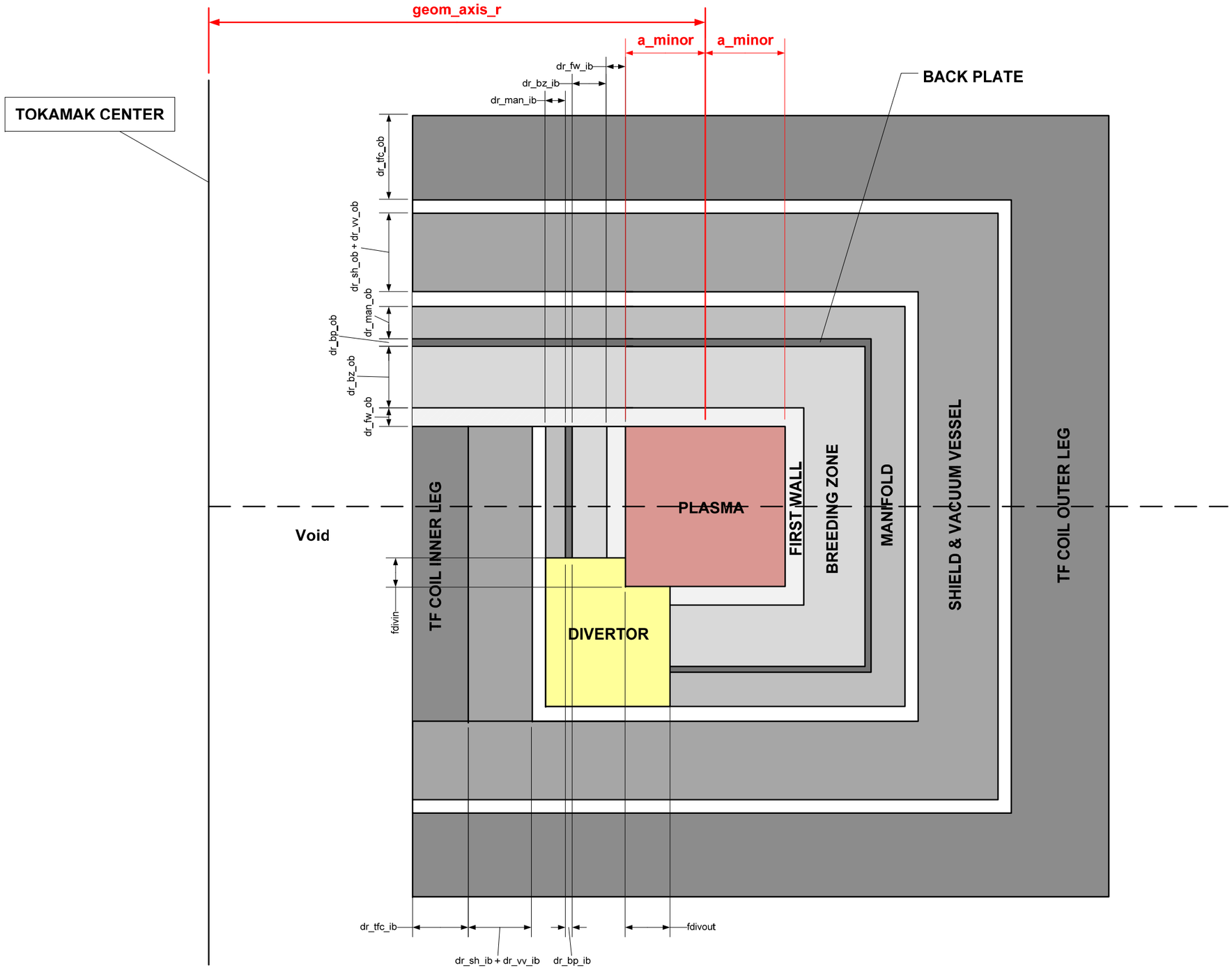

B. Apendix : Results

B.1. Apollo2 Peak Radial Flux Results

1D geometry Apollo2 model performances with different energy grids.

Inboard	Distance to plasma	1968 groupes			1200 groupes			600 groupes		
		Flux>0,1MeV	Flux<0,1MeV	Flux Total	Flux>0,1MeV	Flux<0,1MeV	Flux Total	Flux>0,1MeV	Flux<0,1MeV	Flux Total
First	0,2	1,40E+15	4,75E+14	1,87E+15	1,40E+15	4,77E+14	1,88E+15	1,40E+15	4,80E+14	1,88E+15
Wall	1,7	1,40E+15	4,75E+14	1,87E+15	1,40E+15	4,77E+14	1,00E+00	1,40E+15	4,80E+14	1,88E+15
	3,2	1,29E+15	4,62E+14	1,75E+15	1,29E+15	4,64E+14	1,75E+15	1,28E+15	4,67E+14	1,75E+15
	4,2	1,18E+15	4,36E+14	1,62E+15	1,18E+15	4,38E+14	1,62E+15	1,18E+15	4,41E+14	1,62E+15
	8,2	1,00E+15	3,97E+14	1,40E+15	1,00E+15	3,99E+14	1,40E+15	9,99E+14	4,01E+14	1,40E+15
BZ	13,2	8,28E+14	3,56E+14	1,18E+15	8,29E+14	3,57E+14	1,19E+15	8,24E+14	3,59E+14	1,18E+15
	18,2	6,79E+14	3,17E+14	9,95E+14	6,79E+14	3,17E+14	9,96E+14	6,74E+14	3,19E+14	9,93E+14
	23,2	5,52E+14	2,79E+14	8,31E+14	5,52E+14	2,79E+14	8,31E+14	5,48E+14	2,80E+14	8,28E+14
	28,2	4,47E+14	2,43E+14	6,90E+14	4,46E+14	2,44E+14	6,90E+14	4,43E+14	2,44E+14	6,87E+14
	33,2	2,98E+14	1,87E+14	4,84E+14	2,97E+14	1,87E+14	4,84E+14	2,94E+14	1,88E+14	4,82E+14
	47,7	2,12E+14	1,56E+14	3,68E+14	2,12E+14	1,56E+14	3,68E+14	2,10E+14	1,57E+14	3,66E+14
BP	48,7	2,00E+14	1,53E+14	3,53E+14	2,00E+14	1,53E+14	3,53E+14	1,98E+14	1,54E+14	3,52E+14
	52,7	1,81E+14	1,46E+14	3,27E+14	1,81E+14	1,47E+14	3,28E+14	1,80E+14	1,47E+14	3,27E+14
	57,7	1,57E+14	1,37E+14	2,93E+14	1,56E+14	1,37E+14	2,93E+14	1,55E+14	1,37E+14	2,92E+14
	65,7	1,41E+14	1,29E+14	2,70E+14	1,41E+14	1,30E+14	2,70E+14	1,39E+14	1,30E+14	2,69E+14
	66,7	1,33E+14	1,25E+14	2,58E+14	1,32E+14	1,26E+14	2,58E+14	1,31E+14	1,25E+14	2,56E+14
	70,7	1,19E+14	1,18E+14	2,37E+14	1,18E+14	1,18E+14	2,36E+14	1,17E+14	1,18E+14	2,34E+14
MF	75,7	1,04E+14	1,10E+14	2,14E+14	1,03E+14	1,10E+14	2,13E+14	1,02E+14	1,09E+14	2,11E+14
	80,7	9,02E+13	1,02E+14	1,93E+14	8,92E+13	1,02E+14	1,91E+14	8,74E+13	1,00E+14	1,88E+14
	85,7	7,68E+13	9,54E+13	1,72E+14	7,56E+13	9,44E+13	1,70E+14	7,36E+13	9,19E+13	1,65E+14
	90,7	6,38E+13	9,03E+13	1,54E+14	6,23E+13	8,85E+13	1,51E+14	6,02E+13	8,48E+13	1,45E+14
	105,7	4,73E+13	8,20E+13	1,29E+14	4,59E+13	7,92E+13	1,25E+14	4,40E+13	7,46E+13	1,19E+14
	106,7	2,21E+13	5,05E+13	7,26E+13	2,14E+13	4,76E+13	6,90E+13	2,05E+13	4,35E+13	6,40E+13
	110,7	5,54E+12	1,64E+13	2,19E+13	5,35E+12	1,48E+13	2,02E+13	5,15E+12	1,30E+13	1,82E+13
Shield	115,7	1,18E+12	3,82E+12	5,00E+12	1,13E+12	3,37E+12	4,51E+12	1,09E+12	2,91E+12	4,00E+12
	120,7	2,63E+11	8,38E+11	1,10E+12	2,54E+11	7,30E+11	9,84E+11	2,46E+11	6,27E+11	8,73E+11
	125,7	6,45E+10	1,84E+11	2,48E+11	6,25E+10	1,60E+11	2,22E+11	6,09E+10	1,38E+11	1,98E+11
	130,7	1,77E+10	4,19E+10	5,96E+10	1,72E+10	3,65E+10	5,38E+10	1,69E+10	3,17E+10	4,86E+10
	145,7	7,83E+09	1,88E+10	2,66E+10	7,69E+09	1,64E+10	2,41E+10	7,54E+09	1,44E+10	2,20E+10
	146,7	4,69E+09	9,67E+09	1,44E+10	4,62E+09	9,02E+09	1,36E+10	4,53E+09	8,45E+09	1,30E+10
	150,7	2,14E+09	3,18E+09	5,32E+09	2,11E+09	3,07E+09	5,18E+09	2,07E+09	2,96E+09	5,04E+09
VV	155,7	9,91E+08	1,10E+09	2,09E+09	9,82E+08	1,07E+09	2,05E+09	9,63E+08	1,04E+09	2,00E+09
	160,7	4,90E+08	4,55E+08	9,44E+08	4,86E+08	4,46E+08	9,32E+08	4,76E+08	4,33E+08	9,09E+08
	165,7	2,50E+08	2,12E+08	4,62E+08	2,48E+08	2,09E+08	4,57E+08	2,43E+08	2,03E+08	4,46E+08
	170,7	1,31E+08	1,08E+08	2,39E+08	1,30E+08	1,06E+08	2,36E+08	1,27E+08	1,03E+08	2,30E+08
	175,7	7,41E+07	6,13E+07	1,35E+08	7,36E+07	6,05E+07	1,34E+08	7,18E+07	5,88E+07	1,31E+08
	190,7	6,16E+07	4,51E+07	1,07E+08	6,12E+07	4,44E+07	1,06E+08	5,96E+07	4,31E+07	1,03E+08
TFCS	191,7	5,70E+07	4,05E+07	9,75E+07	5,66E+07	3,99E+07	9,66E+07	5,52E+07	3,86E+07	9,38E+07
	192,7	4,97E+07	3,55E+07	8,52E+07	4,93E+07	3,50E+07	8,43E+07	4,80E+07	3,38E+07	8,18E+07
	194,7	3,86E+07	3,19E+07	7,05E+07	3,83E+07	3,14E+07	6,97E+07	3,72E+07	3,03E+07	6,75E+07
	196,7	2,80E+07	3,28E+07	6,07E+07	2,77E+07	3,24E+07	6,01E+07	2,68E+07	3,13E+07	5,81E+07
	197,7	1,11E+07	1,76E+07	2,87E+07	1,10E+07	1,76E+07	2,85E+07	1,06E+07	1,69E+07	2,76E+07
	206,7	2,09E+06	2,93E+06	5,01E+06	2,07E+06	2,94E+06	5,01E+06	2,00E+06	2,83E+06	4,83E+06
TFC	216,7	4,44E+05	5,29E+05	9,73E+05	4,41E+05	5,30E+05	9,71E+05	4,24E+05	5,10E+05	9,34E+05
	226,7	9,21E+04	1,04E+05	1,96E+05	9,13E+04	1,04E+05	1,95E+05	8,73E+04	9,96E+04	1,87E+05
	236,7	4,09E+04	4,56E+04	8,64E+04	4,05E+04	4,57E+04	8,62E+04	3,86E+04	4,36E+04	8,22E+04
	246,7	1,11E+03	9,58E+02	2,07E+03	1,08E+03	9,43E+02	2,03E+03	9,36E+02	7,93E+02	1,73E+03
	256,7	1,13E+02	1,81E+02	2,95E+02	1,10E+02	1,79E+02	2,89E+02	9,72E+01	1,62E+02	2,59E+02

B.2. Apollo2 Energy Deposition Results

1D geometry Apollo2 model performances with different energy grids.

Apollo2							
		Energie depose Apollo2 1968 MW/m3	Energie depose Apollo2 1200 MW/m3	Energie depose Apollo2 600 MW/m3	1968 vs 1200	1968 vs 600	1200 vs 600
Inboard	First Wall	1,6081E+01	1,5966E+01	1,6014E+01	0,71%	0,41%	-0,30%
	BZ10	7,9949E+00	8,0018E+00	7,9981E+00	-0,06%	-0,04%	0,05%
	BZ	4,1058E+00	4,1082E+00	4,1035E+00	-0,09%	0,06%	0,11%
	BP	2,7114E-01	2,6935E-01	2,7393E-01	0,66%	-1,03%	-1,70%
	MF	2,2170E-01	2,1358E-01	2,0931E-01	3,67%	5,59%	2,00%
	Shield	8,0333E-01	8,0684E-01	7,9087E-01	-0,44%	1,55%	1,98%
	VV	1,2745E-04	1,1514E-04	1,0610E-04	9,66%	16,75%	7,85%
	TFCS	1,7504E-06	1,7214E-06	1,6705E-06	1,66%	4,57%	2,96%
	TFC	2,7137E-07	2,8029E-07	2,7101E-07	-3,29%	0,13%	3,31%

		Energie depose Apollo2 1968 MW/m3	Energie depose Apollo2 1200 MW/m3	Energie depose Apollo2 600 MW/m3	1968 vs 1200	1968 vs 600	1200 vs 600
Outboard	First Wall	2,3593E+01	2,3433E+01	2,3510E+01	0,68%	0,35%	-0,33%
	BZ 10	3,0356E+00	3,0336E+00	8,3920E+00	0,07%	0,09%	0,11%
	BZ	8,3994E+00	8,4011E+00	3,0265E+00	-0,02%	0,30%	0,23%
	BP	6,4796E-02	6,4302E-02	6,5618E-02	0,76%	-1,27%	-2,05%
	MF	4,6572E-02	4,5377E-02	4,5029E-02	2,57%	3,31%	0,77%
	Shield	7,4997E-02	7,4443E-02	7,1527E-02	0,74%	4,63%	3,92%
	VV	1,5617E-07	4,8355E-08	2,6887E-08	69,04%	82,78%	44,40%
	TFCS	2,0167E-12	1,7796E-12	1,8388E-12	11,75%	8,82%	-3,32%
	TFC	2,0414E-13	2,0888E-13	1,9619E-13	-2,32%	3,89%	6,08%

B.3. RZ Apollo2 performances

RZ square-based geometry Apollo2 model performances compared to the 3D DEMO Tripoli4 simulations.

	ΔTBR (%)	ΔTBR Inboard (%)	ΔTBR Outboard (%)	ΔMultiplication Factor (%)
Reference	-1,29	-0,81	-1,43	1,92
RefLi75	-1,15	-0,49	-1,35	2,02
RefLi60	-0,99	0,09	-1,32	2,08
RefLi45	-0,75	0,79	-1,2	2,21
IBminus10	-0,84	1,65	-1,52	2,09
IBMinus20	-0,45	4,65	-1,62	2,26
OBminus10	-0,56	-0,92	-0,44	2,11
OBminus20	0,34	-1,04	0,81	2,34
OBIBminus10	-0,1	1,45	-0,54	2,24
OBIBminus20	1,42	4,5	0,65	2,63

Apollo2	TBR	TBR Inboard	TBR Outboard	Multiplication Factor
Reference	1.10	0.26	0.83	1.18
RefLi75	1.06	0.25	0.81	1.19
RefLi60	1.01	0.24	0.78	1.19
RefLi45	0.95	0.22	0.73	1.20
IBminus10	1.07	0.24	0.83	1.18
IBMinus20	1.03	0.20	0.83	1.18
OBminus10	1.07	0.26	0.81	1.18
OBminus20	1.04	0.26	0.78	1.18
OBIBminus10	1.05	0.24	0.81	1.18
OBIBminus20	0.97	0.20	0.77	1.18

Tripoli4	TBR	TBR Inboard	TBR Outboard	Multiplication Factor
Reference	1.11	0.26	0.85	1.16
RefLi75	1.07	0.25	0.82	1.16
RefLi60	1.02	0.24	0.79	1.17
RefLi45	0.96	0.22	0.74	1.17
IBminus10	1.08	0.23	0.85	1.16
IBMinus20	1.04	0.19	0.84	1.15
OBminus10	1.08	0.26	0.81	1.16
OBminus20	1.03	0.26	0.77	1.15
OBIBminus10	1.05	0.23	0.81	1.16
OBIBminus20	0.96	0.19	0.77	1.15

B.4. 1D Tripoli4 performances

1D geometry Tripoli4 model performances compared to the 3D DEMO Tripoli4 simulations.

	Ref			
	Peakflux (n/cm².s) tripoli4 1D	**Peak flux (n/cm².s) tripoli4 3D**	**Deposited Energy Tripoli4 1D MW/m³**	**Deposited Energy Tripoli4 3D MW/m³**
FW Ib	1,896E+15	1,221E+15	10,81	7,00
FW Ob	2,085E+15	1,265E+15	13,94	7,33
BZ Ib	9,181E+14	6,741E+14	4,13	3,43
BZ Ob	7,002E+14	4,651E+14	3,20	2,23
BP I	2,93E+14	2,64E+14	0,39	0,36
BP O	9,19E+13	8,08E+13	0,09	0,09
	IBminus10			
	Peakflux (n/cm².s) tripoli4 1D	**Peak flux (n/cm².s) tripoli4 3D**	**Deposited Energy Tripoli4 1D MW/m³**	**Deposited Energy Tripoli4 3D MW/m³**
FW Ib	1,892E+15	1,220E+15	10,82	7,06
FW Ob	2,082E+15	1,262E+15	13,94	7,37
BZ Ib	1,044E+15	7,574E+14	4,87	4,02
BZ Ob	6,996E+14	4,645E+14	3,20	2,23
BP I	4,51E+14	3,68E+14	0,65	0,61
BP O	9,18E+13	8,01E+13	0,09	0,09
	IBminus20			
	Peakflux (n/cm².s) tripoli4 1D	**Peak flux (n/cm².s) tripoli4 3D**	**Deposited Energy Tripoli4 1D MW/m³**	**Deposited Energy Tripoli4 3D MW/m³**
FW Ib	1,886E+15	1,215E+15	10,81	6,98
FW Ob	2,078E+15	1,258E+15	13,94	7,30
BZ Ib	1,195E+15	8,514E+14	5,94	4,83
BZ Ob	6,982E+14	4,637E+14	3,19	2,23
BP I	6,71E+14	5,17E+14	1,17	1,12
BP O	9,17E+13	8,01E+13	0,09	0,09
	OBminus10			
	Peakflux (n/cm².s) tripoli4 1D	**Peak flux (n/cm².s) tripoli4 3D**	**Deposited Energy Tripoli4 1D MW/m³**	**Deposited Energy Tripoli4 3D MW/m³**
FW Ib	1,895E+15	1,220E+15	10,81	7,04
FW Ob	2,084E+15	1,262E+15	13,93	7,30
BZ Ib	9,180E+14	6,724E+14	4,13	3,42
BZ Ob	7,866E+14	5,241E+14	3,63	2,55
BP I	2,93E+14	2,64E+14	0,39	0,36
BP O	1,47E+14	1,19E+14	0,15	0,14

	OBminus20			
	Peakflux (n/cm^2.s) tripoli4 1D	**Peak flux (n/cm^2.s) tripoli4 3D**	**Deposited Energy Tripoli4 1D MW/m^3**	**Deposited Energy Tripoli4 3D MW/m^3**
FW Ib	1,895E+15	1,219E+15	10,81	7,01
FW Ob	2,083E+15	1,261E+15	13,94	7,34
BZ Ib	9,175E+14	6,718E+14	4,13	3,42
BZ Ob	8,898E+14	5,940E+14	4,18	2,95
BP I	2,93E+14	2,63E+14	0,39	0,35
BP O	2,30E+14	1,73E+14	0,26	0,21
	IBOBminus10			
	Peakflux (n/cm^2.s) tripoli4 1D	**Peak flux (n/cm^2.s) tripoli4 3D**	**Deposited Energy Tripoli4 1D MW/m^3**	**Deposited Energy Tripoli4 3D MW/m^3**
FW Ib	1,892E+15	1,218E+15	10,82	7,02
FW Ob	2,082E+15	1,260E+15	13,94	7,32
BZ Ib	1,043E+15	7,550E+14	4,87	4,00
BZ Ob	7,859E+14	5,238E+14	3,63	2,55
BP I	4,51E+14	3,68E+14	0,64	0,63
BP O	1,47E+14	1,19E+14	0,15	0,14
	IBOBminus20			
	Peakflux (n/cm^2.s) tripoli4 1D	**Peak flux (n/cm^2.s) tripoli4 3D**	**Deposited Energy Tripoli4 1D MW/m^3**	**Deposited Energy Tripoli4 3D MW/m^3**
FW Ib	1,885E+15	1,214E+15	10,81	7,01
FW Ob	2,076E+15	1,257E+15	13,93	7,31
BZ Ib	1,194E+15	8,499E+14	5,94	4,83
BZ Ob	8,873E+14	5,924E+14	4,17	2,94
BP I	6,70E+14	5,18E+14	1,17	1,11
BP O	2,29E+14	1,72E+14	0,25	0,22
	RefLi75			
	Peakflux (n/cm^2.s) tripoli4 1D	**Peak flux (n/cm^2.s) tripoli4 3D**	**Deposited Energy Tripoli4 1D MW/m^3**	**Deposited Energy Tripoli4 3D MW/m^3**
FW Ib	2,025E+15	1,289E+15	10,86	7,07
FW Ob	2,215E+15	1,330E+15	14,00	7,37
BZ Ib	1,010E+15	7,294E+14	4,09	3,36
BZ Ob	7,758E+14	5,098E+14	3,18	2,21
BP I	3,28E+14	2,89E+14	0,43	0,39
BP O	1,08E+14	9,13E+13	0,11	0,10

	RefLi60			
	Peakflux (n/cm².s) tripoli4 1D	**Peak flux (n/cm².s) tripoli4 3D**	**Deposited Energy Tripoli4 1D MW/m³**	**Deposited Energy Tripoli4 3D MW/m³**
FW Ib	2,186E+15	1,372E+15	10,95	7,15
FW Ob	2,380E+15	1,412E+15	14,08	7,48
BZ Ib	1,127E+15	7,991E+14	4,04	3,29
BZ Ob	8,742E+14	5,669E+14	3,16	2,18
BP I	3,74E+14	3,20E+14	0,48	0,42
BP O	1,28E+14	1,06E+14	0,14	0,12
	RefLi45			
	Peakflux (n/cm².s) tripoli4 1D	**Peak flux (n/cm².s) tripoli4 3D**	**Deposited Energy Tripoli4 1D MW/m³**	**Deposited Energy Tripoli4 3D MW/m³**
FW Ib	2,398E+15	1,476E+15	11,06	7,23
FW Ob	2,596E+15	1,514E+15	14,20	7,54
BZ Ib	1,284E+15	8,882E+14	3,97	3,20
BZ Ob	1,008E+15	6,421E+14	3,13	2,14
BP I	4,35E+14	3,62E+14	0,56	0,47
BP O	1,58E+14	1,24E+14	0,17	0,14

Peak neutron flux on the radial direction calculated with 1D Tripoli4 simulation

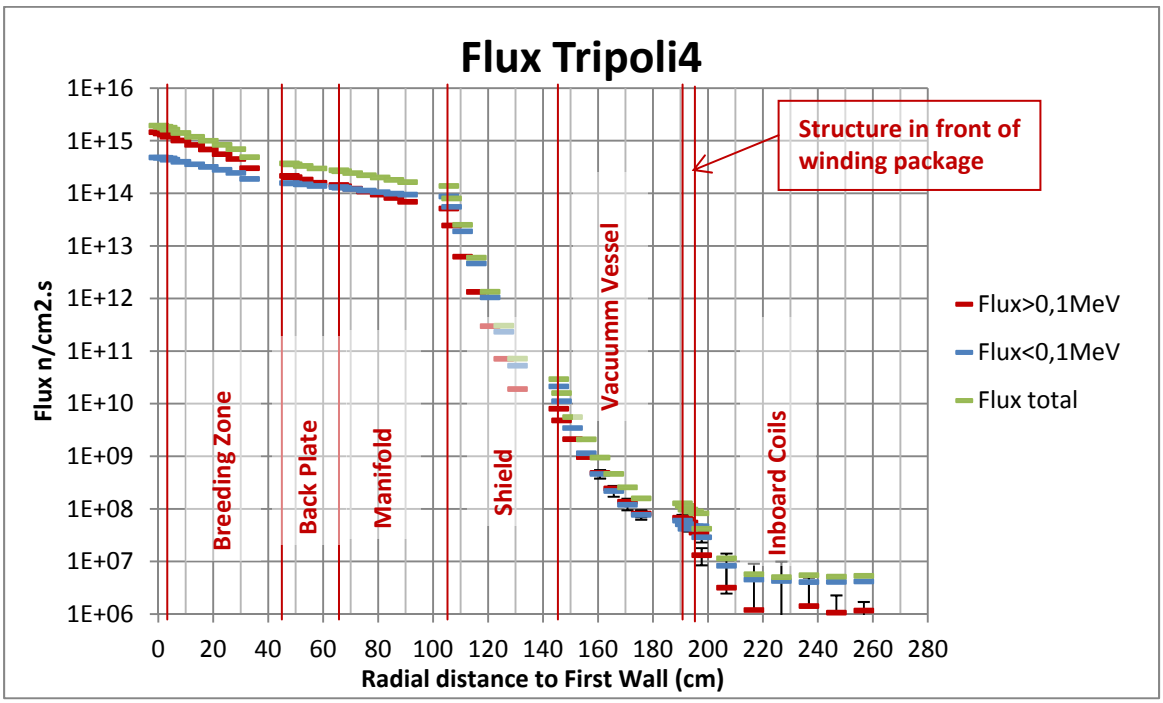

B.5. 1D Apollo2 peak neutron flux performances

1D geometry Apollo2 model performances compared to the 1D Tripoli4 simulations.

Peak Neutron Flux for E_n> 0,1MeV						
	Distance to Plasma (cm)	Fast Flux Apollo2 1968 1/cm^2.s	Fast Flux Apollo2 1200 1/cm^2.s	Fast Flux Apollo2 600 1/cm^2.s	Fast Flux Tripoli4 1D 1/cm^2.s	Sigma (%)
First Wall	0,2	1,40E+15	1,40E+15	1,40E+15	1,46E+015	0,002
	1,7	1,40E+15	1,40E+15	1,40E+15	1,38E+015	0,002
BZ	3,2	1,29E+15	1,29E+15	1,28E+15	1,32E+015	0,002
	4,2	1,18E+15	1,18E+15	1,18E+15	1,20E+015	0,002
	8,2	1,00E+15	1,00E+15	9,99E+14	1,02E+015	0,002
	13,2	8,28E+14	8,29E+14	8,24E+14	8,38E+014	0,002
	18,2	6,79E+14	6,79E+14	6,74E+14	6,86E+014	0,002
	23,2	5,52E+14	5,52E+14	5,48E+14	5,58E+014	0,003
	28,2	4,47E+14	4,46E+14	4,43E+14	4,52E+014	0,003
	33,2	2,98E+14	2,97E+14	2,94E+14	3,02E+014	0,003
BP	47,7	2,12E+14	2,12E+14	2,10E+14	2,16E+014	0,005
	48,7	2,00E+14	2,00E+14	1,98E+14	2,04E+014	0,005
	52,7	1,81E+14	1,81E+14	1,80E+14	1,84E+014	0,005
	57,7	1,57E+14	1,56E+14	1,55E+14	1,60E+014	0,006
MF	65,7	1,41E+14	1,41E+14	1,39E+14	1,44E+014	0,007
	66,7	1,33E+14	1,32E+14	1,31E+14	1,37E+014	0,006
	70,7	1,19E+14	1,18E+14	1,17E+14	1,23E+014	0,007
	75,7	1,04E+14	1,03E+14	1,02E+14	1,09E+014	0,007
	80,7	9,02E+13	8,92E+13	8,74E+13	9,50E+013	0,007
	85,7	7,68E+13	7,56E+13	7,36E+13	8,19E+013	0,008
	90,7	6,38E+13	6,23E+13	6,02E+13	6,94E+013	0,008
Shield	105,7	4,73E+13	4,59E+13	4,40E+13	5,17E+013	0,008
	106,7	2,21E+13	2,14E+13	2,05E+13	2,46E+013	0,009
	110,7	5,54E+12	5,35E+12	5,15E+12	6,28E+012	0,016
	115,7	1,18E+12	1,13E+12	1,09E+12	1,35E+012	0,035
	120,7	2,63E+11	2,54E+11	2,46E+11	2,99E+011	0,074
	125,7	6,45E+10	6,25E+10	6,09E+10	7,17E+010	0,155
	130,7	1,77E+10	1,72E+10	1,69E+10	1,91E+010	0,303
VV	145,7	7,83E+09	7,69E+09	7,54E+09	8,06E+009	0,582
	146,7	4,69E+09	4,62E+09	4,53E+09	4,82E+009	0,616
	150,7	2,14E+09	2,11E+09	2,07E+09	2,13E+009	0,883
	155,7	9,91E+08	9,82E+08	9,63E+08	9,67E+008	1,303
	160,7	4,90E+08	4,86E+08	4,76E+08	4,86E+008	1,835
	165,7	2,50E+08	2,48E+08	2,43E+08	2,46E+008	2,549
	170,7	1,31E+08	1,30E+08	1,27E+08	1,37E+008	3,493
	175,7	7,41E+07	7,36E+07	7,18E+07	8,22E+007	4,887
TFCS	190,7	6,16E+07	6,12E+07	5,96E+07	6,82E+007	6,995
	191,7	5,70E+07	5,66E+07	5,52E+07	6,31E+007	7,840
	192,7	4,97E+07	4,93E+07	4,80E+07	5,53E+007	8,038
	194,7	3,86E+07	3,83E+07	3,72E+07	4,31E+007	8,798
TFC	196,7	2,80E+07	2,77E+07	2,68E+07	3,56E+007	9,955
	197,7	1,11E+07	1,10E+07	1,06E+07	1,32E+007	9,116
	206,7	2,09E+06	2,07E+06	2,00E+06	3,20E+006	16,639
	216,7	4,44E+05	4,41E+05	4,24E+05	1,20E+006	26,108

	226,7	9,21E+04	9,13E+04	8,73E+04	7,86E+005	28,718
	236,7	4,09E+04	4,05E+04	3,86E+04	1,42E+006	35,429
	246,7	1,11E+03	1,08E+03	9,36E+02	1,07E+006	33,944
	256,7	1,13E+02	1,10E+02	9,72E+01	1,17E+006	30,697

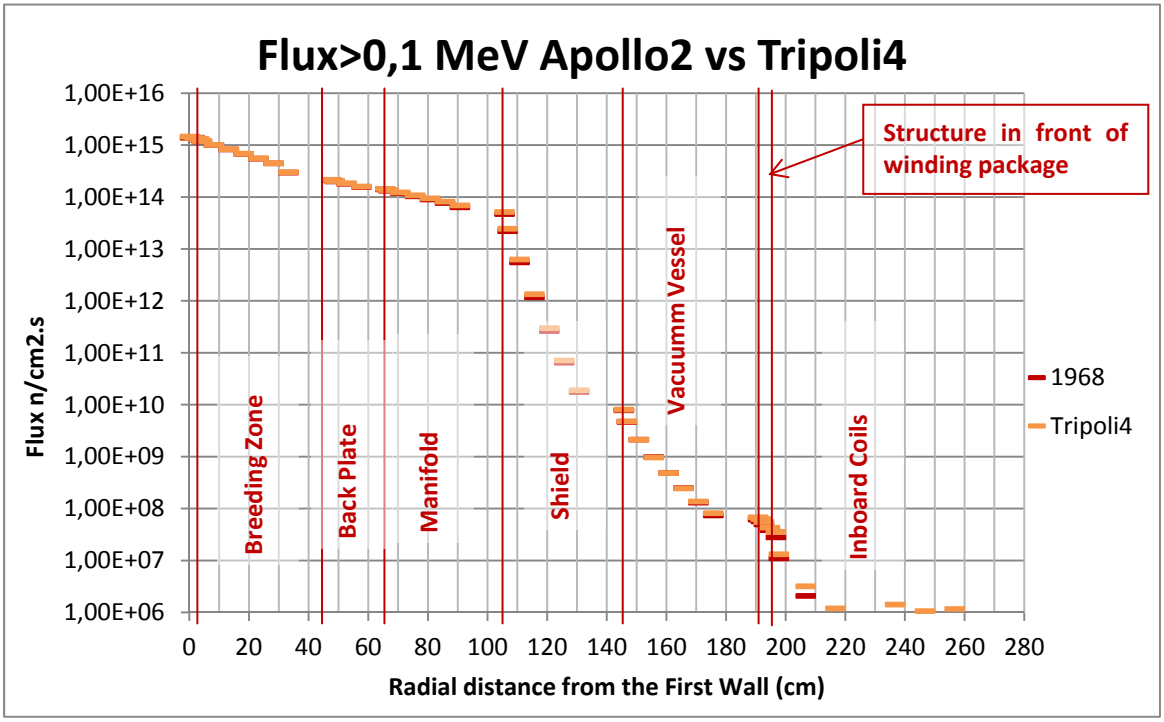

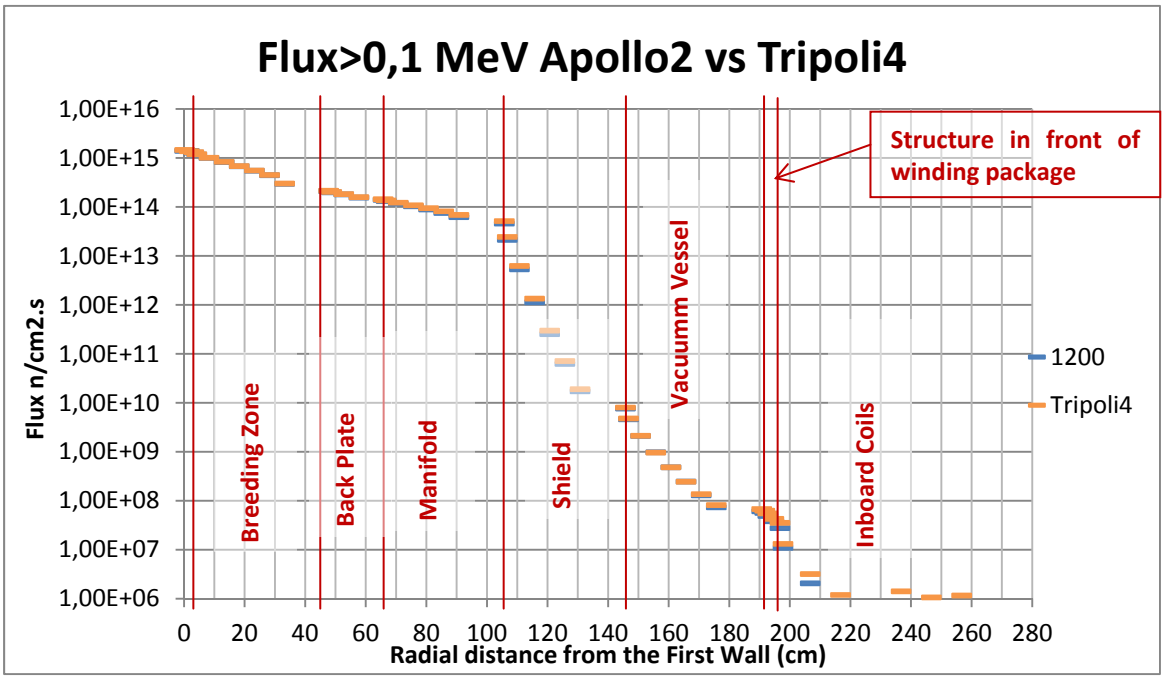

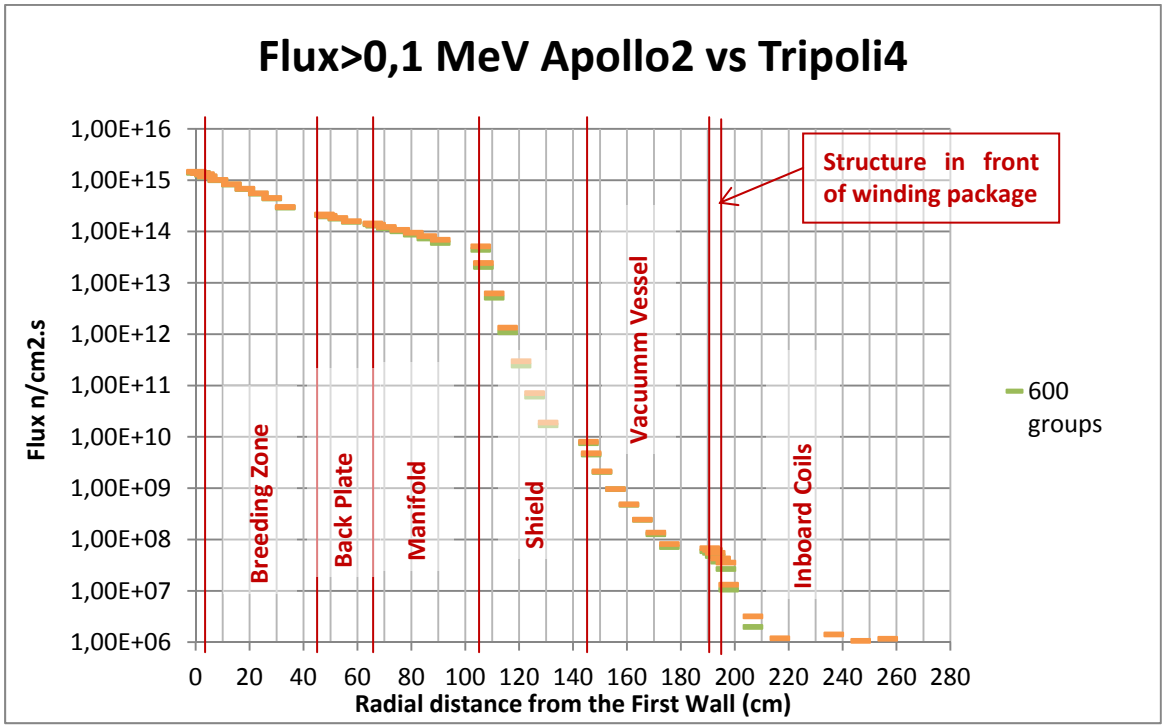
Flux>0,1 MeV Apollo2 vs Tripoli4
Flux n/cm2.s
1,00E+16
1,00E+15
1,00E+14
1,00E+13
1,00E+12
1,00E+11
1,00E+10
1,00E+09
1,00E+08
1,00E+07
1,00E+06
0 20 40 60 80 100 120 140 160 180 200 220 240 260 280
Radial distance from the First Wall (cm)
Breeding Zone
Back Plate
Manifold
Shield
Vacuumm Vessel
Inboard Coils
Structure in front of winding package
600 groups

B.6. 1D Apollo2 deposited energy performances

1D geometry Apollo2 model performances compared to the 1D Tripoli4 simulations.

		Total Deposited Energy (MW/m^3)							
		Distance to plasma	Apollo2 600	Tripoli4 N	Tripoli4 N sigma	Tripoli4 PN Neutron	Tripoli4 PN Photon	Tripoli4 PN Total	Tripoli4 PN sigma
Inboard	FW	0,2	1,601E+01	1,648E+01	0,00	3,141E+00	8,496E+00	1,164E+01	0,01
	BZ10	3,2	7,998E+00	8,133E+00	0,00	4,644E+00	4,920E+00	9,564E+00	0,01
	BZ	13,2	4,104E+00	4,129E+00	0,00	2,775E+00	1,686E+00	4,461E+00	0,00
	BP	47,7	2,739E-01	2,511E-01	0,01	1,161E-01	1,126E-01	2,286E-01	0,03
	MF	65,7	2,093E-01	2,151E-01	0,01	1,056E-01	1,575E-01	2,630E-01	0,02
	Shield	105,7	7,909E-01	8,216E-01	0,01	3,629E-02	7,217E-01	7,580E-01	0,01
	VV	145,7	1,061E-04	1,344E-04	0,40	8,051E-05	1,253E-04	2,058E-04	0,82
	TFSWP	190,7	1,670E-06	1,786E-06	9,32	2,039E-07	2,496E-06	2,700E-06	40,47
	TFC	196,7	2,710E-07	5,650E-07	7,29	8,599E-08	5,577E-07	6,437E-07	14,68
Outboard	FW	0,2	2,351E+01	2,272E+01	0,00	4,299E+00	1,088E+01	1,518E+01	0,01
	BZ10	3,2	8,392E+00	1,020E+01	0,00	5,220E+00	6,676E+00	1,190E+01	0,00
	BZ	13,2	3,027E+00	3,484E+00	0,00	2,263E+00	1,456E+00	3,718E+00	0,00
	BP	80,7	6,562E-02	6,121E-02	0,01	3,083E-02	2,398E-02	5,482E-02	0,04
	MF	98,7	4,503E-02	4,596E-02	0,01	2,308E-02	2,795E-02	5,103E-02	0,03
	Shield	158,7	7,153E-02	8,018E-02	0,01	2,659E-03	7,100E-02	7,366E-02	0,02
	VV	218,7	2,689E-08	7,423E-08	5,97	4,428E-08	3,217E-08	7,645E-08	16,12
	TFCS	308,7	1,839E-12	3,273E-08	29,67	4,157E-09	2,226E-08	2,641E-08	68,08
	TFC	316,7	1,962E-13	4,236E-08	11,06	2,561E-09	2,198E-08	2,454E-08	22,01

B.7. Example of neural network

C++ program containing a neural network that estimates the TBR.

```
#define ActivationFunction(sum)          ( tanh(sum) )
void FctTBR_Total_Rn_9_0(double *param, double *res)
{
  ////////////////////////////////
  //
  //     ******************************************
  //     ** Uranie  Wed Jun  6 15:22:46 2012
  //     **   Version : v2.3/2
  //     **      Date : Wed Mar 07, 2012
  //     ******************************************
  //
  //
  //     ******************************************
  //     ** BF_Rn **
  //     **
  //     **  **
  //     ******************************************
  //
  //    INPUT : 26
  //              Half_Radius_of_the_Plasma ( Half_Radius_of_the_Plasma )
  //              Thickness_VV_Inboard ( Thickness_VV_Inboard )
  //              Thickness_SH_Inboard ( Thickness_SH_Inboard )
  //              Thickness_MAN_Inboard ( Thickness_MAN_Inboard )
  //              Thickness_BZ_Inboard ( Thickness_BZ_Inboard )
  //              Thickness_FW ( Thickness_FW )
  //              Thickness_of_the_Plasma ( Thickness_of_the_Plasma )
  //              Thickness_MAN_Outboard ( Thickness_MAN_Outboard )
  //              Thickness_BZ_Outboard ( Thickness_BZ_Outboard )
  //              Lithium_6_enrichment ( Lithium_6_enrichment )
  //              Composition_FW_He ( Composition_FW_He )
  //              Composition_BZ_EuroFer ( Composition_BZ_EuroFer )
  //              Composition_BZ_He ( Composition_BZ_He )
  //              Composition_MAN_LiPB ( Composition_MAN_LiPB )
  //              Composition_MAN_EuroFer ( Composition_MAN_EuroFer )
  //              Composition_SH_EuroFer ( Composition_SH_EuroFer )
  //              Composition_SH_H2O ( Composition_SH_H2O )
  //              Composition_VV_He ( Composition_VV_He )
  //              Composition_VV_Boron ( Composition_VV_Boron )
  //              Composition_TFSWP_He ( Composition_TFSWP_He )
  //              Composition_TFC_Epoxy ( Composition_TFC_Epoxy )
  //              Composition_TFC_HeLiq ( Composition_TFC_HeLiq )
  //              Triangulation ( Triangulation )
  //              Elongation ( Elongation )
  //              Surface_Div_Inboard ( Surface_Div_Inboard )
  //              Surface_Div_Outboard ( Surface_Div_Outboard )
  //
  //    HIDDEN : 9
  //
  //    OUTPUT : 1
  //              TBR_Total ( TBR_Total )
  //
  ////////////////////////////////
  int nInput   = 26;
  int nOuput   = 1;
  int nHidden  = 9;
  const int nNeurones  = 36;
  double FctTBR_Total_Rn_9_0_act[nNeurones];

  // --- Pretraitment of the inputs and outputs
  double FctTBR_Total_Rn_9_0_minInput[] = {
  700.027, 30.0008, 25.0012, 25.0013, 30.004,
  2.00016, 240.002, 40.0015, 50.0066, 0.600045,
  25.0011, 5.00222, 5.00134, 0.000179968, 25.001,
  5.00087, 20.0018, 35.001, 1.00004, 0.00105174,
  15.001, 13.0002, 0.400003, 1.8, 0.0500017,
  0.0600001,
  };
  double FctTBR_Total_Rn_9_0_minOuput[] = {
```

```
  0.8116,   };
  double FctTBR_Total_Rn_9_0_maxInput[] = {
  899.991, 39.9985, 34.9989, 34.9984, 59.9976,
  3.99996, 259.997, 59.9971, 89.9958, 0.989939,
  34.9996, 19.9977, 19.9998, 9.99884, 34.9992,
  14.9983, 30, 39.9995, 2.99975, 9.99985,
  24.9985, 19.9999, 0.699999, 2.19999, 0.06,
  0.0699996,
  };
  double FctTBR_Total_Rn_9_0_maxOuput[] = {
  1.28595,   };

  // --- Values of the weights
  double FctTBR_Total_Rn_9_0_valW[] = {
  -0.770503, -0.41701, -0.365062, 0.00748932, 0.00295046,
  0.00203292, 0.00796074, 0.122025, 0.10879, -0.00384605,
  0.00355137, -0.0109447, -0.064051, -0.128022, -0.0485073,
  -0.0634014, 0.008742, 0.0127396, -0.00108845, -0.00566644,
  -0.00144493, 0.000365803, 0.0033791, 0.000712315, -0.00141671,
  -0.00729155, -0.00775967, 0.0205796, 0.0161141, -0.0009466,
  -0.286987, -0.673256, 0.690277, 1.62677, 0.879966,
  -1.62892, -0.65816, 0.261458, 1.79952, -0.830435,
  -0.151052, -0.00183584, 0.49168, 2.13363, -0.668357,
  0.381465, 0.0541227, -0.67419, -0.383398, -0.726098,
  -0.0150234, -1.6811, -1.3721, 0.784842, -0.422099,
  -0.858814, 0.0257492, 0.00281103, -0.924063, 0.943711,
  0.296202, -0.0435597, 0.000954333, -0.189686, -0.83575,
  -0.248009, 0.18671, 0.0952223, -0.089727, -1.42836,
  0.476611, -0.0903414, -0.264497, -0.0535293, 0.0165653,
  -0.209324, 0.239533, 0.256478, 0.0943184, -0.269124,
  -0.303051, 0.603791, -0.545882, 0.502966, -0.235403,
  -0.841119, -1.13427, 0.000151469, -0.000460163, -0.00168479,
  1.643e-05, -0.0096084, -0.0198637, -0.000940162, -0.000390213,
  -0.015843, -0.383224, 0.0163927, 0.0273961, 0.0114247,
  -0.0240531, 0.00247994, 0.00183277, 0.000340355, -0.00050983,
  -0.000832667, -0.00155477, -0.00184639, 0.000287451, 8.49932e-05,
  0.000952165, -0.00176677, 0.000828718, 0.797215, 1.0542,
  -0.0494095, -0.00143265, 0.000722249, 0.0242915, 0.414508,
  0.0132581, 0.0138992, 0.00128125, -0.0093475, 0.032112,
  0.0117303, 0.0713432, 0.010499, 0.00607154, 0.0167218,
  -0.00190306, -0.00579686, 0.000489116, -1.35903e-05, 0.00240901,
  0.00157214, -0.000603431, 0.0432602, -0.0116913, 0.00569366,
  -0.00346953, -1.06365, -1.10414, -0.0227595, 0.000412701,
  6.78779e-05, -6.97775e-05, 0.00374682, -0.0592056, 0.00700191,
  -0.0202186, -0.523984, -0.0619691, 0.0115967, -0.077947,
  0.0676499, -0.00823138, -0.0194779, -0.000317695, 0.00369104,
  -0.00113327, -5.3444e-05, 0.000697444, -0.000742812, -3.9401e-05,
  0.0159359, -0.00430074, -0.00274163, -0.00561686, -2.99803,
  0.757833, 0.00609582, -0.000498689, -0.000207196, -0.00107892,
  -0.022916, 0.0958661, -0.00307953, -0.000983546, 0.00554005,
  -0.00829994, -0.000313094, 0.0997375, 0.025635, 0.00264543,
  -0.00412672, 0.000304029, 0.00106788, 0.00101378, 0.000217847,
  -0.000131415, -0.000258623, -0.000182101, 0.000684372, -0.00323913,
  0.00808579, 0.008599, -0.813495, -0.662911, 0.00930383,
  -0.00122413, -0.000216768, -0.00503985, -0.0781939, -0.00713892,
  -0.00649209, 0.000989081, -0.0410093, -0.0916615, 0.00883855,
  0.197953, 0.17109, 0.00445988, -0.00420201, -0.00166514,
  0.00226193, 0.000294848, 0.000568471, -0.000170057, 0.00210311,
  0.0016579, -0.000957386, -0.00168051, 0.00450953, 0.00649519,
  -0.000751702, 1.10303, -0.726772, 0.66379, -0.915479,
  0.411347, -1.11326, -0.381297, 0.512392, 2.16415,
  0.427017, -0.240469, -1.80094, 1.66976, -0.231898,
  -0.0274794, 1.16326, -0.10856, 0.966408, -1.96549,
  0.268139, 0.146961, 2.28708, -1.03568, -1.05558,
  -0.959071, -0.229529, 0.0506664,
  };
  // --- Constantes
  int indNeurone = 0;
  int CrtW;
  double sum;

  // --- Input Layers
  for(int i = 0; i < nInput; i++) {
     FctTBR_Total_Rn_9_0_act[indNeurone++] = 2.0 * ( param[i] -
FctTBR_Total_Rn_9_0_minInput[i] ) / ( FctTBR_Total_Rn_9_0_maxInput[i] -
FctTBR_Total_Rn_9_0_minInput[i] ) - 1.0;
```

```
  }

  // --- Hidden Layers
  for (int member = 0; member < nHidden; member++) {
     int CrtW = member * ( nInput + 2) + 2;
     sum = FctTBR_Total_Rn_9_0_valW[CrtW++];
     for (int source = 0; source < nInput; source++) {
         sum += FctTBR_Total_Rn_9_0_act[source] * FctTBR_Total_Rn_9_0_valW[CrtW++];
       }
       FctTBR_Total_Rn_9_0_act[indNeurone++] = ActivationFunction(sum);
  }

  // --- Output
  for (int member = 0; member < nOuput; member++) {
    sum = FctTBR_Total_Rn_9_0_valW[0];
    for (int source = 0; source < nHidden; source++) {
      CrtW = source * ( nInput + 2) + 1;
      sum += FctTBR_Total_Rn_9_0_act[nInput+source] * FctTBR_Total_Rn_9_0_valW[CrtW];
    }
    FctTBR_Total_Rn_9_0_act[indNeurone++] = sum;
    res[member] = FctTBR_Total_Rn_9_0_minOuput[member] + 0.5 * (
FctTBR_Total_Rn_9_0_maxOuput[member] - FctTBR_Total_Rn_9_0_minOuput[member] ) * ( sum +
1.0);
  }
}
```

B.8. Neural network performances example

Automatically generated file containing the neural network performances for different hiding layers and iterations.

```
Nombre de neurones de la couche cachee : 1
      Essai MSE         moyenne     moyenne_abs ecart type  ecart type perc   ecart Max   ecart Max perc    Note

      0     1.3342e-03  1.2205e-04  7.1559e-03  8.8904e-03  5.1062e-03        4.2868e-02  4.7704e-02        1.0796e-
01
      1     1.2958e-03  1.4131e-04  7.1605e-03  8.8958e-03  5.1011e-03        4.2418e-02  4.6631e-02        1.0747e-
01
      2     1.3556e-03  2.5109e-04  7.1305e-03  8.8963e-03  5.1795e-03        4.5108e-02  4.9093e-02        1.0836e-
01

Nombre de neurones de la couche cachee : 2
      Essai MSE         moyenne     moyenne_abs ecart type  ecart type perc   ecart Max   ecart Max perc    Note

      0     5.6857e-04  7.5366e-05  4.4929e-03  5.6364e-03  3.2701e-03        2.9540e-02  3.0656e-02        6.5541e-
02
      1     5.1697e-04  1.0875e-05  4.4985e-03  5.6416e-03  3.2647e-03        3.0599e-02  3.1720e-02        6.5293e-
02
      2     5.6203e-04  2.8079e-04  4.4975e-03  5.6711e-03  3.3344e-03        3.0075e-02  3.1194e-02        6.5727e-
02

Nombre de neurones de la couche cachee : 3
      Essai MSE         moyenne     moyenne_abs ecart type  ecart type perc   ecart Max   ecart Max perc    Note

      0     2.8943e-04  3.9709e-05  3.1815e-03  4.0299e-03  2.3770e-03        2.1614e-02  2.1973e-02        4.5475e-
02
      1     3.3068e-04  3.3691e-04  3.4391e-03  4.3598e-03  2.5958e-03        2.0543e-02  1.9837e-02        4.8691e-
02
      2     2.7599e-04  2.5864e-05  3.2398e-03  4.1126e-03  2.4410e-03        2.2503e-02  2.4933e-02        4.6455e-
02
```

```
Nombre de neurones de la couche cachee : 4
      Essai MSE         moyenne     moyenne_abs ecart type  ecart type perc   ecart Max   ecart Max perc    Note

      0     9.7440e-05  5.5697e-05  1.7495e-03  2.3165e-03  1.4537e-03        1.2685e-02  1.1935e-02        2.4702e-
02
      1     9.6959e-05  1.9162e-04  1.7298e-03  2.2990e-03  1.4684e-03        1.3220e-02  1.3668e-02        2.4723e-
02
      2     8.5833e-05  6.7761e-05  1.7544e-03  2.2993e-03  1.4246e-03        1.1843e-02  1.2262e-02        2.4537e-
02


Nombre de neurones de la couche cachee : 5
      Essai MSE         moyenne     moyenne_abs ecart type  ecart type perc   ecart Max   ecart Max perc    Note

      0     3.6953e-05  1.4426e-04  1.0895e-03  1.3986e-03  8.4464e-04        7.6229e-03  6.5488e-03        1.4925e-
02
      1     3.4770e-05  4.3617e-05  1.1193e-03  1.4425e-03  8.7213e-04        7.6237e-03  7.5155e-03        1.5369e-
02
      2     4.5417e-05  4.7776e-05  1.1780e-03  1.5270e-03  9.2651e-04        1.1094e-02  1.1286e-02        1.6926e-
02

Nombre de neurones de la couche cachee : 6
      Essai MSE         moyenne     moyenne_abs ecart type  ecart type perc   ecart Max   ecart Max perc    Note

      0     4.2188e-05  7.3508e-06  1.1260e-03  1.4525e-03  8.7899e-04        8.0089e-03  7.8922e-03        1.5603e-
02
      1     2.8112e-05  3.3706e-04  9.4493e-04  1.1618e-03  7.2113e-04        5.6682e-03  5.9067e-03        1.2771e-
02
      2     2.3919e-05  6.1193e-05  8.5781e-04  1.1020e-03  6.7541e-04        5.9896e-03  5.0463e-03        1.1698e-
02

Nombre de neurones de la couche cachee : 7
      Essai MSE         moyenne     moyenne_abs ecart type  ecart type perc   ecart Max   ecart Max perc    Note

      0     2.5492e-05  4.8987e-05  8.8061e-04  1.1686e-03  7.4103e-04        9.4176e-03  9.7755e-03        1.2890e-
02
```

```
      1     2.0434e-05  3.9255e-05  8.1358e-04  1.0507e-03  6.3412e-04        5.3205e-03  5.4757e-03        1.1105e-
02
      2     1.9908e-05  2.2119e-04  8.1431e-04  1.0384e-03  6.5072e-04        4.7585e-03  5.0299e-03        1.1010e-
02

Nombre de neurones de la couche cachee : 8
      Essai MSE         moyenne     moyenne_abs ecart type  ecart type perc   ecart Max   ecart Max perc    Note

      0     2.1540e-05  3.0268e-05  8.0827e-04  1.0451e-03  6.3571e-04        4.8528e-03  4.7436e-03        1.0939e-
02
      1     1.9415e-05  2.4224e-05  7.7984e-04  1.0193e-03  6.2621e-04        5.1436e-03  4.4805e-03        1.0600e-
02
      2     2.1293e-05  9.4595e-05  8.3006e-04  1.0702e-03  6.5203e-04        4.8699e-03  4.8835e-03        1.1211e-
02

Nombre de neurones de la couche cachee : 9
      Essai MSE         moyenne     moyenne_abs ecart type  ecart type perc   ecart Max   ecart Max perc    Note

      0     2.0187e-05  8.2823e-05  8.2545e-04  1.0532e-03  6.2928e-04        4.9867e-03  4.5731e-03        1.1095e-
02
      1     1.3811e-05  2.9151e-05  6.7702e-04  8.7342e-04  5.2745e-04        4.4525e-03  4.2245e-03        9.1769e-
03
      2     3.2663e-05  2.6305e-04  1.0569e-03  1.3278e-03  8.0386e-04        6.3489e-03  7.4607e-03        1.4409e-
02


Nombre de neurones de la couche cachee : 10
      Essai MSE         moyenne     moyenne_abs ecart type  ecart type perc   ecart Max   ecart Max perc    Note

      0     1.8102e-05  2.2629e-05  7.7668e-04  1.0011e-03  6.0337e-04        4.9456e-03  4.5686e-03        1.0504e-
02
      1     3.1249e-05  5.6763e-05  1.0221e-03  1.3141e-03  7.9270e-04        7.3116e-03  7.0855e-03        1.4080e-
02
      2     2.1582e-05  2.2686e-05  8.2993e-04  1.0710e-03  6.5028e-04        4.7191e-03  4.8694e-03        1.1195e-
02
```

```
Nombre de neurones de la couche cachee : 11
      Essai MSE         moyenne     moyenne_abs ecart type  ecart type perc   ecart Max   ecart Max perc    Note

      0     2.3016e-05  8.2102e-05  8.4414e-04  1.1002e-03  6.8435e-04        6.9218e-03  7.2035e-03        1.1869e-
02
      1     2.0537e-05  7.3624e-05  8.3491e-04  1.0782e-03  6.6192e-04        5.6456e-03  6.2438e-03        1.1484e-
02
      2     1.8775e-05  1.3793e-04  7.8505e-04  1.0092e-03  6.1994e-04        5.5018e-03  5.7342e-03        1.0791e-
02

Nombre de neurones de la couche cachee : 12
      Essai MSE         moyenne     moyenne_abs ecart type  ecart type perc   ecart Max   ecart Max perc    Note

      0     2.7996e-05  9.3369e-05  9.7235e-04  1.2506e-03  7.5804e-04        6.3051e-03  6.0606e-03        1.3249e-
02
      1     1.7056e-05  3.4085e-05  7.5807e-04  9.8224e-04  5.9341e-04        5.1772e-03  4.6552e-03        1.0310e-
02
      2     3.6235e-05  1.0255e-04  1.0579e-03  1.3495e-03  8.1430e-04        6.9707e-03  7.2674e-03        1.4529e-
02

Nombre de neurones de la couche cachee : 13
      Essai MSE         moyenne     moyenne_abs ecart type  ecart type perc   ecart Max   ecart Max perc    Note

      0     2.2280e-05  5.9113e-05  8.7419e-04  1.1436e-03  7.1510e-04        7.3071e-03  7.6015e-03        1.2314e-
02
      1     2.1336e-05  2.3286e-05  8.4456e-04  1.0871e-03  6.5307e-04        5.0627e-03  4.5679e-03        1.1362e-
02
      2     1.9212e-05  6.7073e-05  7.7708e-04  1.0017e-03  6.0977e-04        4.7160e-03  4.9852e-03        1.0544e-
02

Nombre de neurones de la couche cachee : 14
      Essai MSE         moyenne     moyenne_abs ecart type  ecart type perc   ecart Max   ecart Max perc    Note

      0     1.7687e-05  1.0746e-04  7.9148e-04  1.0197e-03  6.2136e-04        5.5452e-03  5.3829e-03        1.0826e-
02
      1     2.2655e-05  4.2048e-05  8.5191e-04  1.0957e-03  6.6532e-04        5.2296e-03  5.6590e-03        1.1595e-
02
```

```
      2     1.6385e-05  1.6176e-05  7.1834e-04  9.3907e-04  5.7350e-04        5.5987e-03  4.8653e-03        9.9063e-
03


Nombre de neurones de la couche cachee : 15
      Essai MSE         moyenne     moyenne_abs ecart type  ecart type perc   ecart Max   ecart Max perc    Note

      0     1.8482e-05  1.0738e-04  7.6727e-04  9.8250e-04  5.9169e-04        4.4203e-03  4.8270e-03        1.0356e-
02
      1     2.5554e-05  2.0299e-05  9.4551e-04  1.2242e-03  7.3913e-04        5.7897e-03  5.3606e-03        1.2789e-
02
      2     2.2865e-05  6.3994e-05  8.8242e-04  1.1285e-03  6.7918e-04        6.2335e-03  6.0471e-03        1.2089e-
02


The chosen one...

Nombre de neurones caches = 9
Essai   = 1
Moyenne = 2.9151e-05
Moyenne abs = 6.7702e-04
MSE = 1.3811e-05
Ecart type = 8.7342e-04
Ecart type pourcentage= 5.2745e-04
Ecart maxi = 4.4525e-03
Ecart maxi perc =  4.2245e-03
Note = 9.1769e-03


Parametres en entree :

Half_Radius_of_the_Plasma:Thickness_VV_Inboard:Thickness_SH_Inboard:Thickness_MAN_Inboard:Thickness_BZ_Inboard:Thick
ness_FW:Thickness_of_the_Plasma:Thickness_MAN_Outboard:Thickness_BZ_Outboard:Lithium_6_enrichment:Composition_FW_He:
Composition_BZ_EuroFer:Composition_BZ_He:Composition_MAN_LiPB:Composition_MAN_EuroFer:Composition_SH_EuroFer:Composi
tion_SH_H2O:Composition_VV_He:Composition_VV_Boron:Composition_TFSWP_He:Composition_TFC_Epoxy:Composition_TFC_HeLiq:
Triangulation:Elongation:Surface_Div_Inboard:Surface_Div_Outboard
```

B.9. Chosen neural network performances

Chosen neural networks for the creation of the surrogate model

```
Rn_TBRTot
Nombre de neurones de la couche cachee : 9
      Essai MSE         moyenne     moyenne_abs ecart type  ecart type perc   ecart Max   ecart Max perc    Note
      1     1.3811e-05  2.9151e-05  6.7702e-04  8.7342e-04  5.2745e-04        4.4525e-03  4.2245e-03        9.1769e-
03

Rn_TBRInboard
Nombre de neurones de la couche cachee : 13
      Essai MSE         moyenne     moyenne_abs ecart type  ecart type perc   ecart Max   ecart Max perc    Note
      1     1.1455e-05  9.7215e-06  2.4586e-04  3.1914e-04  7.5818e-04        1.7299e-03  7.7373e-03        4.5972e-
03

Rn_TBROutboard
Nombre de neurones de la couche cachee : 14
      Essai MSE         moyenne     moyenne_abs ecart type  ecart type perc   ecart Max   ecart Max perc    Note
      1     2.4405e-05  8.9766e-05  6.8191e-04  8.6985e-04  6.9636e-04        4.0384e-03  5.0772e-03        9.5410e-
03

Facteur de multiplication
Nombre de neurones de la couche cachee : 9
      Essai MSE         moyenne     moyenne_abs ecart type  ecart type perc   ecart Max   ecart Max perc    Note
      0     2.5049e-05  1.6236e-05  1.0485e-04  1.3868e-04  7.6902e-05        7.7808e-04  6.4845e-04        1.6573e-
03

Energie FWI
Nombre de neurones de la couche cachee : 2
      Essai MSE         moyenne     moyenne_abs ecart type  ecart type perc   ecart Max   ecart Max perc    Note
      0     1.5087e-03  8.2564e-24  2.3766e-22  3.0889e-22  4.0279e-03        1.2503e-21  2.5187e-02        2.1634e-
02

Energie FWO
Nombre de neurones de la couche cachee : 5
```

```
      Essai MSE         moyenne     moyenne_abs ecart type  ecart type perc   ecart Max   ecart Max perc    Note
      0     2.1390e-04  1.7865e-24  1.9654e-22  2.4552e-22  2.3502e-03        9.5821e-22  1.6529e-02        6.1422e-
03



Energie BZI
Nombre de neurones de la couche cachee : 2
      Essai MSE         moyenne     moyenne_abs ecart type  ecart type perc   ecart Max   ecart Max perc    Note
      0     1.1462e-04  6.0330e-24  5.6443e-23  7.2404e-23  2.3794e-03        2.9000e-22  1.3152e-02        4.8408e-
03

Energie BZO
Nombre de neurones de la couche cachee : 6
      Essai MSE         moyenne     moyenne_abs ecart type  ecart type perc   ecart Max   ecart Max perc    Note
      2     6.3801e-05  1.7080e-24  3.8695e-23  5.0698e-23  2.0694e-03        1.8305e-22  1.2539e-02        3.9613e-
03

Energie BZ10I
Nombre de neurones de la couche cachee : 1
      Essai MSE         moyenne     moyenne_abs ecart type  ecart type perc   ecart Max   ecart Max perc    Note
      0     3.8021e-04  8.5045e-24  1.2768e-22  1.6013e-22  2.4908e-03        5.7443e-22  1.3479e-02        7.6408e-
03

Energie BZ10O
Nombre de neurones de la couche cachee : 5
      Essai MSE         moyenne     moyenne_abs ecart type  ecart type perc   ecart Max   ecart Max perc    Note
      0     1.7942e-04  5.3551e-24  1.2514e-22  1.5930e-22  2.0677e-03        6.4539e-22  1.2137e-02        5.0757e-
03

Energie BPI
Nombre de neurones de la couche cachee : 3
      Essai MSE         moyenne     moyenne_abs ecart type  ecart type perc   ecart Max   ecart Max perc    Note
      2     2.9661e-04  2.0103e-25  1.8906e-23  2.4882e-23  1.3870e-02        1.2774e-22  8.1975e-02        2.5033e-
02

Energie BPO
```

```
Nombre de neurones de la couche cachee : 6
      Essai MSE         moyenne     moyenne_abs ecart type  ecart type perc   ecart Max   ecart Max perc    Note
      2     3.0685e-04  1.3761e-25  1.0181e-23  1.3628e-23  2.3607e-02        7.3594e-23  1.7966e-01        4.4641e-
02

Energie MANI
Nombre de neurones de la couche cachee : 4
      Essai MSE         moyenne     moyenne_abs ecart type  ecart type perc   ecart Max   ecart Max perc    Note
      1     3.0373e-04  6.1346e-25  1.9500e-23  2.5852e-23  1.4068e-02        1.8448e-22  9.9401e-02        2.7046e-
02



Energie MANO
Nombre de neurones de la couche cachee : 2
      Essai MSE         moyenne     moyenne_abs ecart type  ecart type perc   ecart Max   ecart Max perc    Note
      1     2.4291e-04  3.4123e-25  7.8202e-24  1.0780e-23  1.7099e-02        5.0724e-23  9.6231e-02        2.9151e-
02

Energie SHI
Nombre de neurones de la couche cachee : 4
      Essai MSE         moyenne     moyenne_abs ecart type  ecart type perc   ecart Max   ecart Max perc    Note
      0     1.7536e-04  3.7263e-25  4.0460e-23  5.4033e-23  9.9887e-03        2.1300e-22  6.2306e-02        1.7973e-
02

Energie SHO
Nombre de neurones de la couche cachee : 2
      Essai MSE         moyenne     moyenne_abs ecart type  ecart type perc   ecart Max   ecart Max perc    Note
      0     2.2230e-04  8.4246e-25  1.0534e-23  1.4775e-23  1.6652e-02        7.7593e-23  1.0939e-01        2.9814e-
02

Energie VV
Nombre de neurones de la couche cachee : 4
      Essai MSE         moyenne     moyenne_abs ecart type  ecart type perc   ecart Max   ecart Max perc    Note
      4     5.0766e-05  8.0903e-26  2.3044e-24  3.9530e-24  1.9609e-02        7.0152e-23  1.6437e-01        3.6554e-
02
```

Energie VVO
Nombre de neurones de la couche cachee : 2

Essai	MSE	moyenne	moyenne_abs	ecart type	ecart type perc	ecart Max	ecart Max perc	Note
5	5.3056e-04	1.7515e-28	1.6890e-26	2.3430e-26	8.1016e-01	2.4769e-25	1.1448e+01	1.9603e+00

Energie TFSWP
Nombre de neurones de la couche cachee : 3

Essai	MSE	moyenne	moyenne_abs	ecart type	ecart type perc	ecart Max	ecart Max perc	Note
1	3.9912e-05	6.7203e-26	3.2249e-25	5.7246e-25	2.3633e-02	1.6735e-23	1.9957e-01	4.3990e-02

Energie TFSWPO
Nombre de neurones de la couche cachee : 1

Essai	MSE	moyenne	moyenne_abs	ecart type	ecart type perc	ecart Max	ecart Max perc	Note
1	1.3674e-05	1.6649e-30	4.0799e-29	9.2181e-29	5.9634e-02	1.2579e-27	3.9095e-01	9.8866e-02

Energie TFC
Nombre de neurones de la couche cachee : 4

Essai	MSE	moyenne	moyenne_abs	ecart type	ecart type perc	ecart Max	ecart Max perc	Note
7	6.3971e-05	9.3692e-27	5.9923e-26	1.1030e-25	2.6476e-02	2.9900e-24	2.3508e-01	5.0624e-02

Energie TFCO
Nombre de neurones de la couche cachee : 1

Essai	MSE	moyenne	moyenne_abs	ecart type	ecart type perc	ecart Max	ecart Max perc	Note
5	1.9533e-05	1.5856e-31	4.4984e-30	1.0654e-29	5.9387e-02	2.3982e-28	3.9853e-01	9.9436e-02

Flux sh1bz1 (1st zone)
fw
Nombre de neurones de la couche cachee : 15

Essai	MSE	moyenne	moyenne_abs	ecart type	ecart type perc	ecart Max	ecart Max perc	Note

```
      0     1.4256e-05  2.0736e-07  5.7367e-07  7.8429e-07  4.7730e-04        4.7939e-06  3.8264e-03        1.0095e-
03

bz
Nombre de neurones de la couche cachee : 9
      Essai MSE         moyenne     moyenne_abs ecart type  ecart type perc   ecart Max   ecart Max perc    Note
      0     1.3258e-05  6.9620e-08  6.1813e-07  8.4528e-07  5.1783e-04        4.9671e-06  3.7553e-03        1.0335e-
03

bp
Nombre de neurones de la couche cachee : 15
      Essai MSE         moyenne     moyenne_abs ecart type  ecart type perc   ecart Max   ecart Max perc    Note
      1     7.6039e-06  5.4340e-08  3.8240e-07  5.0790e-07  1.3198e-03        3.8156e-06  1.4950e-02        2.8956e-
03

man
Nombre de neurones de la couche cachee : 13
      Essai MSE         moyenne     moyenne_abs ecart type  ecart type perc   ecart Max   ecart Max perc    Note
      0     2.2272e-05  1.0455e-08  4.2142e-07  5.6667e-07  2.3728e-03        4.7107e-06  3.0617e-02        5.6624e-
03
sh
Nombre de neurones de la couche cachee : 14
      Essai MSE         moyenne     moyenne_abs ecart type  ecart type perc   ecart Max   ecart Max perc    Note
      0     3.0310e-05  3.5048e-08  1.9278e-07  2.6123e-07  3.3514e-03        1.9885e-06  3.8260e-02        7.4829e-
03



vv
Nombre de neurones de la couche cachee : 12
      Essai MSE         moyenne     moyenne_abs ecart type  ecart type perc   ecart Max   ecart Max perc    Note
      0     8.3889e-05  4.8392e-12  2.5328e-10  3.7401e-10  1.3193e-02        2.8808e-09  1.0837e-01        2.4869e-
02

tfswp
Nombre de neurones de la couche cachee : 9
      Essai MSE         moyenne     moyenne_abs ecart type  ecart type perc   ecart Max   ecart Max perc    Note
```

```
      0     3.2432e-05  1.0970e-12  1.3388e-11  1.9887e-11  1.5313e-02        1.7376e-10  1.7736e-01        3.3373e-
02

tfc
Nombre de neurones de la couche cachee : 4
      Essai MSE         moyenne     moyenne_abs ecart type  ecart type perc   ecart Max   ecart Max perc    Note
      1     4.9855e-05  4.9881e-14  8.2481e-12  1.2487e-11  1.8027e-02        1.1032e-10  1.4710e-01        3.3236e-
02
```

Flux sh1bz2 (2nd zone)

```
fw
Nombre de neurones de la couche cachee : 8
      Essai MSE         moyenne     moyenne_abs ecart type  ecart type perc   ecart Max   ecart Max perc    Note
      4     1.3425e-05  3.3978e-08  6.2845e-07  8.3867e-07  4.5600e-04        4.9953e-06  4.1338e-03        1.0113e-
03


bz
Nombre de neurones de la couche cachee : 9
      Essai MSE         moyenne     moyenne_abs ecart type  ecart type perc   ecart Max   ecart Max perc    Note
      2     1.1874e-05  2.1911e-07  6.3637e-07  7.7751e-07  4.4072e-04        4.5806e-06  3.6446e-03        9.3151e-
04

bp
Nombre de neurones de la couche cachee : 11
      Essai MSE         moyenne     moyenne_abs ecart type  ecart type perc   ecart Max   ecart Max perc    Note
      1     1.1090e-05  8.1910e-09  2.7330e-07  3.6551e-07  1.7888e-03        2.9078e-06  2.2404e-02        4.1435e-
03

man
Nombre de neurones de la couche cachee : 12
      Essai MSE         moyenne     moyenne_abs ecart type  ecart type perc   ecart Max   ecart Max perc    Note
      0     1.5423e-05  5.3051e-09  2.2724e-07  3.0936e-07  2.4392e-03        2.9650e-06  2.7356e-02        5.3319e-
03
sh
Nombre de neurones de la couche cachee : 10
```

```
      Essai MSE         moyenne     moyenne_abs ecart type  ecart type perc   ecart Max   ecart Max perc    Note
      1     2.0201e-05  4.4685e-09  8.5807e-08  1.2026e-07  3.0511e-03        9.3412e-07  3.0846e-02        6.3388e-
03


vv
Nombre de neurones de la couche cachee : 6
      Essai MSE         moyenne     moyenne_abs ecart type  ecart type perc   ecart Max   ecart Max perc    Note
      1     5.9089e-05  1.0065e-11  8.5290e-11  1.2636e-10  1.2450e-02        1.2287e-09  9.6383e-02        2.2680e-
02

tfswp
Nombre de neurones de la couche cachee : 5
      Essai MSE         moyenne     moyenne_abs ecart type  ecart type perc   ecart Max   ecart Max perc    Note
      1     5.4932e-05  4.6132e-13  3.3986e-12  5.3509e-12  1.3891e-02        1.3796e-10  1.1627e-01        2.6067e-
02

tfc
Nombre de neurones de la couche cachee : 4
      Essai MSE         moyenne     moyenne_abs ecart type  ecart type perc   ecart Max   ecart Max perc    Note
      1     8.1275e-05  7.3925e-15  1.9198e-12  2.9865e-12  1.6448e-02        3.3386e-11  1.4580e-01        3.1841e-
02
```

Flux sh2bz1 (3rd zone)

```
fw
Nombre de neurones de la couche cachee : 8
      Essai MSE         moyenne     moyenne_abs ecart type  ecart type perc   ecart Max   ecart Max perc    Note
      3     1.3327e-05  1.5382e-07  5.8328e-07  7.8899e-07  4.5079e-04        5.2682e-06  3.7074e-03        9.6194e-
04

bz
Nombre de neurones de la couche cachee : 7
      Essai MSE         moyenne     moyenne_abs ecart type  ecart type perc   ecart Max   ecart Max perc    Note
      4     1.2327e-05  4.3008e-08  5.9738e-07  8.0241e-07  4.8365e-04        5.1675e-06  3.8725e-03        1.0015e-
03
```

```
bp
Nombre de neurones de la couche cachee : 7
      Essai MSE         moyenne     moyenne_abs ecart type  ecart type perc   ecart Max   ecart Max perc    Note
      1     1.1686e-05  9.3697e-09  4.2704e-07  5.7242e-07  1.4696e-03        3.8583e-06  2.7053e-02        4.2970e-
03

man
Nombre de neurones de la couche cachee : 11
      Essai MSE         moyenne     moyenne_abs ecart type  ecart type perc   ecart Max   ecart Max perc    Note
      0     2.8323e-05  8.0835e-09  4.6222e-07  6.2390e-07  2.5033e-03        3.7029e-06  1.9958e-02        4.7879e-
03

sh
Nombre de neurones de la couche cachee : 11
      Essai MSE         moyenne     moyenne_abs ecart type  ecart type perc   ecart Max   ecart Max perc    Note
      3     1.3548e-05  2.4813e-08  1.3639e-07  1.8067e-07  2.4850e-03        1.3689e-06  3.3675e-02        5.9896e-
03

vv
Nombre de neurones de la couche cachee : 9
      Essai MSE         moyenne     moyenne_abs ecart type  ecart type perc   ecart Max   ecart Max perc    Note
      4     4.5530e-05  1.0927e-11  8.7985e-11  1.2549e-10  1.2362e-02        1.2157e-09  1.0986e-01        2.3803e-
02

tfswp
Nombre de neurones de la couche cachee : 8
      Essai MSE         moyenne     moyenne_abs ecart type  ecart type perc   ecart Max   ecart Max perc    Note
      1     4.7918e-05  1.5457e-13  5.1213e-12  7.5725e-12  1.2330e-02        6.3897e-11  1.1414e-01        2.4223e-
02

tfc
Nombre de neurones de la couche cachee : 7
      Essai MSE         moyenne     moyenne_abs ecart type  ecart type perc   ecart Max   ecart Max perc    Note
      0     6.8000e-05  1.3371e-14  2.7591e-12  4.2064e-12  1.4076e-02        4.7824e-11  1.2631e-01        2.7387e-
02
```

Flux sh2bz2 (4th zone)

```
fw
Nombre de neurones de la couche cachee : 9
      Essai MSE         moyenne     moyenne_abs ecart type  ecart type perc   ecart Max   ecart Max perc    Note
      4     1.5371e-05  6.8993e-08  6.6105e-07  8.9962e-07  5.0115e-04        5.4024e-06  4.2910e-03        1.0920e-
03

bz
Nombre de neurones de la couche cachee : 10
      Essai MSE         moyenne     moyenne_abs ecart type  ecart type perc   ecart Max   ecart Max perc    Note
      3     1.0447e-05  1.0263e-07  5.3557e-07  7.4695e-07  4.7634e-04        4.2271e-06  3.8489e-03        9.7223e-
04

bp
Nombre de neurones de la couche cachee : 10
      Essai MSE         moyenne     moyenne_abs ecart type  ecart type perc   ecart Max   ecart Max perc    Note
      0     1.6672e-05  5.6283e-08  3.2678e-07  4.3223e-07  2.0050e-03        3.8673e-06  1.7518e-02        3.9276e-
03

man
Nombre de neurones de la couche cachee : 11
      Essai MSE         moyenne     moyenne_abs ecart type  ecart type perc   ecart Max   ecart Max perc    Note
      3     2.2187e-05  6.6251e-09  2.8552e-07  3.8647e-07  2.9416e-03        3.5018e-06  2.5397e-02        5.7067e-
03

sh
Nombre de neurones de la couche cachee : 11
      Essai MSE         moyenne     moyenne_abs ecart type  ecart type perc   ecart Max   ecart Max perc    Note
      0     2.4793e-05  5.1289e-10  9.0656e-08  1.2321e-07  3.2041e-03        9.3988e-07  3.3755e-02        6.8286e-
03

vv
Nombre de neurones de la couche cachee : 9
      Essai MSE         moyenne     moyenne_abs ecart type  ecart type perc   ecart Max   ecart Max perc    Note
      4     6.0370e-05  4.0617e-13  2.1959e-11  3.3040e-11  1.0753e-02        3.6414e-10  1.0152e-01        2.1509e-
02
```

```
tfswp
Nombre de neurones de la couche cachee : 8
      Essai MSE         moyenne     moyenne_abs ecart type  ecart type perc   ecart Max   ecart Max perc    Note
      0     6.6995e-05  2.1477e-14  1.3814e-12  2.1162e-12  1.3378e-02        2.0879e-11  1.3489e-01        2.7537e-
02

tfc
Nombre de neurones de la couche cachee : 6
      Essai MSE         moyenne     moyenne_abs ecart type  ecart type perc   ecart Max   ecart Max perc    Note
      4     5.9494e-05  3.7779e-14  6.6616e-13  1.0592e-12  1.3042e-02        1.0835e-11  1.0014e-01        2.3651e-
02
```

C. Apendix : Programs and Codes

C.1. Neutronic Module

- Launcher.py

```
from math import *
import glob
import sys
import math
import os
from ctypes import *
from numpy  import *
from functions import *
from neuralnetworks import *
from inputs import *

###################1. Declaration of the Neural Networks used to perform the calculations
(shared libraries .so) #################


#################### 2. Opening the input file ##############################

#output = open('input.dat','r')

#################### 3. Creation of the output files ######################
print 'LOADING THE PROGRAM...'
output = open('check.out','w')
var = open('variables.out','w')
var.write('NEUTRONIC MODULE\n\n')
var.write('File created automatically by the neutronic module.\n')
var.write('File containing output variables stored in rows \n\n')
output.write('NEUTRONIC MODULE\n\n')
output.write('File created automatically by the neutronic module.\n')
output.write('File containing the geometry check and output variables stored in rows
\n\n')

################ 4. Definition of the variables ############################
print 'GEOMETRY VALIDATION'

#Matrix containing the index, name, value and operable window of each parameter used by
the neural networks
#The matrix columns are: [Index,Name,Value,MinValue,MaxValue,Dimension]

param_values = array([
        [0,'Lithium_6_enrichment', Lithium_6_enrichment,  0.6, 0.99, 'cm'],
        #General parameters
        [1,'Half_Radius_of_the_Plasma',Half_Radius_of_the_Plasma*100,  700, 900, 'cm'],
        #Thickness
        [2,'Thickness_of_the_Plasma', Thickness_of_the_Plasma*100,  240, 250, 'cm'],
        [3,'Thickness_CS_Inboard', Thickness_CS_Inboard*100, 72, 76, 'cm'],
        [4,'Thickness_TFC_Inboard', Thickness_TFC_Inboard*100 ,  70, 78 , 'cm'],
        [5,'Thickness_TFSWP_Inboard', Thickness_TFSWP_Inboard*100 ,   5, 7 , 'cm'],
        [6,'Thickness_VV_Inboard',Thickness_VV_Inboard*100 ,  30, 40, 'cm'],
        [7,'Thickness_SH_Inboard',Thickness_SH_Inboard*100 ,  25, 35 , 'cm'],
        [8,'Thickness_MAN_Inboard',Thickness_MAN_Inboard*100 ,  25, 35 , 'cm'],
        [9,'Thickness_BP_Inboard',Thickness_BP_Inboard*100 ,   15, 25   , 'cm'],
        [10,'Thickness_BZ_Inboard',Thickness_BZ_Inboard*100 ,  30, 60  , 'cm'],
        [11,'Thickness_FW',Thickness_FW*100 ,   2, 4  , 'cm'],
        [12,'Thickness_FWPL_Inboard',Thickness_FWPL_Inboard*100,  0.1, 0.3  , 'cm'],
        [13,'Thickness_TFC_Outboard',Thickness_TFC_Outboard*100 ,  90, 96   , 'cm'],
        [14,'Thickness_TFSWP_Outboard',Thickness_TFSWP_Outboard*100,    7, 9 , 'cm'],
        [15,'Thickness_VV_Outboard', Thickness_VV_Outboard*100,   77, 83   , 'cm'],
        [16,'Thickness_SH_Outboard', Thickness_SH_Outboard*100,   45, 55   , 'cm'],
        [17,'Thickness_MAN_Outboard',Thickness_MAN_Outboard*100 ,   45, 55  , 'cm'],
        [18,'Thickness_BP_Outboard',Thickness_BP_Outboard*100 ,  15, 25  , 'cm'],
        [19,'Thickness_BZ_Outboard', Thickness_BZ_Outboard*100  , 60, 90  , 'cm'],
        [20,'Thickness_FWPL_Outboard',Thickness_FWPL_Outboard*100 ,  0.1, 0.3 , 'cm'],
```

```
        [21,'Tolerance_TFC_CS_Inboard', Tolerance_TFC_CS_Inboard*100,   8, 12 , 'cm'],
               #Tolerances
        [22,'Tolerance_VV_TFC_Inboard', Tolerance_VV_TFC_Inboard*100,   8, 12, 'cm'],
        [23,'Tolerance_SH_VV_Inboard', Tolerance_SH_VV_Inboard*100,   8, 12, 'cm'],
        [24,'Tolerance_BB_SH_Inboard',Tolerance_BB_SH_Inboard*100 ,   8, 12, 'cm'],
        [25,'Tolerance_VV_TFC_Outboard',Tolerance_VV_TFC_Outboard*100 ,  8, 12, 'cm'],
        [26,'Tolerance_SH_VV_Outboard',Tolerance_SH_VV_Outboard*100 ,   8, 12, 'cm'],
        [27,'Tolerance_BB_SH_Outboard', Tolerance_BB_SH_Outboard*100 ,  8, 12, 'cm'],
        [28,'Distance_Plasma_FW_Inboard',Distance_Plasma_FW_Inboard*100 , 5, 15, 'cm'],
        [29,'Distance_Plasma_FW_Outboard',Distance_Plasma_FW_Outboard*100 , 5, 20, 'cm'],
        [30,'Composition_FW_He',Composition_FW_He , 25, 35 , '%'],
        #Materials compositions
        [31,'Composition_BZ_EuroFer', Composition_BZ_EuroFer,   5, 20 , '%'],
        [32,'Composition_BZ_He',Composition_BZ_He ,   5, 20, '%'],
        [33,'Composition_BP_LiPB',Composition_BP_LiPB , 0, 10, '%'],
        [34,'Composition_BP_EuroFer',Composition_BP_EuroFer ,  25, 35   , '%'],
        [35,'Composition_MAN_LiPB',Composition_MAN_LiPB , 0, 10 , '%'],
        [36,'Composition_MAN_EuroFer', Composition_MAN_EuroFer,  25, 35  , '%'],
        [37,'Composition_SH_EuroFer',Composition_SH_EuroFer, 5, 15, '%'],
        [38,'Composition_SH_H2O', Composition_SH_H2O,20, 30 , '%'],
        [39,'Composition_VV_He',Composition_VV_He , 35, 40, '%'],
        [40,'Composition_VV_Boron',Composition_VV_Boron ,  1, 3, '%'],
        [41,'Composition_TFSWP_He',Composition_TFSWP_He , 0, 10, '%'],
        [42,'Composition_TFC_Epoxy', Composition_TFC_Epoxy, 15, 25, '%' ],
        [43,'Composition_TFC_HeLiq',Composition_TFC_HeLiq ,  13, 20, '%'],
        [44,'Triangulation', Triangulation,  0.4, 0.7 , 'no unit'],
        #Plasma parameters
        [45,'Elongation',Elongation ,  1.8, 2.2 , 'no unit'],
        [46,'Surface_Div_Inboard', Surface_Div_Inboard,  5, 6 , '%'],
        [47,'Surface_Div_Outboard',Surface_Div_Outboard ,   6, 7 , '%']])



#Parameters for the validation of the geometry

correctgeom = sel_value(param_values,'Half_Radius_of_the_Plasma') -
(sel_value(param_values,'Thickness_of_the_Plasma') +
sel_value(param_values,'Thickness_CS_Inboard') +
sel_value(param_values,'Thickness_TFC_Inboard') +
sel_value(param_values,'Thickness_TFSWP_Inboard') +
sel_value(param_values,'Thickness_VV_Inboard') +
sel_value(param_values,'Thickness_SH_Inboard') +
sel_value(param_values,'Thickness_MAN_Inboard') +
sel_value(param_values,'Thickness_BP_Inboard') +
sel_value(param_values,'Thickness_BZ_Inboard') + sel_value(param_values,'Thickness_FW') +
sel_value(param_values,'Thickness_FWPL_Inboard') +
sel_value(param_values,'Distance_Plasma_FW_Inboard') +
sel_value(param_values,'Tolerance_TFC_CS_Inboard') +
sel_value(param_values,'Tolerance_VV_TFC_Inboard') +
sel_value(param_values,'Tolerance_SH_VV_Inboard') +
sel_value(param_values,'Tolerance_BB_SH_Inboard'))
norm_1D_flux =
Fusion_Power*1000000/0.00000000000016021773/17.6/(Volume*1000000)*pi*((sel_value(param_val
ues,'Half_Radius_of_the_Plasma')+sel_value(param_values,'Thickness_of_the_Plasma')+sel_val
ue(param_values,'Distance_Plasma_FW_Outboard'))**2-
(sel_value(param_values,'Half_Radius_of_the_Plasma')-
sel_value(param_values,'Thickness_of_the_Plasma')-
sel_value(param_values,'Distance_Plasma_FW_Inboard'))**2)
norm_tripoli =
Fusion_Power*1000000/0.00000000000016021773/17.6/(Volume*1000000)*pi*((sel_value(param_val
ues,'Half_Radius_of_the_Plasma')+sel_value(param_values,'Thickness_of_the_Plasma')+sel_val
ue(param_values,'Distance_Plasma_FW_Outboard'))**2-
(sel_value(param_values,'Half_Radius_of_the_Plasma')-
sel_value(param_values,'Thickness_of_the_Plasma')-
sel_value(param_values,'Distance_Plasma_FW_Inboard'))**2)*200
print norm_tripoli
MeV_to_W = 0.00000000000016021773

################## 5. Validation of the geometry ########################
output.write('BEGINNING OF GEOMETRY CHECK \n')
i=0
while (i<len(param_values)):
       if (sel_min(param_values,param_values[i][1])<=
sel_value(param_values,param_values[i][1]) <= sel_max(param_values,param_values[i][1])):
              output.write('\tCHECK GEOM (%s): OK \n' % param_values[i][1])
       else:
```

```
                output.write('\tCHECK GEOM (%s): FALSE \n' % param_values[i][1])
                output.write('\tThe thickness of %s (%7.2f%s) is not within the limits
(%7.2f-%7.2f%s) \n'
%(param_values[i][1],sel_value(param_values,param_values[i][1]),sel_dim(param_values,param
_values[i][1]),sel_min(param_values,param_values[i][1]),sel_max(param_values,param_values[
i][1]),sel_dim(param_values,param_values[i][1])))
                output.write('PROGRAM STOP\n')
                print 'PROGRAM STOP'
                print 'OPS! The geomtry entered is not valid, check the output file
"check.out'
                sys.exit()
        i=i+1
if (correctgeom<0):
        output.write('\tCHECK GEOM Inboard Total Thicknes: FALSE \n')
        output.write('\tThe thickness of the inboard components exceeds the half radius of
the plasma \n')
        print 'PROGRAM STOP'
        print 'OPS! The geomtry entered is not valid, check the output file "check.out'
else:
        output.write('\tCHECK GEOM Inboard Total Thickness: OK \n')

output.write('END OF GEOMETRY CHECK \n\n')
#################### 6. Creation of the arrays that will be send to the Neural Networks
##########################
output.write('BEGINNING THE CREATION OF THE ARRAYS SEND TO THE NEURAL NETWORKS \n')
#Creation of an array containing the input parameters for the 1D model neural networks
param1D= array([sel_value(param_values,'Half_Radius_of_the_Plasma'),
        sel_value(param_values,'Thickness_CS_Inboard'),
        sel_value(param_values,'Thickness_TFC_Inboard'),
        sel_value(param_values,'Thickness_TFSWP_Inboard'),
        sel_value(param_values,'Thickness_VV_Inboard'),
        sel_value(param_values,'Thickness_SH_Inboard'),
        sel_value(param_values,'Thickness_MAN_Inboard'),
        sel_value(param_values,'Thickness_BP_Inboard'),
        sel_value(param_values,'Thickness_BZ_Inboard'),
        sel_value(param_values,'Thickness_FW'),
        sel_value(param_values,'Thickness_FWPL_Inboard'),
        sel_value(param_values,'Distance_Plasma_FW_Inboard'),
        sel_value(param_values,'Thickness_of_the_Plasma'),
        sel_value(param_values,'Distance_Plasma_FW_Outboard'),
        sel_value(param_values,'Thickness_TFC_Outboard'),
        sel_value(param_values,'Thickness_TFSWP_Outboard'),
        sel_value(param_values,'Thickness_VV_Outboard'),
        sel_value(param_values,'Thickness_SH_Outboard'),
        sel_value(param_values,'Thickness_MAN_Outboard'),
        sel_value(param_values,'Thickness_BP_Outboard'),
        sel_value(param_values,'Thickness_BZ_Outboard'),
        sel_value(param_values,'Thickness_FWPL_Outboard'),
        sel_value(param_values,'Tolerance_TFC_CS_Inboard'),
        sel_value(param_values,'Tolerance_VV_TFC_Inboard'),
        sel_value(param_values,'Tolerance_SH_VV_Inboard'),
        sel_value(param_values,'Tolerance_BB_SH_Inboard'),
        sel_value(param_values,'Tolerance_VV_TFC_Outboard'),
        sel_value(param_values,'Tolerance_SH_VV_Outboard'),
        sel_value(param_values,'Tolerance_BB_SH_Outboard'),
        sel_value(param_values,'Lithium_6_enrichment'),
        sel_value(param_values,'Composition_FW_He'),
        sel_value(param_values,'Composition_BZ_EuroFer'),
        sel_value(param_values,'Composition_BZ_He'),
        sel_value(param_values,'Composition_MAN_LiPB'),
        sel_value(param_values,'Composition_MAN_EuroFer'),
        sel_value(param_values,'Composition_BP_LiPB'),
        sel_value(param_values,'Composition_BP_EuroFer'),
        sel_value(param_values,'Composition_SH_EuroFer'),
        sel_value(param_values,'Composition_SH_H2O'),
        sel_value(param_values,'Composition_VV_He'),
        sel_value(param_values,'Composition_VV_Boron'),
        sel_value(param_values,'Composition_TFSWP_He'),
        sel_value(param_values,'Composition_TFC_Epoxy'),
        sel_value(param_values,'Composition_TFC_HeLiq')])
output.write('\tCHECK ARRAY INPUTS 1D MODEL: OK \n')


#Creation of an array containing the input parameters for the RZ model neural networks
paramRZ= array([sel_value(param_values,'Half_Radius_of_the_Plasma'),
        sel_value(param_values,'Thickness_VV_Inboard'),
```

```
        sel_value(param_values,'Thickness_SH_Inboard'),
        sel_value(param_values,'Thickness_MAN_Inboard'),
        sel_value(param_values,'Thickness_BZ_Inboard'),
        sel_value(param_values,'Thickness_FW'),
        sel_value(param_values,'Thickness_of_the_Plasma'),
        sel_value(param_values,'Thickness_MAN_Outboard'),
        sel_value(param_values,'Thickness_BZ_Outboard'),
        sel_value(param_values,'Lithium_6_enrichment'),
        sel_value(param_values,'Composition_FW_He'),
        sel_value(param_values,'Composition_BZ_EuroFer'),
        sel_value(param_values,'Composition_BZ_He'),
        sel_value(param_values,'Composition_MAN_LiPB'),
        sel_value(param_values,'Composition_MAN_EuroFer'),
        sel_value(param_values,'Composition_SH_EuroFer'),
        sel_value(param_values,'Composition_SH_H2O'),
        sel_value(param_values,'Composition_VV_He'),
        sel_value(param_values,'Composition_VV_Boron'),
        sel_value(param_values,'Composition_TFSWP_He'),
        sel_value(param_values,'Composition_TFC_Epoxy'),
        sel_value(param_values,'Composition_TFC_HeLiq'),
        sel_value(param_values,'Triangulation'),
        sel_value(param_values,'Elongation'),
        (sel_value(param_values,'Surface_Div_Inboard')/100),
        (sel_value(param_values,'Surface_Div_Outboard')/100)])
output.write('\tCHECK ARRAY INPUTS RZ MODEL: OK \n')
output.write('END OF ARRAY CHECK \n\n')

########################### 7. Import of the Neural networks to python using ctypes (import
of a dynamic library.so) ################
print 'LOADING AND PROCESSING THE NEURAL NETWORKS'
output.write('BEGINNING NEURAL NETWORK LOADING AND CALCULATIONS \n')


#Creation of a matrix with the names of the output parameters. The result and dimension
given by the neural networks will be added to the matrix later on
#The matrix columns are: [Index,Name,Value,Corrected Value,Dimension]

output_RZ= array([[0,'TBRTot',float,float,0.],
        [1,'TBRIb',float,float,0.],
        [2,'TBROb',float,float,0.],
        [3,'ME',float,float,0.]])

#The matrix columns for the energy are: [Index,Name,Value,Corrected Value MW/m3,Corrected
Value MW/m2,Dimension]
output_ener=array ([[0,'EnerFWIb',float,float,0.],
        [1,'EnerBZ10Ib',float,float,0.],
        [2,'EnerBZIb',float,float,0.],
        [3,'EnerBPIb',float,float,0.],
        [4,'EnerMANIb',float,float,0.],
        [5,'EnerSHIb',float,float,0.],
        [6,'EnerVVIb',float,float,0.],
        [7,'EnerTFSWPIb',float,float,0.],
        [8,'EnerFWOb',float,float,0.],
        [9,'EnerBZ10Ob',float,float,0.],
        [10,'EnerBZOb',float,float,0.],
        [11,'EnerBPOb',float,float,0.],
        [12,'EnerMANOb',float,float,0.],
        [13,'EnerSHOb',float,float,0.],
        [14,'EnerVVOb',float,float,0.],
        [15,'EnerTFSWPOb',float,float,0.]])

#The matrix columns for the flux are: [Index,Name,Value,Corrected Value,Dimension]
output_flux= array([[0,'FluxFWIb',float,float,0.],
        [1,'FluxBZIb',float,float,0.],
        [2,'FluxBPIb',float,float,0.],
        [3,'FluxMANIb',float,float,0.],
        [4,'FluxSHIb',float,float,0.],
        [5,'FluxVVIb',float,float,0.],
        [6,'FluxTFSWPIb',float,float,0.]])



########################### 8. Import of the Neural networks to python using ctypes (import
of a dynamic library.so) and calculation ################

#Calculation of the TBR and ME
```

```
i=0
while (i<len(output_RZ)):
        res=c_double()
        load_nn(output_RZ[i][1],paramRZ,res) #function that load the neural network and
performs de calculation
        output_RZ[i][2] = res.value
        output_RZ[i][3] = res.value*(1.-sel_error_ph(output_RZ[i][1]))-
3*sel_sigma_nn(output_RZ[i][1])
        output_RZ[i][4]='no unit'
        output.write('\tCHECK CALCULATION (%s): OK \n' % output_RZ[i][1])
        output.write('\t\tNeural Network calculation: %g %s \n' %
(output_RZ[i][2],output_RZ[i][4]))
        output.write('\t\tSigma of the nn: %f \n' % (sel_sigma_nn(output_RZ[i][1])))
        output.write('\t\tStandard Error committed by the nn: %f  \n' %
((sel_error_nn(output_RZ[i][1]))*100))
        output.write('\t\tMaximum Error commited by the nn: %f \n' %
((sel_maxperf_nn(output_RZ[i][1]))*100))
        output.write('\t\tError commited by the physical model: %f \n' %
((sel_error_ph(output_RZ[i][1]))*100))
        output.write('\t\tFinal value after correction: %s %s \n\n' %
(output_RZ[i][3],output_RZ[i][4]))
        i=i+1


#Calculation of the Deposited Energy
i=0
while (i<len(output_ener)):
        if (output_ener[i][1]=='EnerVVIb' or output_ener[i][1]=='EnerTFSWPIb' or
output_ener[i][1]=='EnerVVOb' or output_ener[i][1]=='EnerTFSWPOb'):
                res=c_double()
                load_nn(output_ener[i][1],param1D,res) #function that load the neural
network and performs de calculation
                output_ener[i][2] = res.value
                output_ener[i][3] =
(res.value*(1.+sel_error_ph(output_ener[i][1]))+3*sel_sigma_nn(output_ener[i][1]))*norm_1D
_flux
                output_ener[i][4]='MW.m^-3'
                output.write('\tCHECK CALCULATION (%s): OK \n' % output_ener[i][1])
                output.write('\t\tNeural Network calculation: %e %s \n' %
((output_ener[i][2]),output_ener[i][4]))
                output.write('\t\tNeural Network calculation after normalization: %g %s \n'
% (((output_ener[i][2])*norm_1D_flux),output_ener[i][4]))
        else:
                res=c_double()
                load_nn(output_ener[i][1],param1D,res) #function that load the neural
network and performs de calculation
                output_ener[i][2] = res.value
                output_ener[i][3] =
(res.value*(1.+2*sel_error_ph(output_ener[i][1]))+3*sel_sigma_nn(output_ener[i][1]))*norm_
tripoli
                output_ener[i][4]='MW.m^-3'
                output.write('\tCHECK CALCULATION (%s): OK \n' % output_ener[i][1])
                output.write('\t\tNeural Network calculation: %e MeV/s \n' %
((output_ener[i][2])))
                output.write('\t\tNeural Network calculation after normalization: %g %s \n'
% (((output_ener[i][2])*norm_tripoli),output_ener[i][4]))
        output.write('\t\tSigma of the nn: %g \n' % (sel_sigma_nn(output_ener[i][1])))
        output.write('\t\tStandard Error committed by the nn: %f \n' %
((sel_error_nn(output_ener[i][1]))*100))
        output.write('\t\tMaximum Error commited by the nn: %f \n' %
((sel_maxperf_nn(output_ener[i][1]))*100))
        output.write('\t\tError commited by the physical model: %f \n' %
((sel_error_ph(output_ener[i][1]))*100))
        output.write('\t\tFinal value after correction and normalization: %g %s \n\n' %
(output_ener[i][3],output_ener[i][4]))
        i=i+1


#Function to choose the nn that will calculate the Flux according to the operating window
of both the BZ and SH
if (sel_value(param_values,'Thickness_SH_Inboard')<=30):
        if (sel_value(param_values,'Thickness_BZ_Inboard')<=45):
                oper_zone = 'sh1bz1'
        else :
                oper_zone = 'sh1bz2'
else:
```

```
        if (sel_value(param_values,'Thickness_BZ_Inboard')<=45):
                oper_zone = 'sh2bz1'
        else :
                oper_zone = 'sh2bz2'

#Calculation of the Flux
i=0
while (i<len(output_flux)):
        res=c_double()
        load_nn((output_flux[i][1]+'%s'%oper_zone),param1D,res) #function that load the
neural network and performs de calculation
        output_flux[i][2] = res.value
        output_flux[i][3] =
(res.value*(1.+sel_error_ph(output_flux[i][1]+'%s'%oper_zone))+3*sel_sigma_nn(output_flux[
i][1]+'%s'%oper_zone))*norm_1D_flux
        output_flux[i][4]='n.cm^-2.s^-1'
        output.write('\tCHECK CALCULATION (%s): OK \n' % output_flux[i][1])
        output.write('\t\tNeural Network calculation: %e %s \n' %
((output_flux[i][2]),output_flux[i][4]))
        output.write('\t\tNeural Network calculation after normalization: %e %s \n' %
(((output_flux[i][2])*norm_1D_flux),output_flux[i][4]))
        output.write('\t\tSigma of the nn: %e \n' %
(sel_sigma_nn(output_flux[i][1]+'%s'%oper_zone)))
        output.write('\t\tStandard Error committed by the nn: %f \n' %
((sel_error_nn(output_flux[i][1]+'%s'%oper_zone))*100))
        output.write('\t\tMaximum Error commited by the nn: %f \n' %
((sel_maxperf_nn(output_flux[i][1]+'%s'%oper_zone))*100))
        output.write('\t\tError commited by the physical model: %f \n' %
((sel_error_ph(output_flux[i][1]+'%s'%oper_zone))*100))
        output.write('\t\tFinal value after correction and normalization: %e %s \n\n' %
(output_flux[i][3],output_flux[i][4]))
        i=i+1

output.write('END NEURAL NETWORK LOADING AND CALCULATIONS \n\n')


########################## 9. Writing the output variables in the output file #####
print 'WRITING THE OUTPUT VALUES'
output.write('BEGINNING WRITING THE RESULTS ON DE variables.out FILE \n')
var.write('BEGINNING INPUT PARAMETERS \n')
i=0
while (i<len(param_values)):
        var.write('\t%s = %7.2f%s \n'
%(param_values[i][1],sel_value(param_values,param_values[i][1]),sel_dim(param_values,param
_values[i][1])))
        i=i+1
var.write('END INPUT PARAMETERS \n\n')

var.write('BEGINNING NORMALIZATION FACTORS \n')
var.write('\tNormalization factor: %7.4e n.s^-1 \n' %norm_1D_flux)
var.write('END NORMALIZATION FACTORS \n\n')

var.write('BEGINNING OUTPUT VARIABLES \n')
var.write('note: corrected for the maximum error of the physcal model and 3*sigma of the
Neural Networks \n')
var.write('this correction assures that 95% of the samples present accurate results.
\n\n')

i=0
while (i<len(output_RZ)):
        var.write('\t%s = %7.4f %s \n' % (output_RZ[i][1],
output_RZ[i][3],output_RZ[i][4]))
        i=i+1
var.write('\n')
i=0
while (i<len(output_ener)):
        var.write('\t%s = %7.4g %s \n' % (output_ener[i][1],
output_ener[i][3],output_ener[i][4]))
        i=i+1
var.write('\n')
i=0
while (i<len(output_flux)):
        var.write('\t%s = %7.4e %s \n' % (output_flux[i][1],
output_flux[i][3],output_flux[i][4]))
        i=i+1
var.write('\n')
```

```
var.write('END OUTPUT VARIABLES \n\n')
print 'END OF THE PROGRAM: CONGRATULATIONS!'
print 'RESULTS: available on "variables.out", if you want further information read the
auto-generated file "check.out"'
output.write('END OF THE PROGRAM')
```

- neuralnetworks.py

```
from math import *
import glob
import sys
import math
import os
from ctypes import *
from numpy  import *
from functions import *

################ Creation of a matrix containing the name of the .so files #######

#Creation of a matrix including: name of the output variable,
#neural network file and correction to the value obtained in %
# [Index, Name, NN File, sigmaNN, Percent error, Maxium Percent Error, Percent Error
Physical model,

nn_files= array([[0,'TBRTot','NN/tbr_me/TBR_Total.so',8.7342e-04,5.2745e-04,4.2245e-
03,0.0142],
        [1,'TBRIb','NN/tbr_me/TBR_Inboard.so',3.1914e-04,7.5818e-04,7.7373e-03,0.0465],
        [2,'TBROb','NN/tbr_me/TBR_Outboard.so',8.6985e-04,6.9636e-04,5.0772e-03,0.0081],
        [3,'ME','NN/tbr_me/facteur_de_multiplication.so',1.3868e-04,7.6902e-05,6.4845e-
04,0.0263],
        [4,'EnerFWIb','NN/ener/ener_fw_ib.so',3.0889e-22,4.0279e-03,2.5187e-02,0.0091448],
        [5,'EnerBZ10Ib','NN/ener/ener_bz10_ib.so',1.6013e-22,2.4908e-03,1.3479e-
02,0.00404934],
        [6,'EnerBZIb','NN/ener/ener_bz_ib.so',7.2404e-23,2.3794e-03,1.3152e-
02,0.00309039],
        [7,'EnerBPIb','NN/ener/ener_bp_ib.so',2.4882e-23,1.3870e-02,8.1975e-02,0.0197396],
        [8,'EnerMANIb','NN/ener/ener_man_ib.so',2.5852e-23,1.4068e-02,9.9401e-
02,0.0154213],
        [9,'EnerSHIb','NN/ener/ener_sh_ib.so',5.4033e-23,9.9887e-03,6.2306e-
02,0.00948404],
        [10,'EnerVVIb','NN/ener/ener_vv_ib.so',3.9530e-24,1.9609e-02,1.6437e-01,2],
        [11,'EnerTFSWPIb','NN/ener/ener_tfswp_ib.so',5.7246e-25,2.3633e-02,1.9957e-01,2],
        [12,'EnerTFCIb','NN/ener/ener_tfc_ib.so',1.1030e-25,2.6476e-02,2.3508e-01,2],
        [13,'EnerFWOb','NN/ener/ener_fw_ob.so',2.4552e-22,2.3502e-03,1.6529e-
02,0.00578448],
        [14,'EnerBZ10Ob','NN/ener/ener_bz10_ob.so',1.5930e-22,2.0677e-03,1.2137e-
02,0.0025382],
        [15,'EnerBZOb','NN/ener/ener_bz_ob.so',5.0698e-23,2.0694e-03,1.2539e-
02,0.0017707],
        [16,'EnerBPOb','NN/ener/ener_bp_ob.so',1.3628e-23,2.3607e-02,1.7966e-
01,0.0218179],
        [17,'EnerMANOb','NN/ener/ener_man_ob.so',1.0780e-23,1.7099e-02,9.6231e-
02,0.0142667],
        [18,'EnerSHOb','NN/ener/ener_sh_ob.so',1.4775e-23,1.6652e-02,1.0939e-
01,0.0108162],
        [19,'EnerVVOb','NN/ener/ener_vv_ob.so',2.3430e-26,8.1016e-01,1.1448e+01,2],
        [20,'EnerTFSWPOb','NN/ener/ener_tfswp_ob.so',9.2181e-29,5.9634e-02,3.9095e-01,2],
        [21,'EnerTFCOb','NN/ener/ener_tfc_ob.so',1.0654e-29,5.9387e-02,3.9853e-01,2],
        [22,'FluxFWIbsh1bz1','NN/sh1bz1/FluxSup0_1Mev_fw.so',7.8429e-07,4.7730e-
04,3.8264e-03,0.],
        [23,'FluxBZIbsh1bz1','NN/sh1bz1/FluxSup0_1Mev_bz.so',8.4528e-07,5.1783e-
04,3.7553e-03,0.],
        [24,'FluxBPIbsh1bz1','NN/sh1bz1/FluxSup0_1Mev_bp.so',5.0790e-07,1.3198e-
03,1.4950e-02,0.],
        [25,'FluxMANIbsh1bz1','NN/sh1bz1/FluxSup0_1Mev_man.so',5.6667e-07,2.3728e-
03,3.0617e-02,0.],
        [26,'FluxSHIbsh1bz1','NN/sh1bz1/FluxSup0_1Mev_sh.so',2.6123e-07,3.3514e-
03,3.8260e-02,0.],
        [27,'FluxVVIbsh1bz1','NN/sh1bz1/FluxSup0_1Mev_vv.so',3.7401e-10,1.3193e-
02,1.0837e-01,0.],
        [28,'FluxTFSWPIbsh1bz1','NN/sh1bz1/FluxSup0_1Mev_tfswp.so',1.9887e-11,1.5313e-
02,1.7736e-01,0.],
        [29,'FluxTFCIbsh1bz1','NN/sh1bz1/FluxSup0_1Mev_tfc.so',1.2487e-11,1.8027e-
02,1.4710e-01,0.],
        [30,'FluxFWIbsh1bz2','NN/sh1bz2/FluxSup0_1Mev_fw.so',8.3867e-07,4.5600e-
04,4.1338e-03,0.],
        [31,'FluxBZIbsh1bz2','NN/sh1bz2/FluxSup0_1Mev_bz.so',7.7751e-07,4.4072e-
04,3.6446e-03,0.],
        [32,'FluxBPIbsh1bz2','NN/sh1bz2/FluxSup0_1Mev_bp.so',3.6551e-07,1.7888e-
03,2.2404e-02,0.],
```

```
        [33,'FluxMANIbsh1bz2','NN/sh1bz2/FluxSup0_1Mev_man.so',3.0936e-07,2.4392e-
03,2.7356e-02,0.],
        [34,'FluxSHIbsh1bz2','NN/sh1bz2/FluxSup0_1Mev_sh.so',1.2026e-07,3.0511e-
03,3.0846e-02,0.],
        [35,'FluxVVIbsh1bz2','NN/sh1bz2/FluxSup0_1Mev_vv.so',1.2636e-10,1.2450e-
02,9.6383e-02,0.],
        [36,'FluxTFSWPIbsh1bz2','NN/sh1bz2/FluxSup0_1Mev_tfswp.so',5.3509e-12,1.3891e-
02,1.1627e-01,0.],
        [37,'FluxTFCIbsh1bz2','NN/sh1bz2/FluxSup0_1Mev_tfc.so',2.9865e-12,1.6448e-
02,1.4580e-01,0.],
        [38,'FluxFWIbsh2bz1','NN/sh2bz1/FluxSup0_1Mev_fw.so',7.8899e-07,4.5079e-
04,3.7074e-03,0.],
        [39,'FluxBZIbsh2bz1','NN/sh2bz1/FluxSup0_1Mev_bz.so',8.0241e-07,4.8365e-
04,3.8725e-03,0.],
        [40,'FluxBPIbsh2bz1','NN/sh2bz1/FluxSup0_1Mev_bp.so',5.7242e-07,1.4696e-
03,2.7053e-02,0.],
        [41,'FluxMANIbsh2bz1','NN/sh2bz1/FluxSup0_1Mev_man.so',6.2390e-07,2.5033e-
03,1.9958e-02,0.],
        [42,'FluxSHIbsh2bz1','NN/sh2bz1/FluxSup0_1Mev_sh_Rn_nH11_3_C.so',1.8067e-
07,2.4850e-03,3.3675e-02,0.],
        [43,'FluxVVIbsh2bz1','NN/sh2bz1/FluxSup0_1Mev_vv_Rn_nH9_4_C.so',1.2549e-
10,1.2362e-02,1.0986e-01,0.],
        [44,'FluxTFSWPIbsh2bz1','NN/sh2bz1/FluxSup0_1Mev_tfswp.so',7.5725e-12,1.2330e-
02,1.1414e-01,0.],
        [45,'FluxTFCIbsh2bz1','NN/sh2bz1/FluxSup0_1Mev_tfc.so',4.2064e-12,1.4076e-
02,1.2631e-01,0.],
        [46,'FluxFWIbsh2bz2','NN/sh2bz2/FluxSup0_1Mev_fw.so',8.9962e-07,5.0115e-
04,4.2910e-03,0.],
        [47,'FluxBZIbsh2bz2','NN/sh2bz2/FluxSup0_1Mev_bz.so',7.4695e-07,4.7634e-
04,3.8489e-03,0.],
        [48,'FluxBPIbsh2bz2','NN/sh2bz2/FluxSup0_1Mev_bp.so',4.3223e-07,2.0050e-
03,1.7518e-02,0.],
        [49,'FluxMANIbsh2bz2','NN/sh2bz2/FluxSup0_1Mev_man.so',3.8647e-07,2.9416e-
03,2.5397e-02,0.],
        [50,'FluxSHIbsh2bz2','NN/sh2bz2/FluxSup0_1Mev_sh.so',1.2321e-07,3.2041e-
03,3.3755e-02,0.],
        [51,'FluxVVIbsh2bz2','NN/sh2bz2/FluxSup0_1Mev_vv.so',3.3040e-11,1.0753e-
02,1.0152e-01,0.],
        [52,'FluxTFSWPIbsh2bz2','NN/sh2bz2/FluxSup0_1Mev_tfswp.so',2.1162e-12,1.3378e-
02,1.3489e-01,0.],
        [53,'FluxTFCIbsh2bz2','NN/sh2bz2/FluxSup0_1Mev_tfc.so',1.0592e-12,1.3042e-
02,1.0014e-01,0.]
        ])

#Creation of the arrays for the look up's
nn_names=array(['TBRTot','TBRIb','TBROb','ME','EnerFWIb','EnerBZ10Ib','EnerBZIb','EnerBPIb
','EnerMANIb','EnerSHIb','EnerVVIb','EnerTFSWPIb','EnerTFCIb','EnerFWOb','EnerBZ10Ob','Ene
rBZOb','EnerBPOb','EnerMANOb','EnerSHOb','EnerVVOb','EnerTFSWPOb','EnerTFCOb','FluxFWIbsh1
bz1','FluxBZIbsh1bz1','FluxBPIbsh1bz1','FluxMANIbsh1bz1','FluxSHIbsh1bz1','FluxVVIbsh1bz1'
,'FluxTFSWPIbsh1bz1','FluxTFCIbsh1bz1','FluxFWIbsh1bz2','FluxBZIbsh1bz2','FluxBPIbsh1bz2',
'FluxMANIbsh1bz2','FluxSHIbsh1bz2','FluxVVIbsh1bz2','FluxTFSWPIbsh1bz2','FluxTFCIbsh1bz2',
'FluxFWIbsh2bz1','FluxBZIbsh2bz1','FluxBPIbsh2bz1','FluxMANIbsh2bz1','FluxSHIbsh2bz1','Flu
xVVIbsh2bz1','FluxTFSWPIbsh2bz1','FluxTFCIbsh2bz1','FluxFWIbsh2bz2','FluxBZIbsh2bz2','Flux
BPIbsh2bz2','FluxMANIbsh2bz2','FluxSHIbsh2bz2','FluxVVIbsh2bz2','FluxTFSWPIbsh2bz2','FluxT
FCIbsh2bz2'])
nn_index = arange(53)

#Obtain index of a given parameter
LuT = dict(zip(nn_names, nn_index))

def load_nn(key,param,res):
        function = cdll.LoadLibrary(nn_files[LuT[key],2])
        return function.fct_nn(param.ctypes.data_as(c_void_p), byref(res))

def sel_sigma_nn(key):
    return nn_files[LuT[key],3].astype(float)
def sel_error_nn(key):
    return nn_files[LuT[key],4].astype(float)
def sel_maxperf_nn(key):
    return float(nn_files[LuT[key],5])
def sel_error_ph(key):
    return float(nn_files[LuT[key],6])
```

- functions.py

```
from math import*
from numpy  import *

#-----------------------------------------------------------------------------
#Support functions for Lanceur.py
#-----------------------------------------------------------------------------

############################LOOKUP#################################

#Matrix containing the names of each value used to look up for values on param_values
param_names = array(['Lithium_6_enrichment',
         'Half_Radius_of_the_Plasma',
         'Thickness_of_the_Plasma',
         'Thickness_CS_Inboard',
         'Thickness_TFC_Inboard',
         'Thickness_TFSWP_Inboard',
         'Thickness_VV_Inboard',
         'Thickness_SH_Inboard',
         'Thickness_MAN_Inboard',
         'Thickness_BP_Inboard',
         'Thickness_BZ_Inboard',
         'Thickness_FW',
         'Thickness_FWPL_Inboard',
         'Thickness_TFC_Outboard',
         'Thickness_TFSWP_Outboard',
         'Thickness_VV_Outboard',
         'Thickness_SH_Outboard',
         'Thickness_MAN_Outboard',
         'Thickness_BP_Outboard',
         'Thickness_BZ_Outboard',
         'Thickness_FWPL_Outboard',
         'Tolerance_TFC_CS_Inboard',
         'Tolerance_VV_TFC_Inboard',
         'Tolerance_SH_VV_Inboard',
         'Tolerance_BB_SH_Inboard',
         'Tolerance_VV_TFC_Outboard',
         'Tolerance_SH_VV_Outboard',
         'Tolerance_BB_SH_Outboard',
         'Distance_Plasma_FW_Inboard',
         'Distance_Plasma_FW_Outboard',
         'Composition_FW_He',
         'Composition_BZ_EuroFer',
         'Composition_BZ_He',
         'Composition_BP_LiPB',
         'Composition_BP_EuroFer',
         'Composition_MAN_LiPB',
         'Composition_MAN_EuroFer',
         'Composition_SH_EuroFer',
         'Composition_SH_H2O',
         'Composition_VV_He',
         'Composition_VV_Boron',
         'Composition_TFSWP_He',
         'Composition_TFC_Epoxy',
        'Composition_TFC_HeLiq',
         'Triangulation',
         'Elongation',
         'Surface_Div_Inboard',
         'Surface_Div_Outboard'])

#Matrix containing the index of each parameter used to look up for values on pram_values
param_index = array ([0,
       1,
       2,
       3,
       4,
       5,
       6,
       7,
       8,
       9,
       10,
       11,
```

```
        12,
        13,
        14,
        15,
        16,
        17,
        18,
        19,
        20,
        21,
        22,
        23,
        24,
        25,
        26,
        27,
        28,
        29,
        30,
        31,
        32,
        33,
        34,
        35,
        36,
        37,
        38,
        39,
        40,
        41,
        42,
        43,
        44,
        45,
        46,
        47,
        ])


#Obtain index of a given parameter
LuT = dict(zip(param_names, param_index))

# function to look up for value of a given parameter
def sel_value(matrix,key):
    return float(matrix[LuT[key],2])

# function to look up for min of a given parameter
def sel_min(matrix,key):
    return float(matrix[LuT[key],3])

# function to look up for max of a given parameter
def sel_max(matrix,key):
    return float(matrix[LuT[key],4])

# function to look up for dimension of a given parameter
def sel_dim(matrix,key):
    return matrix[LuT[key],5]
```

- check.out

```
NEUTRONIC MODULE

File created automatically by the neutronic module.
File containing the geometry check and output variables stored in rows

BEGINNING OF GEOMETRY CHECK
        CHECK GEOM (Lithium_6_enrichment): OK
        CHECK GEOM (Half_Radius_of_the_Plasma): OK
        CHECK GEOM (Thickness_of_the_Plasma): OK
        CHECK GEOM (Thickness_CS_Inboard): OK
        CHECK GEOM (Thickness_TFC_Inboard): OK
        CHECK GEOM (Thickness_TFSWP_Inboard): OK
        CHECK GEOM (Thickness_VV_Inboard): OK
        CHECK GEOM (Thickness_SH_Inboard): OK
        CHECK GEOM (Thickness_MAN_Inboard): OK
        CHECK GEOM (Thickness_BP_Inboard): OK
        CHECK GEOM (Thickness_BZ_Inboard): OK
        CHECK GEOM (Thickness_FW): OK
        CHECK GEOM (Thickness_FWPL_Inboard): OK
        CHECK GEOM (Thickness_TFC_Outboard): OK
        CHECK GEOM (Thickness_TFSWP_Outboard): OK
        CHECK GEOM (Thickness_VV_Outboard): OK
        CHECK GEOM (Thickness_SH_Outboard): OK
        CHECK GEOM (Thickness_MAN_Outboard): OK
        CHECK GEOM (Thickness_BP_Outboard): OK
        CHECK GEOM (Thickness_BZ_Outboard): OK
        CHECK GEOM (Thickness_FWPL_Outboard): OK
        CHECK GEOM (Tolerance_TFC_CS_Inboard): OK
        CHECK GEOM (Tolerance_VV_TFC_Inboard): OK
        CHECK GEOM (Tolerance_SH_VV_Inboard): OK
        CHECK GEOM (Tolerance_BB_SH_Inboard): OK
        CHECK GEOM (Tolerance_VV_TFC_Outboard): OK
        CHECK GEOM (Tolerance_SH_VV_Outboard): OK
        CHECK GEOM (Tolerance_BB_SH_Outboard): OK
        CHECK GEOM (Distance_Plasma_FW_Inboard): OK
        CHECK GEOM (Distance_Plasma_FW_Outboard): OK
        CHECK GEOM (Composition_FW_He): OK
        CHECK GEOM (Composition_BZ_EuroFer): OK
        CHECK GEOM (Composition_BZ_He): OK
        CHECK GEOM (Composition_BP_LiPB): OK
        CHECK GEOM (Composition_BP_EuroFer): OK
        CHECK GEOM (Composition_MAN_LiPB): OK
        CHECK GEOM (Composition_MAN_EuroFer): OK
        CHECK GEOM (Composition_SH_EuroFer): OK
        CHECK GEOM (Composition_SH_H2O): OK
        CHECK GEOM (Composition_VV_He): OK
        CHECK GEOM (Composition_VV_Boron): OK
        CHECK GEOM (Composition_TFSWP_He): OK
        CHECK GEOM (Composition_TFC_Epoxy): OK
        CHECK GEOM (Composition_TFC_HeLiq): OK
        CHECK GEOM (Triangulation): OK
        CHECK GEOM (Elongation): OK
        CHECK GEOM (Surface_Div_Inboard): OK
        CHECK GEOM (Surface_Div_Outboard): OK
        CHECK GEOM Inboard Total Thickness: OK
END OF GEOMETRY CHECK

BEGINNING THE CREATION OF THE ARRAYS SEND TO THE NEURAL NETWORKS
        CHECK ARRAY INPUTS 1D MODEL: OK
        CHECK ARRAY INPUTS RZ MODEL: OK
END OF ARRAY CHECK

BEGINNING NEURAL NETWORK LOADING AND CALCULATIONS
        CHECK CALCULATION (TBRTot): OK
                Neural Network calculation: 1.13509 no unit
                Sigma of the nn: 0.000873
                Standard Error committed by the nn: 0.052745
                Maximum Error commited by the nn: 0.422450
                Error commited by the physical model: 1.420000
                Final value after correction: 1.11635116861 no unit

        CHECK CALCULATION (TBRIb): OK
```

```
        Neural Network calculation: 0.291268 no unit
        Sigma of the nn: 0.000319
        Standard Error committed by the nn: 0.075818
        Maximum Error commited by the nn: 0.773730
        Error commited by the physical model: 4.650000
        Final value after correction: 0.276766277737 no unit

CHECK CALCULATION (TBROb): OK
        Neural Network calculation: 0.844204 no unit
        Sigma of the nn: 0.000870
        Standard Error committed by the nn: 0.069636
        Maximum Error commited by the nn: 0.507720
        Error commited by the physical model: 0.810000
        Final value after correction: 0.834756347425 no unit

CHECK CALCULATION (ME): OK
        Neural Network calculation: 1.18494 no unit
        Sigma of the nn: 0.000139
        Standard Error committed by the nn: 0.007690
        Maximum Error commited by the nn: 0.064845
        Error commited by the physical model: 2.630000
        Final value after correction: 1.15336365235 no unit

CHECK CALCULATION (EnerFWIb): OK
        Corrected with 2sigma from Tripoli4 and 3sigma from NN
        Neural Network calculation: 4.974528e-20 MeV/s
        Neural Network calculation after normalization: 11.0415 MW.m^-3
        Sigma of the nn: 3.0889e-22
        Standard Error committed by the nn: 0.402790
        Maximum Error commited by the nn: 2.518700
        Error commited by the physical model: 0.914480
        Final value after correction and normalization: 11.4491 MW.m^-3

CHECK CALCULATION (EnerBZ10Ib): OK
        Corrected with 2sigma from Tripoli4 and 3sigma from NN
        Neural Network calculation: 4.095834e-20 MeV/s
        Neural Network calculation after normalization: 9.09116 MW.m^-3
        Sigma of the nn: 1.6013e-22
        Standard Error committed by the nn: 0.249080
        Maximum Error commited by the nn: 1.347900
        Error commited by the physical model: 0.404934
        Final value after correction and normalization: 9.27141 MW.m^-3

CHECK CALCULATION (EnerBZIb): OK
        Corrected with 2sigma from Tripoli4 and 3sigma from NN
        Neural Network calculation: 1.915665e-20 MeV/s
        Neural Network calculation after normalization: 4.25203 MW.m^-3
        Sigma of the nn: 7.2404e-23
        Standard Error committed by the nn: 0.237940
        Maximum Error commited by the nn: 1.315200
        Error commited by the physical model: 0.309039
        Final value after correction and normalization: 4.32652 MW.m^-3

CHECK CALCULATION (EnerBPIb): OK
        Corrected with 2sigma from Tripoli4 and 3sigma from NN
        Neural Network calculation: 9.937550e-22 MeV/s
        Neural Network calculation after normalization: 0.220575 MW.m^-3
        Sigma of the nn: 2.4882e-23
        Standard Error committed by the nn: 1.387000
        Maximum Error commited by the nn: 8.197500
        Error commited by the physical model: 1.973960
        Final value after correction and normalization: 0.245851 MW.m^-3

CHECK CALCULATION (EnerMANIb): OK
        Corrected with 2sigma from Tripoli4 and 3sigma from NN
        Neural Network calculation: 1.157896e-21 MeV/s
        Neural Network calculation after normalization: 0.257008 MW.m^-3
        Sigma of the nn: 2.5852e-23
        Standard Error committed by the nn: 1.406800
        Maximum Error commited by the nn: 9.940100
        Error commited by the physical model: 1.542130
        Final value after correction and normalization: 0.282149 MW.m^-3

CHECK CALCULATION (EnerSHIb): OK
        Corrected with 2sigma from Tripoli4 and 3sigma from NN
        Neural Network calculation: 3.293703e-21 MeV/s
```

```
        Neural Network calculation after normalization: 0.731074 MW.m^-3
        Sigma of the nn: 5.4033e-23
        Standard Error committed by the nn: 0.998870
        Maximum Error commited by the nn: 6.230600
        Error commited by the physical model: 0.948404
        Final value after correction and normalization: 0.78092 MW.m^-3

CHECK CALCULATION (EnerVVIb): OK
        Neural Network calculation: 9.495278e-23 MW.m^-3
        Neural Network calculation after normalization: 0.000105379 MW.m^-3
        Sigma of the nn: 3.953e-24
        Standard Error committed by the nn: 1.960900
        Maximum Error commited by the nn: 16.437000
        Error commited by the physical model: 200.000000
        Final value after correction and normalization: 0.000329298 MW.m^-3

CHECK CALCULATION (EnerTFSWPIb): OK
        Neural Network calculation: 9.932315e-24 MW.m^-3
        Neural Network calculation after normalization: 1.10229e-05 MW.m^-3
        Sigma of the nn: 5.7246e-25
        Standard Error committed by the nn: 2.363300
        Maximum Error commited by the nn: 19.957000
        Error commited by the physical model: 200.000000
        Final value after correction and normalization: 3.49748e-05 MW.m^-3

CHECK CALCULATION (EnerFWOb): OK
        Corrected with 2sigma from Tripoli4 and 3sigma from NN
        Neural Network calculation: 6.548105e-20 MeV/s
        Neural Network calculation after normalization: 14.5342 MW.m^-3
        Sigma of the nn: 2.4552e-22
        Standard Error committed by the nn: 0.235020
        Maximum Error commited by the nn: 1.652900
        Error commited by the physical model: 0.578448
        Final value after correction and normalization: 14.8659 MW.m^-3

CHECK CALCULATION (EnerBZ10Ob): OK
        Corrected with 2sigma from Tripoli4 and 3sigma from NN
        Neural Network calculation: 5.123015e-20 MeV/s
        Neural Network calculation after normalization: 11.3711 MW.m^-3
        Sigma of the nn: 1.593e-22
        Standard Error committed by the nn: 0.206770
        Maximum Error commited by the nn: 1.213700
        Error commited by the physical model: 0.253820
        Final value after correction and normalization: 11.5349 MW.m^-3

CHECK CALCULATION (EnerBZOb): OK
        Corrected with 2sigma from Tripoli4 and 3sigma from NN
        Neural Network calculation: 1.410535e-20 MeV/s
        Neural Network calculation after normalization: 3.13084 MW.m^-3
        Sigma of the nn: 5.0698e-23
        Standard Error committed by the nn: 0.206940
        Maximum Error commited by the nn: 1.253900
        Error commited by the physical model: 0.177070
        Final value after correction and normalization: 3.17568 MW.m^-3

CHECK CALCULATION (EnerBPOb): OK
        Corrected with 2sigma from Tripoli4 and 3sigma from NN
        Neural Network calculation: 2.393140e-22 MeV/s
        Neural Network calculation after normalization: 0.0531184 MW.m^-3
        Sigma of the nn: 1.3628e-23
        Standard Error committed by the nn: 2.360700
        Maximum Error commited by the nn: 17.966000
        Error commited by the physical model: 2.181790
        Final value after correction and normalization: 0.0645109 MW.m^-3

CHECK CALCULATION (EnerMANOb): OK
        Corrected with 2sigma from Tripoli4 and 3sigma from NN
        Neural Network calculation: 2.273533e-22 MeV/s
        Neural Network calculation after normalization: 0.0504636 MW.m^-3
        Sigma of the nn: 1.078e-23
        Standard Error committed by the nn: 1.709900
        Maximum Error commited by the nn: 9.623100
        Error commited by the physical model: 1.426670
        Final value after correction and normalization: 0.0590817 MW.m^-3

CHECK CALCULATION (EnerSHOb): OK
```

```
        Corrected with 2sigma from Tripoli4 and 3sigma from NN
        Neural Network calculation: 3.392507e-22 MeV/s
        Neural Network calculation after normalization: 0.0753004 MW.m^-3
        Sigma of the nn: 1.4775e-23
        Standard Error committed by the nn: 1.665200
        Maximum Error commited by the nn: 10.939000
        Error commited by the physical model: 1.081620
        Final value after correction and normalization: 0.0867678 MW.m^-3

CHECK CALCULATION (EnerVVOb): OK
        Neural Network calculation: 1.760812e-26 MW.m^-3
        Neural Network calculation after normalization: 1.95416e-08 MW.m^-3
        Sigma of the nn: 2.343e-26
        Standard Error committed by the nn: 81.016000
        Maximum Error commited by the nn: 1144.800000
        Error commited by the physical model: 200.000000
        Final value after correction and normalization: 1.36633e-07 MW.m^-3

CHECK CALCULATION (EnerTFSWPOb): OK
        Neural Network calculation: 1.768877e-28 MW.m^-3
        Neural Network calculation after normalization: 1.96311e-10 MW.m^-3
        Sigma of the nn: 9.2181e-29
        Standard Error committed by the nn: 5.963400
        Maximum Error commited by the nn: 39.095000
        Error commited by the physical model: 200.000000
        Final value after correction and normalization: 8.95841e-10 MW.m^-3

CHECK CALCULATION (FluxFWIb): OK
        Neural Network calculation: 1.258146e-03 n.cm^-2.s^-1
        Neural Network calculation after normalization: 1.396297e+15 n.cm^-2.s^-1
        Sigma of the nn: 7.842900e-07
        Standard Error committed by the nn: 0.047730
        Maximum Error commited by the nn: 0.382640
        Error commited by the physical model: 0.000000
        Final value after correction and normalization: 1.398908e+15 n.cm^-2.s^-1

CHECK CALCULATION (FluxBZIb): OK
        Neural Network calculation: 1.156347e-03 n.cm^-2.s^-1
        Neural Network calculation after normalization: 1.283319e+15 n.cm^-2.s^-1
        Sigma of the nn: 8.452800e-07
        Standard Error committed by the nn: 0.051783
        Maximum Error commited by the nn: 0.375530
        Error commited by the physical model: 0.000000
        Final value after correction and normalization: 1.286134e+15 n.cm^-2.s^-1

CHECK CALCULATION (FluxBPIb): OK
        Neural Network calculation: 1.885853e-04 n.cm^-2.s^-1
        Neural Network calculation after normalization: 2.092929e+14 n.cm^-2.s^-1
        Sigma of the nn: 5.079000e-07
        Standard Error committed by the nn: 0.131980
        Maximum Error commited by the nn: 1.495000
        Error commited by the physical model: 0.000000
        Final value after correction and normalization: 2.109839e+14 n.cm^-2.s^-1

CHECK CALCULATION (FluxMANIb): OK
        Neural Network calculation: 1.254116e-04 n.cm^-2.s^-1
        Neural Network calculation after normalization: 1.391824e+14 n.cm^-2.s^-1
        Sigma of the nn: 5.666700e-07
        Standard Error committed by the nn: 0.237280
        Maximum Error commited by the nn: 3.061700
        Error commited by the physical model: 0.000000
        Final value after correction and normalization: 1.410691e+14 n.cm^-2.s^-1

CHECK CALCULATION (FluxSHIb): OK
        Neural Network calculation: 3.973296e-05 n.cm^-2.s^-1
        Neural Network calculation after normalization: 4.409584e+13 n.cm^-2.s^-1
        Sigma of the nn: 2.612300e-07
        Standard Error committed by the nn: 0.335140
        Maximum Error commited by the nn: 3.826000
        Error commited by the physical model: 0.000000
        Final value after correction and normalization: 4.496559e+13 n.cm^-2.s^-1

CHECK CALCULATION (FluxVVIb): OK
        Neural Network calculation: 6.144883e-09 n.cm^-2.s^-1
        Neural Network calculation after normalization: 6.819622e+09 n.cm^-2.s^-1
        Sigma of the nn: 3.740100e-10
```

```
               Standard Error committed by the nn: 1.319300
               Maximum Error commited by the nn: 10.837000
               Error commited by the physical model: 0.000000
               Final value after correction and normalization: 8.064857e+09 n.cm^-2.s^-1

        CHECK CALCULATION (FluxTFSWPIb): OK
               Neural Network calculation: 2.930061e-10 n.cm^-2.s^-1
               Neural Network calculation after normalization: 3.251796e+08 n.cm^-2.s^-1
               Sigma of the nn: 1.988700e-11
               Standard Error committed by the nn: 1.531300
               Maximum Error commited by the nn: 17.736000
               Error commited by the physical model: 0.000000
               Final value after correction and normalization: 3.913917e+08 n.cm^-2.s^-1

END NEURAL NETWORK LOADING AND CALCULATIONS

BEGINNING WRITING THE RESULTS ON DE variables.out FILE
END OF THE PROGRAM
```

- check.out

```
NEUTRONIC MODULE


File created automatically by the neutronic module.
File containing output variables stored in rows

BEGINNING INPUT PARAMETERS
        Lithium_6_enrichment =    0.90cm
        Half_Radius_of_the_Plasma =  750.00cm
        Thickness_of_the_Plasma =  246.00cm
        Thickness_CS_Inboard =   74.30cm
        Thickness_TFC_Inboard =   74.00cm
        Thickness_TFSWP_Inboard =    6.00cm
        Thickness_VV_Inboard =   35.00cm
        Thickness_SH_Inboard =   30.00cm
        Thickness_MAN_Inboard =   30.00cm
        Thickness_BP_Inboard =   18.00cm
        Thickness_BZ_Inboard =   44.50cm
        Thickness_FW =    3.00cm
        Thickness_FWPL_Inboard =    0.20cm
        Thickness_TFC_Outboard =   93.00cm
        Thickness_TFSWP_Outboard =    8.00cm
        Thickness_VV_Outboard =   80.00cm
        Thickness_SH_Outboard =   50.00cm
        Thickness_MAN_Outboard =   50.00cm
        Thickness_BP_Outboard =   18.00cm
        Thickness_BZ_Outboard =   77.00cm
        Thickness_FWPL_Outboard =    0.20cm
        Tolerance_TFC_CS_Inboard =   10.00cm
        Tolerance_VV_TFC_Inboard =   10.00cm
        Tolerance_SH_VV_Inboard =   10.00cm
        Tolerance_BB_SH_Inboard =   10.00cm
        Tolerance_VV_TFC_Outboard =   10.00cm
        Tolerance_SH_VV_Outboard =   10.00cm
        Tolerance_BB_SH_Outboard =   10.00cm
        Distance_Plasma_FW_Inboard =   13.00cm
        Distance_Plasma_FW_Outboard =   15.00cm
        Composition_FW_He =   30.00%
        Composition_BZ_EuroFer =   10.00%
        Composition_BZ_He =   10.00%
        Composition_BP_LiPB =    5.00%
        Composition_BP_EuroFer =   28.00%
        Composition_MAN_LiPB =    5.00%
        Composition_MAN_EuroFer =   28.00%
        Composition_SH_EuroFer =   10.00%
        Composition_SH_H2O =   25.00%
        Composition_VV_He =   37.00%
        Composition_VV_Boron =    2.00%
        Composition_TFSWP_He =    5.00%
        Composition_TFC_Epoxy =   18.00%
        Composition_TFC_HeLiq =   17.00%
        Triangulation =    0.47no unit
        Elongation =    1.90no unit
        Surface_Div_Inboard =    5.50%
        Surface_Div_Outboard =    6.50%
END INPUT PARAMETERS

BEGINNING NORMALIZATION FACTORS
        Normalization factor Apollo2 based model: 1.1098e+18 n.s^-1
        Normalization factor tripoli4 based model: 2.2196e+20 n.s^-1
END NORMALIZATION FACTORS

BEGINNING OUTPUT VARIABLES
note: corrected for the maximum error of the physcal model and 3*sigma of the Neural
Networks
this correction assures that 95% of the samples present accurate results.

For DepEner on the FW, BZ, BP, MAN and SH the the error of the physical model is estimated
as 3sigma from Tripoli4.

        TBRTot =  1.1164 no unit
        TBRIb =  0.2768 no unit
```

```
        TBROb =  0.8348 no unit
        ME =  1.1534 no unit

        EnerFWIb =   11.45 MW.m^-3
        EnerBZ10Ib =   9.271 MW.m^-3
        EnerBZIb =   4.327 MW.m^-3
        EnerBPIb =  0.2459 MW.m^-3
        EnerMANIb =  0.2821 MW.m^-3
        EnerSHIb =  0.7809 MW.m^-3
        EnerVVIb = 0.0003293 MW.m^-3
        EnerTFSWPIb = 3.497e-05 MW.m^-3
        EnerFWOb =   14.87 MW.m^-3
        EnerBZ10Ob =   11.53 MW.m^-3
        EnerBZOb =   3.176 MW.m^-3
        EnerBPOb = 0.06451 MW.m^-3
        EnerMANOb = 0.05908 MW.m^-3
        EnerSHOb = 0.08677 MW.m^-3
        EnerVVOb = 1.366e-07 MW.m^-3
        EnerTFSWPOb = 8.958e-10 MW.m^-3

        FluxFWIb = 1.3989e+15 n.cm^-2.s^-1
        FluxBZIb = 1.2861e+15 n.cm^-2.s^-1
        FluxBPIb = 2.1098e+14 n.cm^-2.s^-1
        FluxMANIb = 1.4107e+14 n.cm^-2.s^-1
        FluxSHIb = 4.4966e+13 n.cm^-2.s^-1
        FluxVVIb = 8.0649e+09 n.cm^-2.s^-1
        FluxTFSWPIb = 3.9139e+08 n.cm^-2.s^-1

END OUTPUT VARIABLES
```

- Release Notes

HCLL DEMO NEUTRONIC MODEL V1.0

General information

This document presents release notes for the HCLL DEMO NEUTRONIC MODEL V1.0 that is being developed within the frame of the SYCOMORE effort to create an integrated tokamak modelling platform of a thermonuclear fusion reactor.

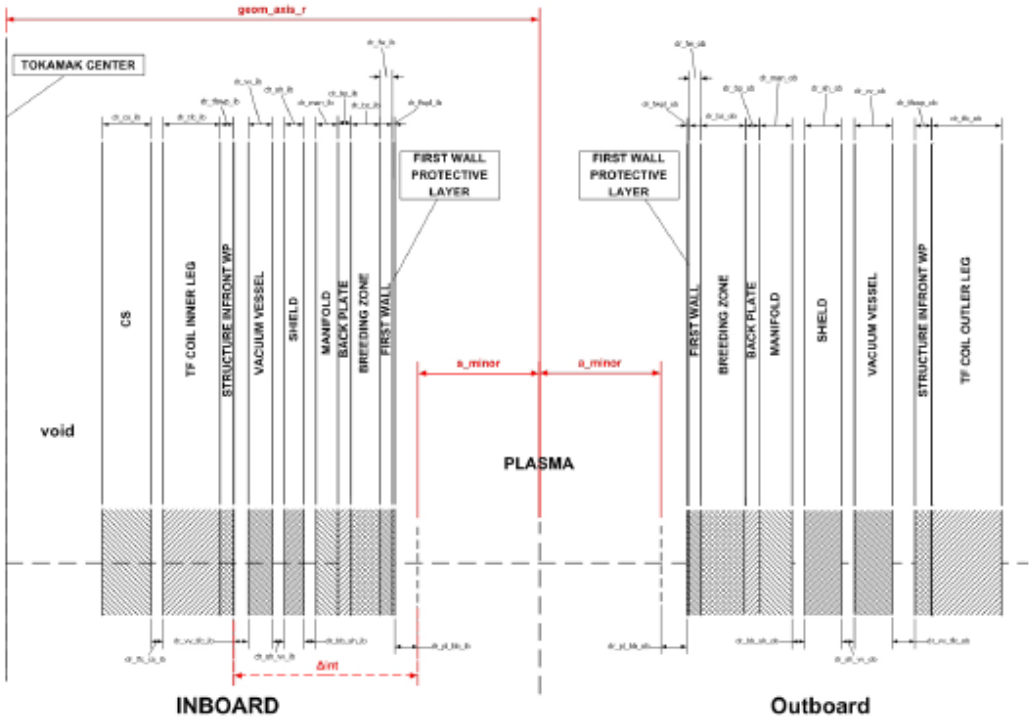

Figure 1. Schema of the tokamak radial inboard torus mid-plane

The target OS and packaging

The NEUTRONIC MODEL V1.0 is available in the form of a universal python program.

The following structure of files can be found on the distribution package:

- `launcher.py` – main python script file that launches the calculations
- `functions.py` – a python file containing support functions for the main script
- `neuralnetworks.py` – a python file containing the path to call the neural networks and its performances
- `inputs.py` – a python file containing the input parameters values
- `NN` – a folder containing the Neural Networks used by the model in form of dynamic libraries ".so"
- `HCLL DEMO NEUTRONIC MODULE ReleaseNotes.pdf` – this file

The NEUTRONIC MODEL V1.0 is implemented as a universal python code that performs neutronic calculations using neural networks presented under the form of dynamic libraries. Thus, it is not dependent on any pre-requisites or special computer configuration.

Installation and launching guidelines

1. In order to install the application just ungzip and untar in desired directory on your hard disk.
2. Edit the *inputs.py* file with the desired tokamak configuration
3. To launch the NEUTRONIC MODULE go to the target directory and run the python launcher *launcher.py*

This sequence will launch the neutronic calculations. Two output files will be created in the launch directory:

- `check.out` – text file containing the description of the steps followed by the NEUTRONIC MODULE
- `variables.out` – text file containing the estimated neutronic parameters stored in rows

Note that the NEUTRONIC MODULE is a python application, thus it requires the installation of python 3.X and the modules numpy and ctypes.

Figure 2. Structure of the NEUTRONIC MODULE

First steps: edition of *inputs.py* and launching the module

1. Open the *inputs.py* file with any text editor software (i.e. nedit on Linux). Introduce the input parameters in the specified dimensions. Note that the values must be within the limits of the operating windows specified in the Appendix A.
2. Now you can launch the NEUTRONIC MODULE to estimate the neutronic parameters. To do so just introduce the next command on the shell:

```
user /target/directory/==> python launcher.py
```

Reading the NEUTRONIC MODULE results

The NEUTRONIC MODULE V1.0 will create two output files containing all informations concerning the neutronic parameters estimated.

- `check.out` – Important information is available on this file:
  - Geometry check: checkup of the geometry consistency.
  - Creation: checkup of the creation of the variables arrays
  - Neural network calculations: writing of the calculated value, the correcting factors and the final estimated value derived corrected and normalised
- `variables.out` – Important information is available on this file:
  - Input parameters: rewriting of the input parameters and dimensions
  - Normalization factor: writing of the normalization factors used by the program
  - Output variables: writing of the estimated neutronic parameters in rows. Dimensions are also specified.

Known problems and limitations

- Limitation: Calculations are only estimations: this is a pre-design tool and must be used carefully.
- Limitation: Estimated parameters are always overestimated. A table specifying the overestimation commited by the model is presented on Table 1. Deviations due to neural networks are presented on Appendix B.
- Limitation: The model is limited to the operating windows presented on Appendix A.
- Limitation: The validation of the model has been done for a small variation window. Estimations beyond these validation windows must be studied carefully.

Neutronic parameters	Unit	Model	Minimum deviation	Maximum deviation	Estimation	Correcting factor
TBR	N.A.	Apollo2 RZ	-1,29%	+1,42%	Underestimate	-1,42%
TBR Ib	N.A.	Apollo2 RZ	-0,92%	+4,65%	Underestimate	-4,65%
TBR Ob	N.A	Apollo2 RZ	-1,62%	+0,81%	Underestimate	-0,81%
Multiplication factor	N.A.	Apollo2 RZ	+1,92%	+2,63%	Underestimate	-2,63%
Peak neutron flux inboard	$1/cm^2.s$	Apollo2 1D	+10,82%	+71,41%	Overestimate	0,00%
Deposited energy (fw-sh)	MW/m^3	Tripoli4 1D neutron-photon	+3,01%	+90,97%	Overestimate	0,00%
Despoited energy (vv-tfc)	MW/m^3	Apollo2 1D	-48,33%	-57,70%	Overestimate	+200%

Table 1 : Correcting factors due to the physical model applied to the obtained results

How to give a feedback

Please send all your requests, bug reports and proposals to:

- Antonella LI PUMA (antonella.li-puma@cea.fr)
- Jean-Charles JABOULAY (jean-charles.jaboulay@ecp.fr)

For further information check HCLL NEUTRONIC MODULE REPORT